EPMA Journal (2020) 11:419–467
https://doi.org/10.1007/s13167-020-00215-0

RESEARCH

Integration of quantitative phosphoproteomics and transcriptomics revealed phosphorylation-mediated molecular events as useful tools for a potential patient stratification and personalized treatment of human nonfunctional pituitary adenomas

Dan Liu[1,2,3,4] · Jiajia Li[2,3,4] · Na Li[2,3,4] · Miaolong Lu[2,3,4] · Siqi Wen[2,3,4] · Xianquan Zhan[2,3,4,5,6]

Received: 2 April 2020 / Accepted: 5 June 2020 / Published online: 13 August 2020

Abstract

Background Invasiveness is a very challenging clinical problem in nonfunctional pituitary adenomas (NFPAs), and currently, there are no effective invasiveness-related molecular biomarkers. The post-neurosurgery treatment is much different as for invasive and noninvasive NFPAs. The aim of this study was to integrate phosphoproteomics and transcriptomics data to reveal phosphorylation-mediated molecular events for invasive characteristics of NFPAs to achieve a potential tool for patient stratification, and prognostic/predictive assessment to discriminate invasive from noninvasive NFPAs for personalized attitude.

Methods The 6-plex tandem mass tag (TMT) labeling reagents coupled with TiO_2 enrichment of phosphopeptides and liquid chromatography-tandem mass spectrometry (LC-MS/MS) were used to identify and quantify each phosphoprotein and phosphosite in NFPAs and controls. Differentially expressed genes (DEGs) between invasive NFPA and control tissues were obtained from the Gene Expression Omnibus (GEO) database. The overlapping analysis was performed between phosphoprotiens and invasive DEGs. Gene Ontology (GO) enrichment, the Kyoto Encyclopedia of Genes and Genomes (KEGG) pathway, and protein–protein interaction (PPI) analyses were used to analyze these overlapped molecules.

Results In total, 1035 phosphoproteins with 2982 phosphorylation sites were identified in NFPAs vs. controls, and 2751 DEGs were identified in invasive NFPAs vs. controls. Overlapping analysis of these phosphoproteins and DEGs exposed 130 overlapped molecules (phosphoproteins; invasive DEGs). GO enrichment and KEGG pathway analyses of 130 overlapped molecules revealed multiple biological processes and signaling pathway network alterations, including cell–cell adhesion, platelet activation, GTPase signaling pathway, protein kinase signaling, calcium signaling pathway, estrogen signaling pathway, glucagon signaling pathway, cGMP–PKG signaling pathway, GnRH signaling pathway, inflammatory mediator regulation of TRP channels, vascular smooth muscle contraction, and Fc gamma R-mediated phagocytosis, which were obviously associated with tumor invasive characteristics. For 130 overlapped molecules, PPI network-based molecular complex detection (MCODE) identified 10 hub molecules, namely SLC2A4, TSC2, AKT1, SCG3, ALB, APOL1, ACACA, SPARCL1, CHGB, and IGFBP5. These hub

Electronic supplementary material The online version of this article (https://doi.org/10.1007/s13167-020-00215-0) contains supplementary material, which is available to authorized users.

✉ Xianquan Zhan
yjzhan2011@gmail.com

[1] Xiangya Nursing School, Central South University, 172 Tong Zi Po Road, Changsha 410013, Hunan, People's Republic of China

[2] University Creative Research Initiatives Center, Shandong First Medical University, 6699 Qingdao Road, Jinan 250117, Shandong, People's Republic of China

[3] Key Laboratory of Cancer Proteomics of Chinese Ministry of Health, Xiangya Hospital, Central South University, 87 Xiangya Road, Changsha 410008, Hunan, People's Republic of China

[4] State Local Joint Engineering Laboratory for Anticancer Drugs, Xiangya Hospital, Central South University, 87 Xiangya Road, Changsha 410008, Hunan, People's Republic of China

[5] Department of Oncology, Xiangya Hospital, Central South University, 87 Xiangya Road, Changsha 410008, Hunan, People's Republic of China

[6] National Clinical Research Center for Geriatric Disorders, Xiangya Hospital, Central South University, 87 Xiangya Road, Changsha 410008, Hunan, People's Republic of China

molecules are involved in multiple signaling pathways and represent potential predictive/prognostic markers in NFPA patients as well as they represent potential therapeutic targets.

Conclusions This study provided the first large-scale phosphoprotein profiling and phosphorylation-related signaling pathway network alterations in human NFPA tissues. Further, overlapping analysis of phosphoproteins and invasive DEGs revealed the phosphorylation-mediated signaling pathway network changes in invasive NFPAs. These findings are the precious resource for in-depth insight into the molecular mechanisms of NFPAs, as well as for the discovery of effective phosphoprotein biomarkers and therapeutic targets for invasive NFPAs.

Keywords Nonfunctional pituitary adenomas · Invasiveness · Tandem mass tag (TMT) labeling · TiO_2 enrichment · Quantitative phosphoproteomics · Transcriptomics · Differentially expressed genes · Overlapped molecule (phosphoprotein · invasive DEG) · Signaling pathway · Patient stratification · Prognostic/predictive assessment · Personalized treatment

Introduction

Pituitary adenoma is a common intracranial tumor that occurs in the anterior lobe of the pituitary gland, which seriously impacts the human endocrine systems [1–4]. Pituitary adenomas are classified into functional pituitary adenomas (FPAs) and nonfunctional pituitary adenomas (NFPAs) [5]. FPAs have the clinically increased levels of the corresponding blood hormones, whereas NFPAs do not have any clinically increased levels of blood hormones to cause the difficulty in its early diagnosis. NFPA is often diagnosed when it grows up to compress its surrounding tissues and organs. Further, NFPAs are classified into invasive and noninvasive NFPAs [6–8]. Noninvasive NFPA is easily treated with neurosurgery. However, the treatment of invasive NFPAs is a big challenge because its invasive behavior injures or damages tumor-surrounding structures, which cannot be completely removed with neurosurgery and causes a risk of recurrence after neurosurgery. Thus, patients with invasive NFPAs are often treated with radiation therapy after neurosurgery. The clinical diagnosis of invasive NFPAs is mainly derived from nuclear magnetic resonance (NMR) image changes and tumor morphological changes observed by neurosurgery, which actually is not fully correct because it is not easy to determine its invasiveness when this tumor is at its early stage with small size [9, 10]. Currently, there are no effective invasiveness-related biomarkers used in clinical practice. Characterizing any invasiveness-related molecular events in NFPAs may benefit the patient stratification and prognostic assessment to discriminate invasive from noninvasive NFPAs for personalized medical procedures. There is an urgent need to discover the changed molecular events for invasive NFPAs.

It is well-known that invasive NFPA is a multicause, multiprocess, and multiconsequence disease, with a series of molecular changes at the levels of genome, transcriptome, proteome, and metabolome, and those molecules interact mutually in a molecular network system [4, 11, 12]. It is driving one to shift the previous single factor model to multiparameter systematic model. Multiomics is an effective approach to realize this multiparameter systematic model shift [13–15]. The proteome and transcriptome are the functional performer of genome, and the proteome and transcriptome are regulated by extensive post-translational modifications (PTMs) [16, 17].

Among those PTMs, phosphorylation is an important and extensively studied PTM with the addition of phosphorus group ($–HPO_3$ to –OH or $–H_3PO_4$ to $–NH_2$) to residues such as serine (Ser, S), threonine (Thr, T), and tyrosine (Tyr, Y) in a protein, which plays crucial roles in signaling pathways and many pathophysiological processes [18]. Phosphorylation and dephosphorylation are reversibly dynamic reactions that are catalyzed by kinases and phosphatases, respectively, which regulate the basic biological functions [19, 20]. Phosphorylation in a protein promotes the conformational changes through interacting with other hydrophilic and hydrophobic residues [19]. Human genome sequencing identifies 107 human phosphatase genes and 518 human protein kinase genes including 90 known tyrosine kinases that include 58 receptor tyrosine kinases. These kinases and phosphatases are the potential targets of anticancer drugs, and tyrosine kinases accounting for 0.3% of genome contribute to 30% of 100 known dominant oncogenes [18, 21]. In eukaryotic cells, protein phosphorylation is a low abundance event, and serine phosphorylation accounts for ~ 90%, threonine phosphorylation for ~ 10%, and tyrosine phosphorylation for ~ 0.05% [18]. Identification and characterization of the altered phosphorylation and functional activities of phosphoproteins in different types of cancers have directly assisted in the discovery of protein kinase inhibitors to treat a tumor [22, 23]. Therefore, it emphasizes the scientific merits of investigating phosphoproteins in pituitary adenomas.

Tandem mass tag (TMT) labeling/TiO_2 phosphopeptide enrichment-based quantitative phosphoproteomics [24, 25] is an effective method to identify phosphoprotein amino acid sequence and phosphorylation sites, and quantify the level of phosphorylation in cancers compared to controls. Briefly, the proteins from cancer and control tissues, respectively, are digested with trypsin, followed by TiO_2 enrichment of phosphopeptides, and liquid chromatography-tandem mass spectrometry (LC-MS/MS) analysis. The MS/MS data are used to determine the amino acid sequence and

phosphorylation sites, and the TMT reporter ions were used to quantify the level of phosphorylation. The studies on phosphorylation in single molecules have been extensively carried out in pituitary adenomas with documented 267 publications when the key words "phosphorylation and pituitary adenoma" were used to search the PubMed database, and those studies are mainly involved in phosphorylation-involved signaling pathways. However, only five publications were found in the PubMed database that are about phosphoproteome or phosphoproteomics in pituitaries or pituitary adenomas [26–30]. Of these publications, Carretero et al. studied the phosphorylation of ERK (extracellular signal–regulated kinase) and RSK (ribosomal S6 kinase) for thyrotropin-releasing hormone (TRH)-induced inhibition of rat *ether-à-go-go*-related (r-ERG) channel potassium currents in rat pituitary growth hormone 3 (GH3) cells [26]. Zhao et al. used proteomics to reveal abnormally phosphorylated AMPK (AMP-activated protein kinase) and ATF2 (activating transcription factor 2) involved in glucose metabolism and tumorigenesis of growth hormone (GH)-secreting pituitary adenomas [27]. Delcout et al. found the role of phosphorylation in pituitary adenylyl cyclase activating polypeptide (PACAP) type I receptor transactivation for insulin growth factor-1 (IGF-1) receptor signaling and antiapoptotic activity in neurons [28]. Beranova-Giorgianni et al. performed phosphoproteomics analysis of the human pituitary and identified 28 phosphoproteins [29]. Zhan et al. used PTMScan experiment that combined immunoaffinity enrichment and LC-MS/MS to analyze a total of 1006 unique phosphorylation sites within 409 proteins in more than 19 signaling pathways in human NFPAs relative to control pituitary tissues [30], and found that lots of hub molecules in many signaling pathways such as mTOR (mammalian target of rapamycin), PI3K/Akt (phosphatidylinositol 3 kinase/protein kinase B), NFκB (nuclear factor kappa-B), Wnt, p38, ERK/MAPK (extracelluar signal-regulated kinase/mitogen-activated protein kinase), and JNK signaling pathways in NFPAs were phosphorylated in NFPAs, and that mTOR, PI3K/AKT, NFκB, Wnt, p38, ERK/MAPK, and JNK signaling pathways were excessively activated in NFPAs [30]. Those publications clearly demonstrated the important roles of protein phosphorylations in pituitary adenoma pathophysiological processes. However, the large-scale global phosphoproteomics analysis has not been carried out in human NFPA tissues. The large-scale profiling of phosphoproteome in human NFPA tissues has important scientific value to understand in-depth the molecular mechanism of NFPAs and discover effective phosphoprotein biomarkers in NFPA patients.

Transcriptome is another level of functional performer of genome. In-depth investigation of transcriptome alterations in invasive NFPAs will directly benefit for the discovery of invasiveness-related molecular events. The public Gene Expression Omnibus (GEO) dataset includes the transcriptomics data between invasive NFPAs and controls, which can be directly extracted to identify differentially expressed genes (DEGs), followed by integration with phosphoproteomics data for comprehensive consideration of invasiveness-related molecular events in invasive NFPAs, from the view point of the multiparameter systematic model.

This study used quantitative phosphoproteomics based on TMT labeling in combination with TiO_2 enrichment of phosphopeptides to identify the large-scale phosphoprotein profile in human NFPA relative to control pituitary tissues, followed by bioinformatics analysis to determine the functional characteristics of phosphoproteins in NFPAs. Further, these identified phosphoproteins and DEG data identified between invasive NFPAs and controls were integrated to determine the overlapped molecules (phosphoproteins; invasive DEGs). Gene ontology (GO) enrichment and the Kyoto Encyclopedia Gene and Genome (KEGG) pathway analysis were performed to determine the functional roles of invasiveness-related phosphoproteins (the overlapped molecules) in NFPAs. These overlapped molecules (phosphoproteins; invasive DEGs) were the precious resource to understand the molecular mechanisms of invasive NFPAs and discover invasiveness-related phosphoprotein biomarkers for potential prognostic/predictive assessment, and patient stratification to discriminate invasive from noninvasive NFPAs, for personalized attitude in medical services of invasive NFPAs. Figure 1 shows the experimental flowchart to identify phosphoproteins in NFPAs and the integrative analysis of phosphoproteomics and transcriptomics data of invasive NFPAs.

Methods

Pituitary adenoma and control tissue samples

Control post-mortem pituitary tissues (n = 4; tissues from 3 white and 1 black patients) were from the Memphis Regional Medical Center (n = 4), which were approved by the University of Tennessee Health Science Center Internal Review Board. Pituitary adenoma biopsy tissues (n = 4; tissues from 4 Chinese patients) were from the Department of Neurosurgery of Xiangya Hospital, China, and were approved by the Xiangya Hospital Medical Ethics Committee of Central South University (Table 1). Written informed consent was obtained from each patient for pituitary adenoma biopsy tissues or the family of each control post-mortem pituitary subject after full explanation of the purpose and nature of all experimental procedures. Quantitative phosphoproteomics was performed with the four mixed NFPA samples and the four mixed control samples.

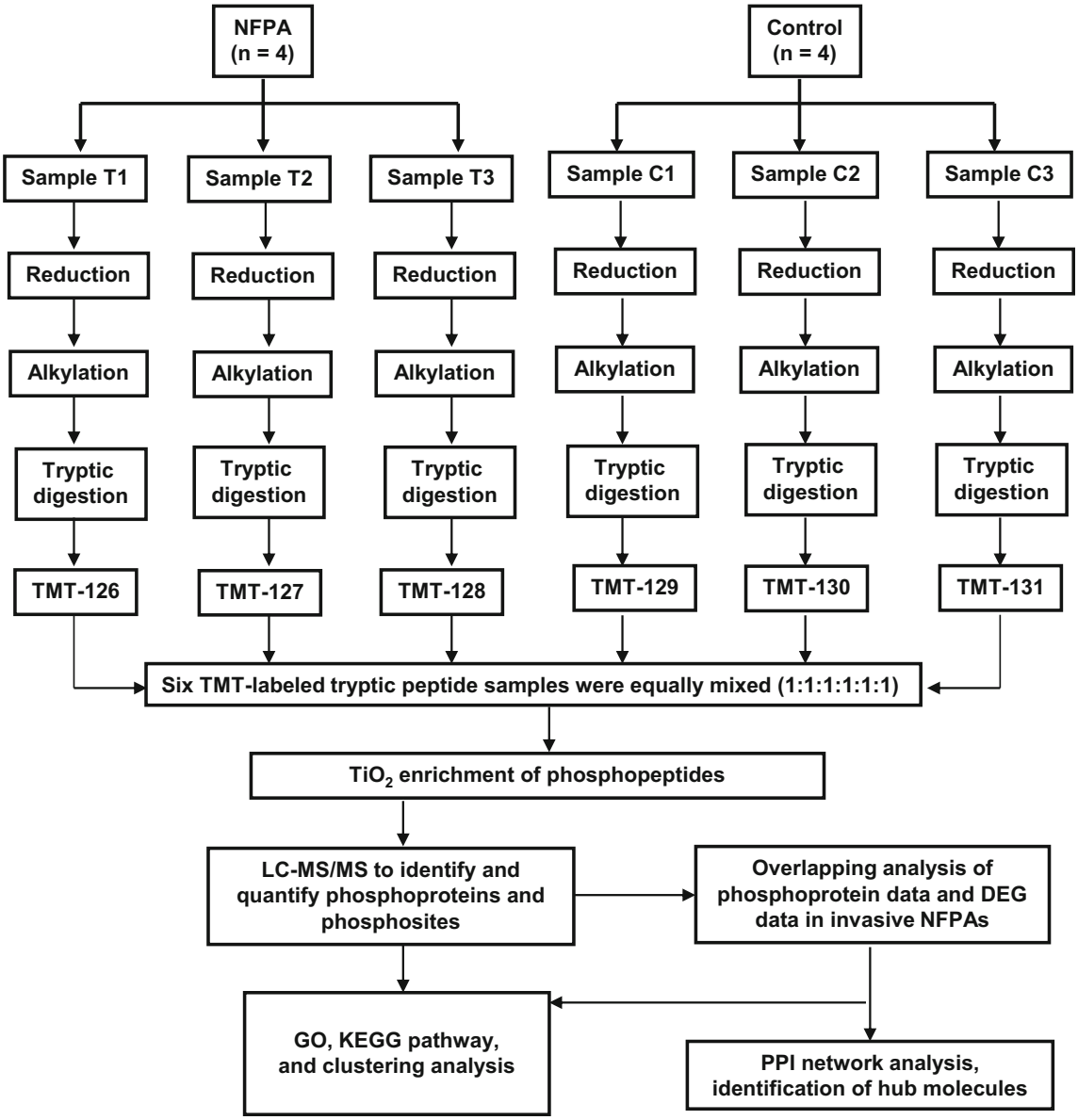

Fig. 1 Experimental flowchart to identify phosphoproteins in NFPAs. Thanks to the 6-plex TMT labeling, it is possible to run six samples at one MS analysis. T1, T2, and T3 were three equal amounts of NFPA protein samples. C1, C2, and C3 were three equal amounts of control pituitary protein samples. The amount of T1, T2, and T3 was equal to that of C1, C2, and C3. Each protein sample was reduced with dithiothreitol (DTT), alkylated with iodoacetamide, and digested with trypsin. NFPA, nonfunctional pituitary adenoma; TMT, tandem mass tag; LC, liquid chromatography; MS/MS, tandem mass spectrometry; GO, gene ontology; KEGG, Kyoto Encyclopedia Gene and Genome; DEG, differentially expressed gene

Protein extraction and quantification

A volume (1 mL) of urea pyrolysis solution [9 M urea, 2.5 mM sodium pyrophosphate, 20 mM 2-hydroxyethyl (HEPES), 1 mM β-glycerophosphate, and 1 mM sodium orthovanadate, and pH 8.0] was added to each tissue sample (100 mg), which was treated with an ultrasonic ice bath (100 W, 10 s; interval 10 s; 10 times), and then followed by centrifugation (18,000×*g*, 10 min, 4 °). The supernatant was the sample of extracted proteins, whose protein content was measured with a Bradford protein quantification kit (YEASEN, Cat# 20202ES76).

Protein digestion with trypsin

Four control protein samples were equally mixed as control protein sample (1.5 mg/sample × 4 = 6 mg), and four NFPA protein samples were equally mixed as NFPA protein sample (1.5 mg/sample × 4 = 6 mg). An amount (300 μg) of each mixed sample (control; NFPA) was mixed with a volume of

Table 1 Clinical information of NFPA and control tissue samples

Group	Sex	Age	Clinical information	Immunohistochemistry	Experiments
NFPA	Male	58	Chinese, NFPA in sellar region. Sellar floor bone destruction, enriched blood supply in tumor, and tumor size 4.5 × 3 × 3 cm^3	ACTH (−), hGH (−), PRL (−), FSH (−), LH (−), TSH (−)	Proteomicst
	Male	53	Chinese, NFPA in sellar region. Sellar floor bone thinning and tumor size 3 × 3 × 2.5 cm^3	ACTH (−), hGH (−), PRL (−), FSH (−), LH (−), TSH (−)	Proteomics
	Female	43	Chinese, NFPA in sellar region. Sellar floor bone thinning, enriched blood supply in tumor, and tumor size 4 × 3 × 3 cm^3	ACTH (−), hGH (−), PRL (−), FSH (+), LH (−), TSH (−)	Proteomics
	Female	43	Chinese, NFPA in sellar region. Adhesion of surrounding tissues, and tumor size 4.5 × 4 × 6 cm^3	ACTH (−), hGH (−), PRL (−), FSH (+), LH (−), TSH (−)	Proteomics
Control	Male	36	White American, multiple toxic materials. Blood alcohol = 0.5 g/L. Blood: HepB (+), HepC (−), HIV (−)	DNT	Proteomics
	Female		White American, 15 h gunshot wound to head. No drugs or alcohol. Blood: HepB (−), HepC (−), HIV (−)	DNT	Proteomics
	Female	34	Black African American, gunshot wound to chest. Blood alcohol = 0.3 g/L; no drugs. Blood: HepB (+), HepC (−), HIV (−)	DNT	Proteomics
	Female	40	White American, multiple toxic compounds. Blood: HepB (+), HepC (+), HIV(−)	DNT	Proteomics

DNT, did not test, which means hormone expressions were not tested in each control pituitary tissue with immunohistochemistry; *ACTH*, adrenocorticotropic hormone; *hGH*, human growth hormone; *PRL*, prolactin; *FSH*, follicle-stimulating hormone; *LH*, luteinizing hormone; *TSH*, thyrotropin-stimulating hormone or thyrotropin; −, negative; +, positive

1 M dithiothreitol (DTT) (the final DTT concentration was 10 mM) (control: $n = 3$; tumor: $n = 3$), followed by incubation (37 °C; 2.5 h) and cooling to room temperature, and then mixed with a volume of 1 M iodoacetamide (the final iodoacetamide concentration was 50 mM), followed by incubation (in the dark; 30 min). The urea concentration was diluted to 1.5 M with five volumes of water. Finally, the mixture was mixed with trypsin (2 μg/μL) at 1:50 (v:v) and then was digested (37 °C; 18 h), followed by desaltation and lyophilization using an SPE C18 column (Waters WAT051910).

TMT labeling of tryptic peptides and enrichment of phosphopeptides

For each sample (control and NFPA, respectively), a total of 300 μg tryptic peptides was equally divided into three parts (100 μg/part) (control: $n = 3$ parts; NFPA: $n = 3$ parts). The 6-plex TMT sixplex™ isobaric label reagent set (Thermo Scientific) was used to label those six parts of tryptic peptides, respectively. The six labeled tryptic peptide samples were equally mixed and lyophilized in vacuum. The lyophilized TMT-labeled peptide was resuspended in 1× DHB buffer that was mixed (1:4) with one volume of 5× DHB [3% DHB, 80% acetonitrile (ACN), and 0.1% trifluoroacetic acid (TFA)] and four volumes of water. The TiO_2 beads were added to the resuspended TMT-labeled peptide mixture and shaken for 40 min, followed by centrifugation (5000×*g*, 1 min) to remove the supernatant. The TiO_2 beads with phosphopeptides were washed with 50 μL of washing buffer I (30% ACN and 3% TFA) (3×) and then with 50 μL of washing buffer II (80% ACN and 0.3% TFA) (3×) to remove the remaining nonbinding peptides. The phosphopeptides were eluted with 50 μL of elution buffer (40% ACN and 15% $NH_3 \cdot H_2O$) (3×) and then lyophilized. The dried TiO_2-enriched phosphopeptides were redissolved in a volume (30 μL) of 0.1% TFA for LC-MS/MS analysis.

LC-MS/MS of enriched phosphopeptides

A volume (20 μL) of TiO_2-enriched phosphopeptides was analyzed with LC-MS/MS. First, phosphopeptides were separated with a high-performance liquid chromatography (HPLC) system EASY-nLC1000 at nanoliter flow rate. The enriched phosphopeptide sample was automatically loaded onto Thermo Scientific EASY column (2 cm × 100 μm; 5 μm C18) that was balanced in 95% of liquid A (0.1% formic acid aqueous solution), then the enriched phosphopeptides were separated by an analytical column (75 μm × 250 mm 3 μm C18 at a flow rate of 250 nL/min) with a linear gradient of solution B (0.1% formic acid in 84% ACN aqueous solution): from 0 to 55% during 0–220 min, 55 to 100% during 220–228 min, and maintaining at 100% during 228–240 min. The LC-separated peptides were online input into a Q-Exactive mass spectrometer (Thermo Finnigan) for MS/MS analysis. The MS parameters

were set as follows: positive-ion scan mode, precursor ion scan range 350–1800 *m*/*z* with a resolution 70,000 at *m*/*z* 200, automatic gain control (AGC) target 3e6, maximum inject time 20 ms, number of scan ranges 1, and dynamic exclusion 30.0 s. For each MS scan, the 10 most abundant precursor ions were selected for MS/MS analysis. The MS/MS parameters were set as follows: high-energy collision dissociation (HCD) ion fragmentation, isolation window 2 *m*/*z*, resolution 17,500 at *m*/*z* 200, maximum injection time 60 ms, normalized collision energy 29 eV, and underfill ratio 0.1%. The MS/MS spectra were used to search the protein database (Uniprot_human_154578_20160815.fasta; 154,578 human sequences; downloaded on 15 August 2016) with MASCOT engine (Matrix Science, London, UK; version 2.2) embedded into Proteome Discoverer 1.4 (Thermo Scientific).

Database searching and functional characteristics of phosphoproteins

Phosphoproteins and phosphosites were identified with MS/MS data using the MASCOT software. The searching parameters were set as follows: MS/MS ion search, trypsin, 2 max missed cleavages, fixed modifications (carbamidomethyl at residue C, TMT 6 plex at the N-terminal, TMT 6 plex at residue K), variable modifications (oxidation at residue M, phosphorylation at residues S, T, and Y), ± 20 ppm for peptide mass tolerance, ± 0.1 Da for fragment mass tolerance, ESI-TRAP (electrospray ionization-ion trap) for instrument type, unrestricted protein mass, true for decoy database pattern, decoy for database pattern, and peptide FDR (false discovery rate) < 0.01. The MS/MS data were used to determine phosphoprotein amino acid sequences and phosphosites. The intensities of TMT-reporter ions were used to determine the phosphorylation level in NFPAs compared to controls. GO enrichments, including cellular components (CCs), molecular functions (MFs), and biological processes (BPs), were analyzed with Cytoscape ClueGO to reveal the functional characteristics of identified phosphoproteins. KEGG pathway enrichment analysis was used to obtain the statistically significant signaling pathways found on the basis of identified phosphoproteins. *P* value for GO enrichment analysis was obtained by two-sided hypergeometric test and corrected by Benjamini–Hochberg. *P* value for pathway enrichment analysis was obtained by two-sided hypergeometric test and corrected by *Q* value. The level of statistical significance was set as $P < 0.05$.

Transcriptomics data of invasive NFPAs relative to control pituitaries

The microarray gene data GSE51618 datasets of human pituitary adenomas were obtained from the public GEO database (http://www.ncbi.nlm.nih.gov/geo/) at the National Center for Biotechnology Information (NCBI). It contained 4 invasive NFPA tissue samples and 3 control pituitary tissue samples, which were analyzed with a gene chip human genome platform (Agilent-014850 Whole Human Genome Microarray 4x44K G4112F) in another laboratory. The R-software (The R Foundation for Statistical Computing, https://www.r-project.org/) was used to analyze DEGs between invasive NFPAs and controls. FDR < 0.05 and fold changes (FC) ≥ 2 were used to determine each DEG.

Overlapping analysis of phosphoprotein data and invasive DEG data

The gene name of each phosphoprotein was obtained from the UniProt human database. The overlapping analysis was carried out between the gene names of phosphoproteins in NFPAs and DEG data between invasive NFPAs and controls to obtain the overlapped molecules (invasive DEGs; phosphoproteins). DAVID GO and KEGG pathway enrichments were used to analyze those overlapped molecules, with statistically significant parameters ($P < 0.05$ and gene count > 3). Each *P* value was corrected with FDR for multiple testing.

Protein–protein interaction and hub molecules with molecular complex detection based on overlapped molecules (invasive DEGs; phosphoproteins)

To investigate their interactive associations, all overlapped molecules between phosphoprotein data and invasive DEG data were mapped to the STRING database. The protein–protein interactions were analyzed by Cytoscape software (version 3.2.1; National Resource for Network Biology) to obtain the protein–protein interaction (PPI) network. The criteria of hub molecule searching were set as a molecular complex detection (MCODE) score > 5 and a statistically significant difference ($P < 0.05$).

Results

Phosphorylation profiling in NFPAs

Totally, 2982 phosphorylation sites within 2076 phosphopeptides derived from 1035 phosphoproteins were identified with TMT–TiO_2 enrichment–LC-MS/MS in NFPAs and controls, including 1207 (1207/2076 = 58%) quantified phosphopeptides with 1660 phosphorylation sites and 869 (869/2076 = 42%) qualified phosphopeptides with 1322 phosphorylation sites (Supplemental Table 1). A representative MS/MS spectrum was from the phosphorylated peptide ^{132}ERADEPQWSLYPSDSQVS*EEVK^{153} ($[M+3H]^{3+}$, *m*/*z* = 1039.83, S* = phosphorylated serine residue) derived from secretogranin-1 (Swiss-Prot No. P05060) (Fig. 2), with a

high-quality MS/MS spectrum, excellent signal-to-noise (S/N) ratio, and extensive product-ion b-ion and y-ion series (b_4, b_5, b_6, b_7, b_8, b_9, b_{10}, b_{11}, y_1, y_2, y_3, y_4, y_5, y_6, y_7, y_8, y_9, y_{10}, y_{11}, y_{12}, and y_{16}). The phosphorylation site was localized to amino acid residue Ser149, and the phosphorylation level was significantly decreased in NFPAs compared to controls (ratio of T/N = 0.29; P = 2.80E-05) (Supplemental Table 1). With the same method, each phosphopeptide and phosphorylation site was identified with MS/MS data (Supplemental Table 1). Among 2076 identified phosphopeptides, 1362 (1362/2076 = 66%) phosphopeptides only contained one single phosphorylation site, and 714 (714/2076 = 34%) phosphopeptides contained at least two phosphorylation sites. Among 2982 identified phosphorylation sites, 2591 (2591/2982 = 86.89%) phosphorylation sites occurred on residue Ser, 357 (357/2982 = 11.97%) phosphorylation sites on residue Thr, and 34 (34/2982 = 1.14%) phosphorylation sites on residue Tyr. Among 1035 phosphoproteins, 486 phosphoproteins were identified with only one phosphorylation site, 242 phosphoproteins with 2 phosphorylation sites, 133 phosphoproteins with 3 phosphorylation sites, 61 phosphoproteins with 4 phosphorylation sites, 39 phosphoproteins with 5 phosphorylation sites, and 74 phosphoproteins with over 5 phosphorylation sites (Supplemental Table 1), including CIC (n = 6 sites), C2CD2L (n = 6), ARHGEF11 (n = 6), EPB41L2 (n = 6), PHF2 (n = 6), POMC (n = 6), VIM (n = 6), NEFH (n = 6), BRAF (n = 6), HTT (n = 6), MECP2 (n = 6), MSH6 (n = 6), SRSF2 (n = 6), TJP1 (n = 6), EPB49 (n = 6), TCOF1 (n = 6), SAFB (n = 6), SMN1 (n = 6), CTR9 (n = 6), KIF21A (n = 6), ZC3H18 (n = 6), RSF1 (n = 6), IRF2BPL (n = 6), THRAP3 (n = 6), CTAGE5 (n = 7), EIF5B (n = 7), MAP4 (n = 7), SUB1 (n = 7), MFAP1 (n = 7), HNRNPUL2 (n = 7), AAK1 (n = 7), ZC3H13 (n = 7), TNKS1BP1 (n = 7), HNRNPC (n = 8), PRPF4B (n = 8), SMARCC2 (n = 8), LMNA (n = 8), PML (n = 8), ADD1 (n = 8), ADD2 (n = 8), PSIP1 (n = 9), ANK1 (n = 9), ANK2 (n = 9), TOP2B (n = 9), TRIM2 (n = 9), TGOLN2 (n = 10), AHNAK (n = 10), SPARCL1 (n = 10), MARCKS (n = 11), HIRIP3 (n = 11), SCG2 (n = 12), LEO1 (n = 12), ACIN1 (n = 12), SPTBN1 (n = 13), FAM169A (n = 13), ATRX (n = 14), AKAP12 (n = 14), EPB41L3 (n = 14), MAPT (n = 15), NEFM (n = 15), MAP2 (n = 15), BCLAF1 (n = 15), HTATSF1 (n = 17), CHGA (n = 19), NUCKS1 (n = 22), IWS1 (n = 23), MAP1A (n = 24), TP53BP1 (n = 26), FGA (n = 35), SRRM1 (n = 42), MAP1B (n = 42), CHGB (n = 50), and SRRM2 (n = 76). These highly phosphorylated proteins might play important roles in the NFPA pathogenesis.

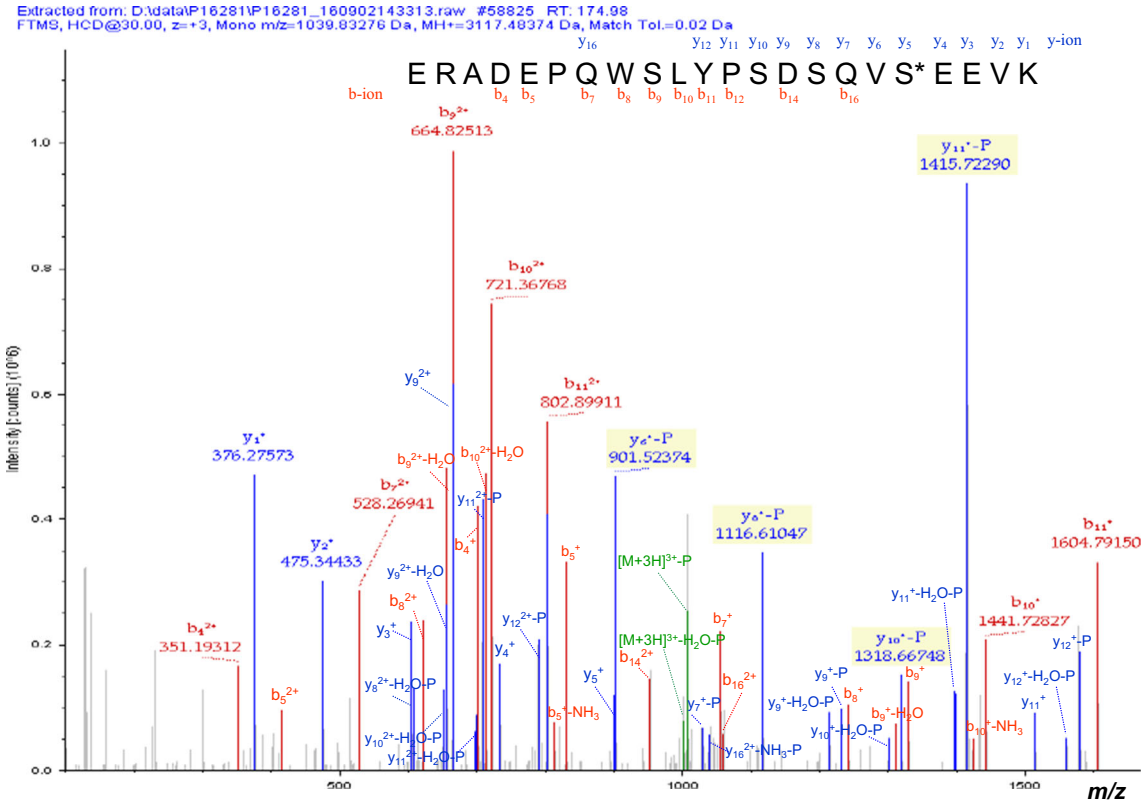

Fig. 2 A representative MS/MS spectrum of phosphopeptide derived from NFPAs. The identified phosphopeptide ^{132}ERADEPQWSLYPSDSQVS*EEVK^{153} ([M+3H]$^{3+}$, m/z = 1039.83, S* = phosphorylated serine residue) was derived from secretogranin-1 (Swiss-Prot No. P05060)

Functional characteristics of phosphoproteins

Those identified 1035 phosphoproteins between NFPAs and controls were analyzed with GO enrichment analysis, including CCs (Supplemental Table 2), MFs (Supplemental Table 3), and BPs (Supplemental Table 4).

CC analysis revealed those phosphoproteins were mainly distributed in the nucleoplasm, cytosol, cell–cell adherens junction, cytoplasm, nuclear speck, nucleus, membrane, focal adhesion, cytoskeleton, protein complex, nuclear matrix, spliceosomal complex, perinuclear region of cytoplasm, Golgi apparatus, chromatin, intracellular ribonucleoprotein complex, Z disc, extracellular exosome, actomyosin, secretory granule, postsynaptic density, costamere, spectrin, microtubule, cell cortex, nuclear heterochromatin, spindle, synaptic vesicle, nuclear membrane, microtubule-associated complex, T-tubule, chromosome, transport vesicle, nuclear envelope, transcriptional repressor complex, PcG protein complex, npBAF complex, Sin3 complex, cAMP-dependent protein kinase complex, soluble N-ethylmaleimide-sensitive factor attachment protein receptor (SNARE) complex, and centrosome (Supplemental Table 2).

MF analysis revealed that the identified phosphoproteins were mainly involved in RNA binding, protein binding, cadherin binding involved in cell–cell adhesion, nucleotide binding, actin filament binding, structural constituent of cytoskeleton, chromatin binding, calmodulin binding, structural molecule activity, microtubule binding, mRNA binding, actin binding, protein kinase binding, 14-3-3 protein binding, spectrin binding, vinculin binding, nucleosomal DNA binding, protein domain–specific binding, translation initiation factor activity, helicase activity, protein binding bridging, protein serine/threonine kinase activity, ion channel binding, histone deacetylase binding, kinase activity, intramolecular transferase activity phosphotransferases, and GTPase activator activity (Supplemental Table 3).

BP analysis revealed that those identified phosphoproteins were mainly involved in multiple biological processes, including cell–cell adhesion, mRNA splicing via spliceosome, RNA splicing, mRNA processing, viral process, RNA processing, mRNA export from nucleus, RNA export from nucleus, microtubule cytoskeleton organization, mRNA 3′-end processing, regulation of alternative mRNA splicing via spliceosome, termination of RNA polymerase II transcription, regulation of cellular response to heat, negative regulation of mRNA splicing via spliceosome, ER to Golgi vesicle-mediated transport, protein sumoylation, membrane fusion, ATP-dependent chromatin remodeling, regulation of mRNA stability, chromatin remodeling, platelet aggregation, regulation of translational initiation, positive regulation of axon extension, negative regulation of transcription DNA-templated, protein phosphorylation, IRE1-mediated unfolded protein response, covalent chromatin modification, platelet activation, and actomyosin structure organization (Supplemental Table 4).

KEGG pathway network analysis identified 31 statistically significant signaling pathways involved in phosphoproteins (Table 2), including spliceosome, platelet activation, RNA transport, endocytosis, mTOR signaling pathway, vascular smooth muscle contraction, SNARE interactions in vesicular transport, proteoglycans in cancer, insulin signaling pathway, glucagon signaling pathway, cGMP–PKG signaling pathway, focal adhesion, estrogen signaling pathway, progesterone-mediated oocyte maturation, protein processing in endoplasmic reticulum, gap junction, gonadotropin-releasing hormone (GnRH) signaling pathway, mitogen-activated protein kinase (MAPK) signaling pathway, and mRNA surveillance pathway.

Further, functional clustering analysis based on CCs, MFs, BPs, and KEGG pathways grouped those identified phosphoproteins into 8 functional clusters (Table 3). Cluster 1 mainly functions in cell–cell adherens junction, cadherin binding involved in cell–cell adhesion, and cell–cell adhesion. Cluster 2 mainly functions in SNARE interactions in vesicular transport, SNAP (soluble N-ethylmaleimide-sensitive fusion attachment proteins) receptor activity, and SNARE complex. Cluster 3 mainly functions in histone H2B ubiquitination, histone monoubiquitination, endodermal cell fate commitment, and Cdc73/Paf1 complex. Cluster 4 mainly functions in myosin II complex and myosin II filament. Cluster 5 mainly functions in oxygen transporter activity, oxygen transport, haptoglobin binding, haptoglobin–hemoglobin complex, and hemoglobin complex. Cluster 6 functions in cAMP-dependent protein kinase complex, protein kinase A catalytic subunit binding, and cAMP-dependent protein kinase regulator activity. Cluster 7 functions in ESCRT (endosomal sorting complex required for transport) III complex disassembly and positive regulation of viral release from host cell. Cluster 8 functions in eukaryotic 43S preinitiation complex. Those findings clearly demonstrate that protein phosphorylations are extensively involved in multiple biological processes and molecular functions in NFPAs.

Integration of phosphoproteomics data and transcriptomics data in invasive NFPAs relative to controls

Microarray transcriptomic data between invasive NFPAs and controls were obtained from the GEO database, which identified 2751 DEGs, consisting of 1477 (53.69%) downregulated and 1274 (46.31%) upregulated DEGs (Supplemental Table 5). An overlapping analysis was performed between 1035 phosphoproteins identified in NFPAs relative to controls and 2751 DEGs identified in invasive NFPAs relative to controls, which identified 130 overlapped molecules (invasive DEGs; phosphoproteins) (Table 4). Those 130 invasiveness-related molecules (DEGs, phosphoproteins) were the precious resource to identify phosphorylation-mediated invasive

Table 2 Statistically significant KEGG signaling pathways identified from 1035 phosphoproteins in NFPAs. Count means the number of genes enriched in this pathway

Category	Pathway name	Count	%	Fold enrichment	*P* value	Benjamini	Gene name of phosphoprotein
KEGG_PATHWAY	hsa03040:Spliceosome	32	3.41	4.57	8.32E-13	1.83E-10	SRSF1, NCBP1, CHERP, SRSF10, TRA2A, WBP11, CTNNBL1, SF3B1, DDX23, RBM8A, PCBP1, USP39, ACIN1, HNRNPC, PRPF40B, RBM25, PRPF40A, DDX42, SNW1, PRPF3, HNRNPA1, SF3A1, HNRNPU, SRSF2, SRSF7, SRSF6, SRSF9, SNRNP200, SLU7, PRPF38B, THOC1, RBM17
KEGG_PATHWAY	hsa04611:Platelet activation	22	2.35	3.22	3.32E-06	3.65E-04	TLN1, LYN, TLN2, STIM1, ARHGAP35, MYL12B, PRKG1, ARHGEF12, ITPR1, ITPR2, AKT1, MAPK1, FGA, FGB, GP1BB, MAPK3, PPP1R12A, GP1BA, GNAS, PRKACB, SNAP23, ITGA2B
KEGG_PATHWAY	hsa03013:RNA transport	24	2.56	2.65	2.89E-05	2.12E-03	CLNS1A, NCBP1, NUP98, EIF5B, RNPS1, NUP155, SMN1, PNN, PABPC4L, EIF4B, EIF4G1, EIF3CL, EIF4G2, EIF4G3, NUP214, EIF3B, EIF3G, RAE1, RBM8A, SRRM1, ACIN1, RANBP2, THOC1, EIF2B5
KEGG_PATHWAY	hsa04144:Endocytosis	28	2.99	2.21	1.40E-04	7.70E-03	CHMP2A, USP8, ASAP2, PML, ASAP1, EPS15L1, ARFGEF2, CHMP2B, GBF1, VPS4B, DNAJC6, VPS4A, VPS35, EHD2, IQSEC1, GIT1, PARD6A, DNM3, FAM21A, EPS15, RABEP1, ARRB1, IGF2R, ACAP2, SH3KBP1, SNX12, BIN1, DNM1
KEGG_PATHWAY	hsa04150:mTOR signaling pathway	12	1.28	3.93	1.75E-04	7.67E-03	PRKCA, EIF4B, AKT1, MAPK1, RPS6KA3, AKT1S1, BRAF, TSC2, MAPK3, PRKAA1, RRAGD, RPTOR
KEGG_PATHWAY	hsa04270:Vascular smooth muscle contraction	16	1.71	2.60	1.11E-03	3.98E-02	PRKCA, BRAF, CALD1, MRVI1, PRKCE, ARHGEF12, PRKG1, PRKCD, ITPR1, ITPR2, ARHGEF11, MAPK1, MAPK3, PPP1R12A, GNAS, PRKACB
KEGG_PATHWAY	hsa04130:SNARE interactions in vesicular transport	8	0.85	4.47	1.62E-03	4.98E-02	STX1A, STX4, SEC22B, VAMP4, BET1L, SNAP23, VAMP2, STX1B
KEGG_PATHWAY	hsa05205:Proteoglycans in cancer	22	2.35	2.09	1.77E-03	4.75E-02	PRKCA, BRAF, ARHGEF12, PDCD4, FLNA, PXN, ITPR1, ITPR2, AKT1, EIF4B, MAPK1, CTTN, ANK1, ANK2, ANK3, SOS1, MAPK3, PPP1R12A, CAMK2D, PRKACB, SLC9A1, FN1
KEGG_PATHWAY	hsa04910:Insulin signaling pathway	17	1.81	2.34	2.24E-03	5.34E-02	PHKA2, IRS2, BRAF, PHKB, ACACA, RPTOR, AKT1, PRKAR2B, MAPK1, PRKAR2A, SLC2A4, SOS1, PRKAR1A, MAPK3, TSC2, PRKAA1, PRKACB
KEGG_PATHWAY	hsa04666:Fc gamma R-mediated phagocytosis	12	1.28	2.71	4.21E-03	8.86E-02	PRKCA, AKT1, MAPK1, LYN, MARCKSL1, MAPK3, ASAP2, ASAP1, MARCKS, PRKCE, BIN1, PRKCD
KEGG_PATHWAY	hsa04114:Oocyte meiosis	14	1.49	2.40	5.18E-03	9.86E-02	ANAPC1, YWHAZ, CDC23, YWHAE, SMC3, ITPR1, ITPR2, MAPK1, RPS6KA3, SLK, MAPK3, CAMK2D, PPP3CB, PRKACB
KEGG_PATHWAY	hsa04922:Glucagon signaling pathway	13	1.39	2.50	5.39E-03	9.44E-02	PHKA2, PHKB, PGAM1, ACACA, ITPR1, ITPR2, AKT1, SLC2A1, PPP3CB, CAMK2D, GNAS, PRKAA1, PRKACB
KEGG_PATHWAY	hsa04720:Long-term potentiation	10	1.07	2.88	7.12E-03	1.14E-01	PRKCA, MAPK1, RPS6KA3, BRAF, MAPK3, PPP3CB, CAMK2D, PRKACB, ITPR1, ITPR2
KEGG_PATHWAY	hsa04962:Vasopressin-regulated water reabsorption	8	0.85	3.46	7.37E-03	1.10E-01	DYNC1LI1, STX4, DYNC1LI2, AVP, GNAS, PRKACB, VAMP2, DYNC1I2
KEGG_PATHWAY	hsa04022:cGMP–PKG signaling pathway	17	1.81	2.04	8.48E-03	1.17E-01	MEF2C, IRS2, SLC8A2, MRVI1, PRKCE, VDAC2, PRKG1, ITPR1, ITPR2, VDAC1, ATP2B1, AKT1, MAPK1, ATP2B4, MAPK3, PPP1R12A, PPP3CB

Table 2 (continued)

Category	Pathway name	Count	%	Fold enrichment	*P* value	Benjamini	Gene name of phosphoprotein
KEGG_PATHWAY	hsa04510:Focal adhesion	20	2.13	1.84	1.15E-02	1.47E-01	PRKCA, TLN1, BRAF, TLN2, TNC, ARHGAP35, MYL12B, PXN, FLNA, VCL, AKT1, MAPK1, ARHGAP5, PAK2, SOS1, MAPK3, PPP1R12A, SPP1, FN1, ITGA2B
KEGG_PATHWAY	hsa04730:Long-term depression	9	0.96	2.85	1.25E-02	1.50E-01	PRKCA, MAPK1, BRAF, LYN, MAPK3, GNAS, PRKG1, ITPR1, ITPR2
KEGG_PATHWAY	hsa04970:Salivary secretion	11	1.17	2.43	1.41E-02	1.59E-01	PRKCA, ATP2B1, ATP2B4, SLC12A2, GNAS, PRKACB, VAMP2, PRKG1, ITPR1, SLC9A1, ITPR2
KEGG_PATHWAY	hsa04915:Estrogen signaling pathway	12	1.28	2.30	1.42E-02	1.53E-01	HSP90AB1, AKT1, MAPK1, HSP90AA1, FKBP5, SOS1, MAPK3, GNAS, PRKACB, PRKCD, ITPR1, ITPR2
KEGG_PATHWAY	hsa04530:Tight junction	11	1.17	2.40	1.52E-02	1.55E-01	PARD6A, TJP1, CTTN, MYH11, MYL12B, MYH14, PRKCE, MYH9, TJP2, TJAP1, MYH10
KEGG_PATHWAY	hsa04914:Progesterone-mediated oocyte maturation	11	1.17	2.40	1.52E-02	1.55E-01	HSP90AB1, ANAPC1, AKT1, MAPK1, CCNB3, RPS6KA3, HSP90AA1, BRAF, MAPK3, CDC23, PRKACB
KEGG_PATHWAY	hsa04141:Protein processing in endoplasmic reticulum	17	1.81	1.91	1.56E-02	1.52E-01	HSP90AB1, SEC31A, HSP90AA1, WFS1, RRBP1, NSFL1C, PDIA6, SEC62, CANX, STUB1, STT3B, HYOU1, DNAJB11, SIL1, DNAJC1, UBE2E2, SSR3
KEGG_PATHWAY	hsa04540:Gap junction	11	1.17	2.38	1.64E-02	1.52E-01	PRKCA, MAPK1, TJP1, SOS1, MAPK3, GNAS, PRKACB, PRKG1, TUBA1B, ITPR1, ITPR2
KEGG_PATHWAY	hsa04919:Thyroid hormone signaling pathway	13	1.39	2.15	1.70E-02	1.52E-01	PRKCA, AKT1, MAPK1, NCOA2, HDAC2, HDAC1, TSC2, MAPK3, SLC2A1, RCAN1, PRKACB, NCOR1, SLC9A1
KEGG_PATHWAY	hsa05100:Bacterial invasion of epithelial cells	10	1.07	2.44	2.03E-02	1.71E-01	DNM3, CTTN, SEPT2, ARHGEF26, CTNNA1, DNM1, PXN, CTNNA2, FN1, VCL
KEGG_PATHWAY	hsa04912:GnRH signaling pathway	11	1.17	2.30	2.03E-02	1.65E-01	PRKCA, MAPK1, MAP3K3, SOS1, MAPK3, CAMK2D, GNAS, PRKACB, PRKCD, ITPR1, ITPR2
KEGG_PATHWAY	hsa05132:*Salmonella* infection	10	1.07	2.29	2.91E-02	2.21E-01	MAPK1, DYNC1LI1, TJP1, DYNC1LI2, MAPK3, PKN2, KLC4, KLC2, FLNA, DYNC1I2
KEGG_PATHWAY	hsa04010:MAPK signaling pathway	21	2.24	1.58	4.26E-02	2.99E-01	PRKCA, MEF2C, BRAF, TAOK2, TAOK1, GNG12, FLNA, AKT1, MAPK1, RPS6KA3, PAK2, MAP3K3, ARRB1, SOS1, MAPT, MAPK3, PPP3CB, HSPB1, MAPK8IP3, STMN1, PRKACB
KEGG_PATHWAY	hsa04068:FoxO signaling pathway	13	1.39	1.84	4.82E-02	3.22E-01	USP7, IRS2, SGK3, BRAF, RBL2, AKT1, MAPK1, CCNB3, SLC2A4, HOMER3, SOS1, MAPK3, PRKAA1
KEGG_PATHWAY	hsa03015:mRNA surveillance pathway	10	1.07	2.09	4.84E-02	3.14E-01	PABPC4L, NCBP1, FIP1L1, CSTF3, RBM8A, SRRM1, RNPS1, ACIN1, CPSF2, PNN
KEGG_PATHWAY	hsa04810:Regulation of actin cytoskeleton	18	1.92	1.63	4.90E-02	3.08E-01	GIT1, BRAF, ARHGEF6, ARHGAP35, MYL12B, GNG12, ARHGEF12, PXN, VCL, MAPK1, PAK2, SOS1, MAPK3, PIKFYVE, PPP1R12A, SLC9A1, FN1, ITGA2B

characteristics in NFPAs for potential prognostic/predictive assessment, patient stratification, and personalized treatment of NFPA patients. Further, the functional characteristics of those 130 overlapped molecules (phosphoproteins; invasive DEGs) were revealed with GO and clustering enrichment analyses.

Gene ontology enrichment analysis The GO enrichment analysis of those identified 130 overlapped molecules (phosphoproteins; invasive DEGs) was annotated with CCs (Supplemental Table 6), MFs (Supplemental Table 7), and BPs (Supplemental Table 8). CC analysis revealed those 130 overlapped molecules (phosphoproteins; invasive DEGs) were mainly distributed in the cytosol, focal adhesion, secretory granule, actin cytoskeleton, cell–cell adherens junction, cytoskeleton, plasma membrane, cell–cell junction, cell cortex, membrane, stress, protein complex, COP9 signalosome, cytoplasm, Golgi apparatus, nuclear speck, SNARE complex, and kinesin complex (Supplemental Table 6). MF analysis revealed that those overlapped molecules (phosphoproteins; invasive DEGs) were significantly involved in cadherin binding involved in cell–cell adhesion, actin filament binding, protein binding, actin binding, structural constituent of cytoskeleton, guanyl-nucleotide exchange factor activity, Rho guanyl-nucleotide exchange factor activity, calmodulin binding, GTPase activator activity, ankyrin binding, structural molecule activity, calcium ion transmembrane transporter activity, spectrin binding, poly(A) RNA binding, microtubule binding, neuropeptide hormone activity, inositol 1,4,5-trisphosphate-sensitive calcium-release channel activity, phosphatidylinositol binding, hormone activity, phosphatidylinositol-3,4,5-trisphosphate binding, and protein kinase activity (Supplemental Table 7). BP analysis revealed multiple statistically significant biological processes, including cell–cell adhesion, regulation of insulin secretion, striated muscle cell differentiation, positive regulation of GTPase activity, neurotransmitter secretion, glucose homeostasis, cellular response to prostaglandin E stimulus, regulation of small GTPase-mediated signal transduction, regulation of Rho protein signal transduction, positive regulation of apoptotic process, renal water homeostasis, glucose transport, positive regulation of endodeoxyribonuclease activity, peptidyl-threonine phosphorylation, transmembrane transport, positive regulation of cAMP biosynthetic process, cellular response to hydroperoxide, signal transduction, platelet degranulation and activation, cellular iron ion homeostasis, and peripheral nervous system myelin maintenance (Supplemental Table 8).

Clustering analysis The clustering analysis of 130 overlapped molecules (phosphoproteins; invasive DEGs) identified 6 significantly functional categories (Table 5). Cluster 1 was mainly associated with cell–cell adherens and regulation, which was involved in the important overlapped molecules (phosphoproteins; invasive DEGs), including ALDOA, TNKS1BP1, LIMA1, CALD1, ASAP1, EPS15L1, H1FX, NDRG1, PLEC, CHMP2B, and PGM5. Cluster 2 was involved in platelet activation, which was involved in the important overlapped molecules (phosphoproteins; invasive DEGs), including AKT1, TLN2, STIM1, GNAS, SNAP23, PRKG1, ARHGEF12, ITPR1, ITPR2, and ITGA2B. Cluster 3 was mainly associated with GTPase signaling and regulation, which was involved in the important overlapped molecules (phosphoproteins; invasive DEGs), including AKT1, ARHGEF11, ARHGEF11, ARHGEF12, ARHGEF6, ASAP1, ASAP2, BCLAF1, CDC42EP4, DOCK11, DOCK7, GAL, GNAS, NGEF, SPTB, STXBP5L, and TSC2. Cluster 4 was associated with the microtubule and its regulation, which was involved in the overlapped molecules (phosphoproteins; invasive DEGs), including CLASP2, KIF13B, KIF16B, KIF1A, MAP4, NDRG1, and STIM1. Cluster 5 was mainly associated with protein kinase activity and peptidyl-threonine phosphorylation, which was involved in the important overlapped molecules (phosphoproteins; invasive DEGs), including AKT1, AVP, CASK, STK39, PRKCD, CDK14, and DCLK1. Cluster 6 was mainly associated with calcium signaling pathway and regulation, which was involved in the overlapped molecules (phosphoproteins; invasive DEGs), including SLC8A2, STIM1, ITPR1, ITPR2, and GNAS. Thereby, those phosphoproteins participated in the corresponding biological functions in NFPAs. It clearly demonstrated the important roles of phosphorylation in invasive NFPA pathogenesis.

Signaling pathways involved in overlapped molecules (phosphoproteins; invasive DEGs)

The KEGG pathway enrichment analysis of 130 overlapped molecules (phosphoproteins; invasive DEGs) identified 14 statistically significant signaling pathways (Table 6; Supplemental Fig. 1) that were related to tumor invasiveness and involved in protein phosphorylations (Table 4), including (i) platelet activation involved in phosphorylation at residues Ser122 and Ser124 in AKT1; Thr1843 (ratio of T/N = 1.16, P = 1.17E-02) in TLN2; Ser257 in STIM1; Ser995 (ratio of T/N = 2.77, P = 2.32E-05) in GNAS; Ser110 (ratio of T/N = 2.13, P = 6.07E-04) in SNAP23; Thr515 in PRKG1; Ser309 (ratio of T/N = 2.94, P = 9.07E-04) in ARHGEF12; Ser1177, Thr1178, Ser1180, and Tyr1181 in ITPR1; Ser1687 (ratio of T/N = 0.67, P = 2.20E-03) in ITPR2; and Ser880 in ITGA2B (Table 6; Supplemental Fig. 1.1); (ii) vascular smooth muscle contraction involved in phosphorylation at residues Ser207 (ratio of T/N = 3.30, P = 2.31E-06) in CALD1; Ser995 (ratio of T/N = 2.77, P = 2.32E-05) in GNAS; Thr515 in PRKG1; Ser309 (ratio of T/N = 2.94, P = 9.07E-04) in ARHGEF12; Tyr514 in PRKCD; Ser1177, Thr1178, Ser1180, and Tyr1181 in ITPR1;, Ser663 (ratio of T/N = 2.32, P = 4.24E-04); Thr668

Table 3 Functional characteristics of 1035 phosphoproteins in NFPAs, clustered with GO and KEGG pathway enrichments. Count means the number of genes enriched in each item

Category	Function characteristics	Count	%	Fold enrichment	*P* value	Gene name of phosphoprotein
Annotation cluster 1						
GOTERM_CC_DIRECT	GO:0005913~cell–cell adherens junction	71	7.57	4.44	2.23E-26	CAST, HSP90AB1, LIMA1, TLN1, SEPT2, ZC3HAV1, VAPB, H1FX, EIF2A, EPS15L1, VCL, LARP1, BZW1, CTTN, PAK2, SLK, PCBP1, ARHGAP1, FAM129B, AHNAK, GOLGA3, DAB2IP, BSG, LYN, PKN2, KTN1, MYH9, CTNNA1, FLNA, CTNNA2, RSL1D1, EIF4G1, EIF4G2, EPB41L1, PGM5, DHX29, SERBP1, USO1, EEF1D, CD226, DBN1, ADD1, ALDOA, HDLBP, YWHAZ, USP8, PPME1, CALD1, ASAP1, CTNND1, KLC2, ESYT2, TAGLN2, SCRIB, CHMP2B, MACF1, NDRG1, PLEC, ZC3H15, YWHAE, MPRIP, TNKS1BP1, EPS15, TJP1, LASP1, TMOD3, SPTBN1, NOP56, TMPO, TJP2, SPTAN1
GOTERM_MF_DIRECT	GO:0098641~cadherin binding involved in cell–cell adhesion	68	7.25	4.49	9.96E-26	CAST, HSP90AB1, LIMA1, TLN1, SEPT2, ZC3HAV1, VAPB, H1FX, EIF2A, EPS15L1, VCL, LARP1, BZW1, CTTN, PAK2, SLK, PCBP1, ARHGAP1, FAM129B, AHNAK, GOLGA3, DAB2IP, BSG, PKN2, KTN1, MYH9, CTNNA1, FLNA, CTNNA2, RSL1D1, EIF4G1, EIF4G2, EPB41L1, DHX29, SERBP1, USO1, EEF1D, DBN1, ADD1, ALDOA, YWHAZ, HDLBP, USP8, PPME1, CALD1, ASAP1, CTNND1, KLC2, ESYT2, TAGLN2, SCRIB, CHMP2B, MACF1, NDRG1, PLEC, ZC3H15, YWHAE, MPRIP, EPS15, TNKS1BP1, TJP1, LASP1, TMOD3, SPTBN1, NOP56, TMPO, TJP2, SPTAN1
GOTERM_BP_DIRECT	GO:0098609~cell–cell adhesion	60	6.40	4.33	6.80E-22	CAST, HSP90AB1, LIMA1, SEPT2, ZC3HAV1, VAPB, H1FX, EPS15L1, EIF2A, LARP1, BZW1, CTTN, SLK, PAK2, PCBP1, ARHGAP1, FAM129B, AHNAK, GOLGA3, DAB2IP, BSG, PKN2, KTN1, RSL1D1, EIF4G1, EIF4G2, EPB41L1, DHX29, SERBP1, USO1, EEF1D, DBN1, ADD1, ALDOA, YWHAZ, HDLBP, USP8, PPME1, CALD1, ASAP1, KLC2, TAGLN2, ESYT2, CHMP2B, MACF1, NDRG1, PLEC, ZC3H15, YWHAE, MPRIP, EPS15, TNKS1BP1, TJP1, LASP1, TMOD3, SPTBN1, TMPO, NOP56, TJP2, SPTAN1
Annotation cluster 2						
KEGG_PATHWAY	hsa04130:SNARE interactions in vesicular transport	8	0.85	4.47	1.62E-03	STX1A, STX4, SEC22B, VAMP4, BET1L, SNAP23, VAMP2, STX1B
GOTERM_MF_DIRECT	GO:0005484~SNAP receptor activity	8	0.85	3.93	3.66E-03	STX1A, STX4, SEC22B, VAMP4, BET1L, SNAP23, VAMP2, STX1B
GOTERM_CC_DIRECT	GO:0031201~SNARE complex	9	0.96	3.43	4.28E-03	STX1A, STX4, SEC22B, VAMP4, BET1L, SNAP23, VAMP2, STX1B, STXBP5L

Table 3 (continued)

Category	Function characteristics	Count	%	Fold enrichment	*P* value	Gene name of phosphoprotein
Annotation cluster 3						
GOTERM_BP_DIRECT	GO:0033523~histone H2B ubiquitination	4	0.43	9.79	6.11E-03	LEO1, PAF1, RNF20, CTR9
GOTERM_BP_DIRECT	GO:0010390~histone monoubiquitination	4	0.43	7.12	1.61E-02	LEO1, PAF1, RNF20, CTR9
GOTERM_BP_DIRECT	GO:0001711~endodermal cell fate commitment	3	0.32	9.79	3.40E-02	LEO1, PAF1, CTR9
GOTERM_CC_DIRECT	GO:0016593~Cdc73/Paf1 complex	3	0.32	8.65	4.35E-02	LEO1, PAF1, CTR9
Annotation cluster 4						
GOTERM_CC_DIRECT	GO:0016460~myosin II complex	4	0.43	11.53	3.64E-03	MYL12B, MYH14, MYH9, MYH10
GOTERM_CC_DIRECT	GO:0097513~myosin II filament	3	0.32	20.18	7.10E-03	MYH14, MYH9, MYH10
Annotation cluster 5						
GOTERM_MF_DIRECT	GO:0005344~oxygen transporter activity	5	0.53	6.84	4.84E-03	IPCEF1, HBA2, HBA1, HBB, HBD
GOTERM_BP_DIRECT	GO:0015671~oxygen transport	5	0.53	6.52	5.85E-03	IPCEF1, HBA2, HBA1, HBB, HBD
GOTERM_MF_DIRECT	GO:0031720~haptoglobin binding	3	0.32	19.14	7.88E-03	HBA2, HBA1, HBB
GOTERM_CC_DIRECT	GO:0031838~haptoglobin–hemoglobin complex	3	0.32	15.14	1.37E-02	HBA2, HBA1, HBB
GOTERM_CC_DIRECT	GO:0005833~hemoglobin complex	4	0.43	6.73	1.90E-02	HBA2, HBA1, HBB, HBD
Annotation cluster 6						
GOTERM_CC_DIRECT	GO:0005952~cAMP-dependent protein kinase complex	4	0.43	11.53	3.64E-03	PRKAR2B, PRKAR2A, PRKAR1A, PRKACB
GOTERM_MF_DIRECT	GO:0034236~protein kinase A catalytic subunit binding	4	0.43	5.47	3.35E-02	PRKAR2B, PRKAR2A, GSK3A, PRKAR1A
GOTERM_MF_DIRECT	GO:0008603~cAMP-dependent protein kinase regulator activity	3	0.32	8.20	4.80E-02	PRKAR2B, PRKAR2A, PRKAR1A
Annotation cluster 7						
GOTERM_BP_DIRECT	GO:1904903~ESCRT III complex disassembly	4	0.43	7.83	1.21E-02	CHMP2A, VPS4B, VPS4A, CHMP2B
GOTERM_BP_DIRECT	GO:1902188~positive regulation of viral release from host cell	4	0.43	7.12	1.61E-02	CHMP2A, VPS4B, VPS4A, CHMP2B
Annotation cluster 8						
GOTERM_CC_DIRECT	GO:0016282~eukaryotic 43S preinitiation complex	4	0.43	5.38	3.52E-02	EIF3CL, EIF3B, EIF3G, DHX29

Table 4 A total of 130 overlapped molecules between 1035 phosphoproteins and 2751 invasive DEGs

DEG name	logFC	AveExpr	*t*	*P* value	Adjusted *P* value	B	Protein accession ID	Protein name	Phosphopeptide
ABCA2	1.9524	9.4927	8.1782	1.28E-05	1.26E-03	3.7214	Q9BZC7	ATP-binding cassette subfamily A member 2	VSEEDQS*LENS*EADVK
ACACA	1.1822	6.8754	3.3664	7.62E-03	4.22E-02	− 2.8421	Q13085	Acetyl-CoA carboxylase 1	FIIGSVSEDNS*EDEISNLVK FIIGSVS*EDNS*EDEISNLVK
ADD2	1.6533	6.9033	5.2921	4.08E-04	7.59E-03	0.1686	P35612	Beta-adducin	EAETKS*PLVS*PSK EAETKS*PLVS*PSK KLELDGEKETAPEEPGS*PAK S*APAS*PVQSPAK EAET*KSPLVS*PSK SAPAS*PVQS*PAK
ADD3	1.0662	11.6287	4.4111	1.46E-03	1.57E-02	− 1.1500	Q9UEY8	Gamma-adducin	IEEVLSPEGS*PSKS*PS*K IEEVLSPEGS*PS*KSPSK IEEVLS*PEGS*PSK IEEVLSPEGS*PSKS*PS*K IEEVLSPEGS*PSKS*PSK
AKAP12	− 4.1353	10.1654	− 4.9159	6.93E-04	1.03E-02	− 0.3808	Q02952	A-kinase anchor protein 12	GLAEVQQDGEAEEGAT*SDGEK SPPS*PVER ETCVSGEDPTQGADLS*PDEK GLAEVQQDGEAEEGATS*DGEK ADS*QDAGQETEK RGS*S*S*DEEGGPK EDEKGDDVDDPENQNSALADT*DASGGLTKESPDTNGPK EVSSLEGS*PPPCLGQEEAVCTK SAESPT*S*PVTSETGSTFK VVGQTT*PESFEK
AKT1	1.1801	6.8509	5.4900	3.11E-04	6.55E-03	0.4493	P31749	RAC-alpha serine/threonine-protein kinase	S*GSPSDNSGAEEMEVSLAKPK
ALB	1.9536	6.1289	4.5055	1.27E-03	1.45E-02	− 1.0035	P02768-1	Serum albumin	TCVADES*AENCDK
ALDOA	1.2343	14.3796	5.4707	3.19E-04	6.64E-03	0.4222	P04075	Fructose-bisphosphate aldolase A	GILAADES*TGSIAK GILAADEST*GSIAK GILAADESTGS*IAK LQS*IGTENTEENR
ANAPC1	1.1050	8.8290	4.9940	6.20E-04	9.67E-03	− 0.2650	Q9H1A4	Anaphase-promoting complex subunit 1	NFDFEGSLS*PVIAPK
ANK1	2.2500	8.5296	3.7930	3.82E-03	2.75E-02	− 2.1377	P16157	Ankyrin-1	LGYIS*VTDVLK ELQFS*VEDINR LST*PPPLAEEEGLASR LS*T*PPPLAEEEGLASR LEGALS*EEPR IT*HSPTVSQVTER ITHS*PTVSQVTER ITHS*PT*VSQVTER
AP3B1	− 1.2102	11.2042	− 4.7116	9.33E-04	1.22E-02	− 0.6877	O00203	AP-3 complex subunit beta-1	NFYES*DDDQKEK

Table 4 (continued)

DEG name	logFC	AveExpr	*t*	*P* value	Adjusted *P* value	B	Protein accession ID	Protein name	Phosphopeptide
APIP	1.1934	8.6558	4.5636	1.16E-03	1.38E-02	− 0.9140	Q96GX9	Probable methylthioribulose-1-phosphate dehydratase	DISGPS*PSK
APOL1	− 1.1936	9.8189	− 3.2480	9.26E-03	4.79E-02	− 3.0397	A5PL32	Apolipoprotein L1	VTEPIS*AES*GEQVER
ARHGEF11	1.5982	6.3788	7.6133	2.33E-05	1.74E-03	3.1111	O15085	Rho guanine nucleotide exchange factor 11	S*LENPT*PPFTPK NS*GIWESPELDR HQVLLEDPEQEGS*AEEEELGVLPCPSTSLDGENR WTDGS*LS*PPAKEPLASDSR
ARHGEF12	1.0544	7.6127	5.9598	1.67E-04	4.70E-03	1.0924	Q9NZN5	Rho guanine nucleotide exchange factor 12	TDCSSGDASRPSSDNADS*PK
ARHGEF6	1.5519	6.6394	4.1475	2.19E-03	1.99E-02	− 1.5656	Q15052	Rho guanine nucleotide exchange factor 6	KDS*IPQVLLPEEEK
ASAP1	1.4735	6.5041	5.7914	2.08E-04	5.30E-03	0.8655	Q9ULH1	Arf-GAP with SH3 domain, ANK repeat and PH domain-containing protein 1	QEEIDES*DDDLDDKPSPIK
ASAP2	− 2.6231	8.6901	− 4.5167	1.25E-03	1.43E-02	− 0.9862	O43150	Arf-GAP with SH3 domain, ANK repeat and PH domain-containing protein 2	LLHEDLDES*DDDMDEK
ATP8A1	1.5729	8.3920	5.5795	2.75E-04	6.14E-03	0.5743	Q9Y2Q0	Probable phospholipid-transporting ATPase IA	TDDVS*EKT*S*LADQEEVR TDDVS*EKT*SLADQEEVR TS*LADQEEVR
AVP	− 1.0570	7.0007	− 3.3755	7.51E-03	4.18E-02	− 2.8269	P01185	Vasopressin-neurophysin 2-copeptin	CQEENYLPS*PCQSGQK
BAIAP3	− 7.0454	10.8238	− 22.2592	1.46E-09	5.00E-06	11.8821	O94812	BAI1-associated protein 3	S*GSPAPPEPVDPSLGLR SGS*PAPPEPVDPSLGLR
BASP1	− 2.4499	11.6391	− 3.2822	8.75E-03	4.61E-02	− 2.9825	P80723	Brain acid–soluble protein 1	S*DGAPASDSKPGSSEAAPSSK AEGAATEEEGT*PK ETPAATEAPS*S*T*PK ETPAATEAPSST*PK
BCLAF1	1.2108	6.8562	6.4198	9.33E-05	3.40E-03	1.6913	Q9NYF8	Bcl-2-associated transcription factor 1	KAEGEPQEES*PLK AEGEWEDQEALDYFS*DKESGK DLFDYS*PPLHK ETQS*PEQVK FNDS*EGDDT*EETEDYR KET*QSPEQVK QKS*PEIHR YS*PSQNSPIHHIPSR YSPS*QNS*PIHHIPSR IDIS*PSTLR SSATSGDIWPGLSAYDNS*PR DTFEHDPSES*IDEFNK SSATSGDIWPGLS*AYDNSPR
CALD1	1.1936	4.5492	3.8770	3.34E-03	2.54E-02	− 2.0009	Q05682	Caldesmon	RGS*IGENQIKDEK
CASC4	− 1.1339	10.5848	− 4.4287	1.42E-03	1.54E-02	− 1.1227	Q6P4E1	Protein CASC4	FFDENES*PVDPQHGSK

Table 4 (continued)

DEG name	logFC	AveExpr	*t*	*P* value	Adjusted *P* value	B	Protein accession ID	Protein name	Phosphopeptide
CASK	2.8830	11.3140	7.5385	2.53E-05	1.82E-03	3.0275	B7ZKY2	Calcium/calmodulin-dependent serine protein kinase (MAGUK family)	TQSS*S*CEDLPSTTQPK TQS*SSCEDLPSTTQPK
CBX8	1.0985	6.6357	3.9595	2.93E-03	2.35E-02	− 1.8672	Q9HC52	Chromobox protein homolog 8	VDDKPS*SPGDSSK
CCDC48	− 3.3166	8.0575	− 9.1213	5.02E-06	7.68E-04	4.6616	Q9HA90	Coiled-coil domain-containing protein 48	TLGTS*EEEAELQQK T*LGTSEEEAELQQK
CCDC86	− 2.5059	12.1490	− 4.2785	1.79E-03	1.76E-02	− 1.3580	Q9H6F5	Coiled-coil domain-containing protein 86	LQQGAGLESPQGQPEPGAAS*PQR LGGLRPES*PESLTSVSR ALVEFESNPEETREPGS*PPSVQR
CDC42EP4	2.2410	9.6096	3.4168	7.02E-03	4.01E-02	− 2.7581	Q9H3Q1	Cdc42 effector protein 4	AGPDLPSLPSHALEDEGWAAAAPS*PGSAR
CDK14	1.1778	11.3632	3.5667	5.50E-03	3.45E-02	− 2.5096	O94921	Cyclin-dependent kinase 14	VHS*ENNACINFK
CENPA	1.5999	4.3832	4.5900	1.12E-03	1.35E-02	− 0.8733	P49450	Histone H3-like centromeric protein A	RRS*PS*PTPTPGPSR
CHD3	1.1576	8.0852	4.7990	8.21E-04	1.13E-02	− 0.5558	Q12873	Chromodomain-helicase-DNA-binding protein 3	ELQGDGPPS*SPTNDPTVK
CHGA	− 3.8263	14.4379	− 4.6354	1.04E-03	1.30E-02	− 0.8038	P10645	Chromogranin-A	S*GELEQEEERLS*KEWEDSK S*GELEQEEERLS*K HSGFEDELSEVLENQS*S*QAELK YPGPQAEGDSEGLS*QGLVDR GEQEHS*QQKEEEEEMAVVPQGLFR S*GEATDGARPQALPEPMQESK EAVEEPS*SKDVMEK EAVEEPSS*KDVMEK REDS*KEAEK YPGPQAEGDS*EGLSQGLVDR GWRPS*S*REDS*LEAGLPLQVR LEGQEEEEDNRDS*SMK EDS*LEAGLPLQVR GLS*AEPGWQAK HSGFEDELS*EVLENQS*SQAELK RPEDQELESLS*AIEAELEK GWRPS*SREDS*LEAGLPLQVR KHS*GFEDELSEVLENQS*SQAELK RPEDQELES*LSAIEAELEK
CHGB	− 1.3288	14.5253	− 3.2997	8.51E-03	4.53E-02	− 2.9533	P05060	Secretogranin-1	SETHAAGHS*QEK GRGS*EEYR AS*EEEPEYGEEIK EKSS*QES*GEETGS*QENHPQESK ADEPQWSLYPSDS*QVS*EEVK SSQESGEET*GSQENHPQESK GERGEDS*S*EEK AS*EEEPEY*GEEIK SSQES*GEETGS*QENHPQESK S*QREDEEEEEGENYQK

Table 4 (continued)

DEG name	logFC	AveExpr	*t*	*P* value	Adjusted *P* value	B	Protein accession ID	Protein name	Phosphopeptide
									SAEFPDFYDS*EEPVSTHQEAENEKDR
									S*QEES*EEGEEDATS*EVDK
									SSQGGS*LPSEEK
									DPADASEAHES*SSR
									NYPS*LELDK
									ADEPQWSLYPS*DS*QVSEEVK
									EKSS*QES*GEET*GSQENHPQESK
									SSQGGSLPS*EEK
									S*AEFPDFYDSEEPVSTHQEAENEKDR
									S*AEFPDFY*DSEEPVSTHQEAENEKDR
									SQEESEEGEEDAT*SEVDK
									M#AHGY*GEES*EEER
									ERADEPQWSLYPSDSQVS*EEVK
									PQS*EES*WDEEDKR
									SAEFPDFYDS*EEPVS*THQEAENEK
									SS*QGGSLPSEEK
									S*SQGGSLPSEEK
									GHPQEES*EESNVSMASLGEK
									SAEFPDFYDSEEPVS*T*HQEAENEK
									EKS*S*QES*GEET*GS*QENHPQESK
									WQQQGDLQDT*KENR
									GHPQEES*EESNVS*M#ASLGEK
									ADEPQWSLY*PSDSQVS*EEVK
									GHPQEES*EESNVS*MAS*LGEK
									WAEGGGHS*R
									GHPQEES*EES*NVS*MASLGEK
									CIIEVLSNALS*K
									DHHS*THYRASEEEPEY*GEEIK
									DPADASEAHESS*S*RGEAGAPGEEDIQGPTK
									LLRDPADAS*EAHESSSR
									S*ETHAAGHS*QEK
CHMP2B	− 1.5915	9.4237	− 9.3648	3.99E-06	6.71E-04	4.8895	Q9UQN3	Charged multivesicular body protein 2b	ATIS*DEEIER
CIC	1.0491	11.3820	6.0126	1.56E-04	4.52E-03	1.1627	I3L2J0	Protein capicua homolog	KNS*TDLDSAPEDPTS*PK
									KNST*DLDSAPEDPTS*PK
									S*S*PPLPPPAEER
									SS*PPLPPPAEER
CLASP2	1.1382	9.5975	6.8774	5.38E-05	2.59E-03	2.2577	O75122	CLIP-associating protein 2	VLNT*GSDVEEAVADALK
									VLNTGS*DVEEAVADALK
CTAGE5	− 1.5080	8.1531	− 6.2874	1.10E-04	3.78E-03	1.5219	O15320	Cutaneous T cell lymphoma-associated antigen 5	AFLS*PPTLLEGPLR
									APSDTGS*LS*PPWDQDRR
									S*NS*ELEDEILCLEK
									SNS*ELEDEILCLEK
									SFNMPS*LDK

Table 4 (continued)

DEG name	logFC	AveExpr	*t*	*P* value	Adjusted *P* value	B	Protein accession ID	Protein name	Phosphopeptide
CYBRD1	− 2.4812	7.6514	− 4.6620	1.00E-03	1.27E-02	− 0.7633	Q53TN4	Cytochrome b reductase 1	GSMPAY*SGNNMDK
DCLK1	− 4.0867	9.7240	− 7.5568	2.48E-05	1.80E-03	3.0480	O15075	Serine/threonine-protein kinase DCLK1	SPSPSPTS*PGSLR VCSS*MDENDGPGEEVSEEGFQIPATITER
DENR	1.0387	8.3264	3.5168	5.96E-03	3.62E-02	− 2.5921	O43583	Density-regulated protein	LTVENS*PK
DMXL2	1.2471	8.1839	7.6581	2.22E-05	1.70E-03	3.1609	Q8TDJ6	DmX-like protein 2	KQS*EVEADLGYPGGK RQS*ENISAPPVLSEDIDK
DOCK11	− 2.9596	8.1805	− 7.3717	3.05E-05	1.98E-03	2.8384	Q5JSL3	Dedicator of cytokinesis protein 11	ETVETAQDDET*SSQGK
DOCK7	− 1.0075	9.0073	− 3.4301	6.87E-03	3.96E-02	− 2.7360	Q96N67	Dedicator of cytokinesis protein 7	SLSNS*NPDISGTPT*SPDDEVR
ELAVL4	2.1977	9.9185	4.3468	1.61E-03	1.66E-02	− 1.2507	P26378	ELAV-like protein 4	NCPS*PMQTGATTDDSK
EPB41L2	1.9271	8.3372	6.2524	1.15E-04	3.86E-03	1.4768	O43491	Band 4.1-like protein 2	EIS*PGSGPGEIR S*YTLVVAK EISPGS*GPGEIR EVAENQQNQS*S*DPEEEK EVAENQQNQSS*DPEEEK
EPB49	1.1990	8.2266	6.2015	1.22E-04	4.01E-03	1.4108	Q08495	Dematin	GNS*LPCVLEQK RGAEEEEEEEDDDS*GEEMK STS*PPPS*PEVWADSR STS*PPPSPEVWADSR ESVGGS*PQTK SSS*LPAYGR DSSVPGS*PSSIVAK
EPS15L1	1.0173	7.5204	5.6410	2.54E-04	5.89E-03	0.6596	Q9UBC2	Epidermal growth factor receptor substrate 15-like 1	TVFPGAVPVLPAS*PPPK STPSHGSVSSLNSTGSLS*PK
FKBP5	2.6927	9.7556	4.9688	6.43E-04	9.84E-03	− 0.3023	Q13451	Peptidyl-prolyl cis-trans isomerase FKBP5	NNEES*PTATVAEQGEDITSK
FLVCR1	− 1.0780	9.4860	− 5.7358	2.24E-04	5.54E-03	0.7898	Q9Y5Y0	Feline leukemia virus subgroup C receptor-related protein 1	AIPADS*PTDQEPK
FOXK1	− 1.0565	7.7540	− 4.9965	6.18E-04	9.66E-03	− 0.2613	P85037	Forkhead box protein K1	EGS*PI*DPEFGSK
GAL	− 8.5314	9.5656	− 12.9818	2.17E-07	1.45E-04	7.6993	P22466	Galanin peptides	LLDLPAAAS*SEDIERS LLDLPAAAS*SEDIERS* LLDLPAAAS*SEDIERS*
GATAD2A	1.0255	8.6559	4.3609	1.58E-03	1.64E-02	− 1.2285	Q86YP4	Transcriptional repressor p66-alpha	RPPS*PDVIVLS*DNEQPS*S*PR
GH1	− 12.5607	10.1374	− 20.6323	2.98E-09	7.99E-06	11.3526	P01241	Somatotropin	FDTNS*HNDDALLK FDT*NSHNDDALLK SVFANSLVYGAS*DSNVYDLLK
GH2	− 11.4395	7.8750	− 30.7801	6.85E-11	5.16E-07	13.8468	P01242	Growth hormone variant	S*HNDDALLK YSFLQNPQT*SLCFSESIPTPSNR
GNAS	− 2.6651	5.5317	− 5.7789	2.11E-04	5.36E-03	0.8486	Q5JWF2	Guanine nucleotide-binding protein G(s) subunit alpha isoforms XLas	ISTAS*GDGR
GPATCH8	1.0279	9.8805	7.4027	2.94E-05	1.96E-03	2.8738	Q9UKJ3	G patch domain-containing protein 8	GSEGDCS*PEDK

Table 4 (continued)

DEG name	logFC	AveExpr	*t*	*P* value	Adjusted *P* value	B	Protein accession ID	Protein name	Phosphopeptide
H1FX	1.2641	10.5253	5.0038	6.11E-04	9.60E-03	− 0.2505	Q92522	Histone H1x	AGGSAALS*PSK
HIST1H1D	2.2738	9.1170	3.4293	6.87E-03	3.96E-02	− 2.7374	P16402	Histone H1.3	GTGASGS*FK KAS*GPPVSELITK
HNRNPA1	− 1.0812	8.4803	− 4.0578	2.51E-03	2.15E-02	− 1.7091	P09651	Heterogeneous nuclear ribonucleoprotein A1	SES*PKEPEQLR
HTATSF1	− 2.5483	13.6709	− 11.7593	5.31E-07	2.15E-04	6.8570	O43719	HIV Tat-specific factor 1	LFEDDDS*NEKLFDEEEDSSEK EFDEDS*DEKEEEEDTYEK ESEDDLNKES*EEEVGPTK LFDEEEDS*S*EKLFDDSDER LFDDS*DER ELHENVLDKELEENDS*ENS*EFEDDGS*EK VFDDES*DEKEDEEYADEK DLDEEGS*EKELHENVLDK LFEES*DDKEDEDADGKEVEDADEK ESS*PEKEAEEGCPEK TEDGGEFEEGAS*ENNAKES*SPEKEAEEGCPEK VLDEEGS*ER ESEEDDSEKES*DEDCSEK
IGFBP5	− 2.6828	10.6639	− 4.1430	2.20E-03	1.99E-02	− 1.5728	P24593	Insulin-like growth factor-binding protein 5	EHEEPT*TSEMAEETYSPK
IPCEF1	1.0260	5.0367	4.7825	8.41E-04	1.15E-02	− 0.5806	Q8WWN9	Interactor protein for cytohesin exchange factors 1	AS*PAPDDTDDTPQELK
ITGA2B	2.0755	7.4627	7.3744	3.04E-05	1.98E-03	2.8416	P08514	Integrin alpha-IIb	AGSEPQALFCS*GVPK
ITPR1	− 1.2600	12.0938	− 5.0407	5.80E-04	9.29E-03	− 0.1962	Q14643	Inositol 1,4,5-trisphosphate receptor type 1	PQKHES*T*SS*Y*NYRVVK
ITPR2	1.8582	7.8515	10.0154	2.22E-06	5.18E-04	5.4714	Q14571	Inositol 1,4,5-trisphosphate receptor type 2	DS*FVEEGNTLRK
KBTBD11	− 3.5584	10.5689	− 4.7908	8.31E-04	1.14E-02	− 0.5681	O94819	Kelch repeat and BTB domain-containing protein 11	AGS*RPQS*PSGDADAR
KIF13B	− 1.0053	12.0356	− 5.8909	1.82E-04	4.94E-03	1.0001	Q9NQT8	Kinesin-like protein KIF13B	SIS*SPNVNR SISS*PNVNR
KIF16B	− 1.3826	8.3241	− 5.2223	4.49E-04	8.02E-03	0.0682	Q96L93	Kinesin-like protein KIF16B	S*KT*T*IT*NLK
KIF1A	1.6590	7.9552	6.7867	5.98E-05	2.74E-03	2.1477	Q12756	Kinesin-like protein KIF1A	SDS*LILDHQWELEK
LIMA1	1.5971	11.6365	8.0040	1.53E-05	1.41E-03	3.5371	Q53GG0; Q9UHB6	LIM domain and actin-binding protein 1	ET**SPGVEDAPIAK
								LIM domain and actin-binding protein 1	QQS*PQEPK ET*S*PGVEDAPIAK EGHSLEMENENLVENGADS*DEDDNSFLK S*QDVELWEGEVVK
MAP4	1.0684	8.1047	4.7053	9.42E-04	1.22E-02	− 0.6974	P27816	Microtubule-associated protein 4	DVT*PPPETEVVLIK VGS*LDNVGHLPAGGAVK

Table 4 (continued)

DEG name	logFC	AveExpr	*t*	*P* value	Adjusted *P* value	B	Protein accession ID	Protein name	Phosphopeptide
									DM#ES*PTKLDVTLAK
									DMESPT*KLDVTLAK
									DMS*PLSETEMALGK
									KCS*LPAEEDSVLEK
									LATNTS*APDLK
MARCKS	− 1.2368	12.4473	− 4.0541	2.53E-03	2.16E-02	− 1.7149	P29966	Myristoylated alanine-rich C-kinase substrate	GEAAAERPGEAAVASS*PSK
									GEAAAERPGEAAVAS*SPSK
									AEDGATPSPSNET*PK
									AEDGATPS*PSNETPK
									AEDGATPSPS*NETPK
									EAPAEGEAAEPGS*PTAAEGEAASAASSTSSPK
									EAPAEGEAAEPGS*PTAAEGEAASAASSTSSPK
									EAPAEGEAAEPGS*PTAAEGEAASAASSTSSPK
									GEPAAAAAPEAGAS*PVEK
MPP2	2.5276	8.8393	8.7985	6.85E-06	8.95E-04	4.3503	Q14168	MAGUK p55 subfamily member 2	TYET*PPPS*PGLDPTFSNQPVPPDAVR
									T*YETPPPS*PGLDPTFSNQPVPPDAVR
MYH14	− 1.1390	8.6919	− 7.3970	2.96E-05	1.97E-03	2.8674	Q7Z406	Myosin-14	LEEGVAS*DEEAEEAQPGSGPSPEPEGSPPAHPQ
NBEAL1	− 1.0097	7.8731	− 4.4773	1.32E-03	1.47E-02	− 1.0471	H7C3C8	Neurobeachin-like protein 1 (Fragment)	SSDQTNYETEGASIQS*RK
NCOA7	− 1.4212	7.9855	− 5.1172	5.21E-04	8.71E-03	− 0.0842	H0UI55	Nuclear receptor coactivator 7	DALPS*PGEWEDLASEK
									VLS*ST*S*EEDEPGVVK
									VLSS*TS*EEDEPGVVK
NDRG1	− 3.0949	12.3453	− 3.9310	3.07E-03	2.42E-02	− 1.9133	Q92597	Protein NDRG1	TASGSS*VTS*LDGTR
NGEF	− 3.0287	7.9883	− 4.7608	8.68E-04	1.17E-02	− 0.6133	Q8N5V2	Ephexin-1	SVPIIS*HS*RWLLK
NPDC1	1.0179	15.1785	5.9750	1.63E-04	4.64E-03	1.1127	Q5SPY9	Neural proliferation differentiation and control protein 1	APGS*PAAPR
									IS*PGDQR
NUP155	1.1429	8.4281	5.2846	4.12E-04	7.62E-03	0.1579	O75694	Nuclear pore complex protein Nup155	AAPQS*PSVPK
									AAPQSPS*VPK
OGFR	− 2.1155	15.1596	− 4.0398	2.59E-03	2.19E-02	− 1.7379	Q9NZT2	Opioid growth factor receptor	SQGDEAGGHGEDRPEPLS*PK
OTUB1	1.4872	9.2341	8.6065	8.28E-06	9.95E-04	4.1600	F5GYJ8	Ubiquitin thioesterase OTUB1	QEPLGSDS*EGVNCLAYDEAIMAQQDR
OXR1	1.1946	5.7526	3.3704	7.57E-03	4.20E-02	− 2.8353	Q8N573	Oxidation resistance protein 1	VVSSTS*EEEEAFTEK
PDLIM4	− 3.5737	9.5064	− 5.5832	2.74E-04	6.13E-03	0.5795	P50479	PDZ and LIM domain protein 4	IHIDPEIQDGS*PTTSR
PEA15	1.1346	10.2397	4.5028	1.27E-03	1.45E-02	− 1.0077	Q15121	Astrocytic phosphoprotein PEA-15	QPS*EEEIIK
PGM5	− 1.0253	5.8422	− 3.2170	9.75E-03	4.94E-02	− 3.0915	Q15124	Phosphoglucomutase-like protein 5	AAGGIILTAS*HCPGGPGGEFGVK
PKM2	1.1738	12.2601	6.1513	1.31E-04	4.15E-03	1.3453	P14618	Pyruvate kinase	LDIDS*PPITAR
PLEC	1.1685	10.5703	3.6270	4.98E-03	3.25E-02	− 2.4100	Q15149	Plectin	SDEGQLS*PATR
									RAS*FAEK
									TQLAS*WSDPTEETGPVAGILDTETLEK
PLXNC1	1.8664	7.1756	5.5181	2.99E-04	6.40E-03	0.4886	O60486	Plexin-C1	KQS*QQLELLESELR
POMC	− 7.4874	13.4887	− 3.8110	3.71E-03	2.70E-02	− 2.1083	P01189	Pro-opiomelanocortin	ACKPDLS*AETPMFPGNGDEQPLTENPR
									REDVS*AGEDCGPLPEGGPEPR

Table 4 (continued)

DEG name	logFC	AveExpr	*t*	*P* value	Adjusted *P* value	B	Protein accession ID	Protein name	Phosphopeptide
									ACKPDLSAET*PM#FPGNGDEQPLTENPR VYPNGAEDES*AEAFPLEFK EGDGPDGPADDGAGAQADLEHS*LLVAAEK S*DGAKPGPR
PRKAR2B	− 1.0157	9.9746	− 3.4835	6.29E-03	3.75E-02	− 2.6473	P31323	cAMP-dependent protein kinase type II-beta regulatory subunit	RAS*VCAEAYNPDEEEDDAESR
PRKCD	1.9942	9.0704	7.0482	4.40E-05	2.33E-03	2.4620	Q05655	Protein kinase C delta type	ASTFCGTPDY*IAPEILQGLK
PRKG1	− 2.0409	5.5427	− 4.3580	1.58E-03	1.65E-02	− 1.2331	Q13976	cGMP-dependent protein kinase 1	T*WTFCGTPEYVAPEIILNK
PXN	1.0331	7.0094	3.5188	5.94E-03	3.61E-02	− 2.5888	P49023	Paxillin	S*SPGGQDEGGFMAQGK TGSSS*PPGGPPKPGSQLDSMLGSLQSDLNK T*GS*SSPPGGPPKPGSQLDSMLGSLQSDLNK T*GSSSPPGGPPKPGSQLDSMLGSLQSDLNK
QSOX2	− 1.2837	6.3713	− 4.1443	2.20E-03	1.99E-02	− 1.5708	Q6ZRP7	Sulfhydryl oxidase 2	DNLLDTYSADQGDS*SEGGTLAR DNLLDTYSADQGDSS*EGGTLAR
RCAN1	− 1.0836	9.4397	− 3.4404	6.75E-03	3.91E-02	− 2.7189	P53805	Calcipressin-1;Calcipressin-3	QFLIS*PPAS*PPVGWK
RRBP1	− 1.3657	10.4681	− 3.9869	2.81E-03	2.30E-02	− 1.8230	Q9P2E9	Ribosome-binding protein 1	NTDVAQS*PEAPK
SCG3	1.2843	10.4326	4.3052	1.72E-03	1.72E-02	− 1.3159	Q8WXD2	Secretogranin-3	ELS*AERPLNEQIAEAEEDKIK LFPAPS*EKSHEETDSTK
SET	− 1.7108	7.9953	− 8.2175	1.23E-05	1.23E-03	3.7624	Q01105	Protein SET	LNEQAS*EEILK
SLC2A4	− 1.3065	5.1362	− 4.4148	1.45E-03	1.56E-02	− 1.1444	P14672	Solute carrier family 2, facilitated glucose transporter member 4	T*PSLLEQEVKPSTELEYLGPDEND
SLC46A1	− 1.1586	7.9882	− 4.9777	6.35E-04	9.78E-03	− 0.2891	A0A024QZ15	Proton-coupled folate transporter	AD*LEFQQFPQS*P
SLC7A14	− 1.3388	10.1699	− 4.9424	6.68E-04	1.01E-02	− 0.3414	Q8TBB6	Probable cationic amino acid transporter	EACS*PVS*EGDEFSGPATNTCGAK
SLC8A2	2.0827	10.6502	5.7643	2.15E-04	5.42E-03	0.8287	Q9UPR5	Sodium/calcium exchanger 2	GIS*ALLLNQGDGDR
SMARCA2	− 1.0693	9.4559	− 3.2347	9.47E-03	4.85E-02	− 3.0619	P51531	Probable global transcription activator SNF2L2	AKPVVS*DFDS*DEEQDER
SNAP23	1.0040	6.7468	4.8842	7.26E-04	1.05E-02	− 0.4280	O00161	Synaptosomal-associated protein; synaptosomal-associated protein 23	TTWGDGGENS*PCNVVSK
SNX17	1.1624	8.6272	4.3682	1.56E-03	1.63E-02	− 1.2171	Q15036	Sorting nexin-17	VTSSVPLPSGSTSS*PGR VTSSVPLPS*GS*T*S*S*PGR
SORBS2	− 2.2906	6.9395	− 3.2557	9.15E-03	4.75E-02	− 3.0267	O94875	Sorbin and SH3 domain-containing protein 2	QNAEIWSS*T*EET*VS*PKIK
SORT1	1.0872	11.4517	5.0676	5.58E-04	9.09E-03	− 0.1567	Q99523	Sortilin	SGYHDDS*DEDLLE
SPAG9	1.1290	9.1942	3.9292	3.08E-03	2.42E-02	− 1.9163	O60271	C-Jun-amino-terminal kinase-interacting protein 4	SAS*QS*SLDKLDQELK SAS*QS*S*LDKLDQELK
SPARCL1	− 3.1871	13.6134	− 4.7627	8.66E-04	1.17E-02	− 0.6103	Q14515	SPARC-like protein 1	EES*HEQS*AEQGK SSS*QELGLK SKEES*HEQS*AEQGK

Table 4 (continued)

DEG name	logFC	AveExpr	*t*	*P* value	Adjusted *P* value	B	Protein accession ID	Protein name	Phosphopeptide
									EHANS*KQEEDNTQSDDIL EESDQPTQVSK
									HIQETEWQS*QEGK
									DQGNQEQDPNIS *NGEEEEEKEPGEVGTHNDNQER
									EHANS*KQEEDNT*QS *DDILEESDQPTQVSK
									S*KEES*HEQSAEQGK
SPTB	1.0905	6.8402	3.9457	3.00E-03	2.38E-02	− 1.8895	P11277	Spectrin beta chain, erythrocyte	LS*S*S*WESLQPEPSHPY
									WDAPDDELDNDNSS*AR
									LSS*S*WESLQPEPSHPY
									LSSS*WES*LQPEPSHPY
									VLS*PVDSGNK
SRRM2	1.1850	7.1163	6.1599	1.29E-04	4.14E-03	1.3566	Q9UQ35	Serine/arginine repetitive matrix protein 2	TS*PPLLDR
									EISS*S*PTSK
									RPS*PQPS*PR
									SGMS*PEQSR
									SST*PPRQS*PSR
									S*S*T*PPRQSPSR
									SS*RSSPELTR
									S*RS*PLAIR
									ENSFGS*PLEFR
									EIS*SS*PTSK
									S*S*RS*SPELTR
									T*SPPLLDR
									S*RS*PATAK
									SCFES*S*PDPELK
									SLS*YS*PVER
									VPS*PTPAPK
									GEFSAS*PMLK
									SGS*S*PGLR
									QGSITS*PQANEQSVT*PQRR
									AQT*PPGPSLSGSKS*PCPQEK
									SATRPS*PS*PER
									S*RT*PPVTR
									GDS*RS*PSHK
									S*PS*PASGR
									S*SSPVTELASRS*PIR
									S*VS*PCSNVESR
									S*LS*GSSPCPK
									AQT*PPGPSLSGS*KSPCPQEK
									SS*SPVTELASR
									S*RS*PSSPELNNK
									RGEGDAPFSEPGTTSTQRPS*S*PETATK

Table 4 (continued)

DEG name	logFC	AveExpr	*t*	*P* value	Adjusted *P* value	B	Protein accession ID	Protein name	Phosphopeptide
									SSS*PVTELASR GRS*ECDS*S*PEPK AQT*PPGPSLS*GSKSPCPQEK EISSSPT*SK ERS*GS*ESSVDQK GQSQT*SPDHR HGGS*PQPLATTPLSQEPVNPPSEAS*PT*R HGGS*PQPLATTPLSQEPVNPPS*EASPTR MALPPQEDAT*ASPPR QSHSES*PSLQSK RGEGDAPFSEPGT*T*S*T*QRPS*S*PETATK RGEGDAPFSEPGT*T*S*T*QRPS*S*PETATK S*DTSSPEVR S*GS*S*QELDVKPS*AS*PQER S*SS*PVTELASR
SSBP3	1.2570	7.2589	4.6141	1.08E-03	1.32E-02	− 0.8364	Q9BWW4	Single-stranded DNA-binding protein 3	NS*PNNISGISNPPGTPR
STIM1	1.0481	9.8564	4.9079	7.01E-04	1.03E-02	− 0.3927	Q13586	Stromal interaction molecule 1	AEQS*LHDLQER
STK39	1.4339	11.9102	6.9767	4.79E-05	2.42E-03	2.3769	Q9UEW8	STE20/SPS1-related proline-alanine-rich protein kinase	TEDGDWEWS*DDEMDEK
STX1A	1.8823	8.2932	5.5539	2.85E-04	6.25E-03	0.5386	Q16623	Syntaxin-1A	TAKDS*DDDDDVAVTVDR
STXBP5L	1.5925	9.9115	4.8616	7.50E-04	1.07E-02	− 0.4617	Q9Y2K9	Syntaxin-binding protein 5-like	SS*SISS*IDKDSK
SYN1	− 1.0498	11.9626	− 5.4376	3.34E-04	6.79E-03	0.3755	P17600	Synapsin-1	PVAGGPGAPPAARPPAS*PS*PQR
TCEA1	− 1.0289	8.8480	− 4.2602	1.84E-03	1.79E-02	− 1.3868	P23193	Transcription elongation factor A protein 1	EPAITSQNS*PEAR
TCF12	− 1.1897	9.1467	− 3.9273	3.09E-03	2.42E-02	− 1.9193	A0A024R5Z0	Transcription factor 12	T*S*ST*NEDEDLNPEQK
TLN2	1.5289	7.8000	4.3424	1.62E-03	1.67E-02	− 1.2575	Q9Y4G6	Talin-2	LDEGT*PPEPK
TNKS1BP1	1.0225	7.5659	4.1437	2.20E-03	1.99E-02	− 1.5717	Q9C0C2	182 kDa tankyrase-1-binding protein	AS*PEPPGPESSSR VPS*S*DEEVVEEPQSR GWS*QEGPVK LDS*PPPSPITEASEAAEAAEAGNLAVSSR LDS*PPPSPITEASEAAEAAEAGNLAVSSR
TPI1	1.7746	10.1649	6.8527	5.53E-05	2.64E-03	2.2279	P60174	Triosephosphate isomerase	KQS*LGELIGTLNAAK IIYGGS*VTGATCK
TPMT	1.0815	6.1567	4.4016	1.48E-03	1.58E-02	− 1.1650	P51580	Thiopurine S-methyltransferase	TSLDIEEYS*DTEVQK
TRIM3	1.4660	5.4120	4.1545	2.16E-03	1.97E-02	− 1.5544	O75382	Tripartite motif-containing protein 3	REDS*PGPEVQPMDK
TSC2	2.1795	10.7866	6.3857	9.73E-05	3.49E-03	1.6479	P49815	Tuberin	S*SSSPELQTLQDILGDPGDK
USP24	1.3950	11.1223	9.0626	5.31E-06	7.86E-04	4.6057	Q9UPU5	Ubiquitin carboxyl-terminal hydrolase 24	VSDQNS*PVLPK
WBP4	1.0929	7.4877	4.0214	2.66E-03	2.23E-02	− 1.7675	O75554	WW domain-binding protein 4	NSDGGS*DPETQK

Table 4 (continued)

DEG name	Phosphorylated amino acid residue	Phosphorylated position	Phosphorylated probabilities	PEP	Score	Phosphorylated level (N)	Phosphorylated level (T)	Ratio (T/N)	*P* value (*t* test)
ABCA2	S; S	1327; 1331	1; 1	3.62E-06	92	10,518	32,589	3.10	1.60E-04
ACACA	S	29	1	3.35E-32	154	2551	7604	2.98	6.08E-05
	S; S	25; 29	0.82; 0.892	7.89E-07	54				
ADD2	S	613; 617	0.885; 0.981	1.79E-04	88	11,989	36,075	3.01	1.28E-05
	S	613; 617	0.877; 1	1.79E-04	88	11,989	36,075	3.01	1.28E-05
	S	592	1	8.36E-06	84	14,454	20,046	1.39	9.74E-04
	S; S	596; 600	1; 1	8.36E-06	70	1895	3649	1.93	1.08E-03
	T	611	0.998	1.24E-02	52				
	S; S	599; 604	0.998; 1	4.07E-03	94				
ADD3	S; S; S	677; 681; 683	0.993; 0.498; 0.498	4.80E-10	105	17,730	41,658	2.35	1.10E-04
	S; S	677; 679	0.906; 0.548	6.72E-04	69	10,380	17,649	1.70	1.34E-04
	S; S	673; 677	1; 0.986	3.87E-04	72				
	S; S; S	677; 681; 683	0.993; 0.498; 0.498	4.80E-10	105				
	S	677; 681	0.522; 0.761	4.80E-10	105				
AKAP12	T	597	0.932	7.78E-31	146	4946	11,387	2.30	9.59E-05
	S	1331	0.999	4.18E-03	91	6418	4875	0.76	2.79E-04
	S	483	1	1.91E-22	135	25,062	14,371	0.57	4.98E-04
	S	598	0.847	7.54E-39	156	15,714	22,991	1.46	1.77E-03
	S	1587	1	1.69E-145	133	4482	8736	1.95	2.36E-03
	S; S; S	696; 697; 698	1; 1; 1	1.42E-03	87	52,712	37,364	0.71	3.64E-03
	T; S	1717; 1720	0.221; 0.221	7.03E-11	68				
	S	1395	0.927	1.21E-12	58				
	T; S	285; 286	0.749; 0.749	3.61E-04	50				
	T	1116	0.956	1.48E-02	84				
AKT1	S; S	122; 124	0.457; 0.457	1.16E-07	92				
ALB	S	82	1	1.24E-47	197	114,813	84,746	0.74	3.24E-04
ALDOA	S	36	0.97	2.14E-30	166				
	T	37	0.555	7.28E-05	95				
	S	39	0.983	1.65E-30	168				
	S	46	0.994	1.17E-03	66				
ANAPC1	S	688	0.839	1.86E-02	40				
ANK1	S	781	1	4.25E-15	146	47,985	171,943	3.58	4.13E-06
	S	1428	1	1.62E-03	107	7814	13,457	1.72	1.74E-05
	T	961	0.979	1.29E-08	106	18,331	29,532	1.61	4.31E-04

Table 4 (continued)

DEG name	Phosphorylated amino acid residue	Phosphorylated position	Phosphorylated probabilities	PEP	Score	Phosphorylated level (N)	Phosphorylated level (T)	Ratio (T/N)	*P* value (*t* test)
	S; T	960; 961	0.5; 0.5	1.29E-08	105	10,530	17,926	1.70	5.29E-04
	S	1607	1	1.17E-03	105	10,600	8027	0.76	3.19E-03
	T	1684	0.745	2.33E-02	51				
	S	1686	0.962	8.25E-04	76				
	S; T	1686; 1688	0.327; 0.327	2.14E-02	47				
AP3B1	S	276	1	1.03E-45	117	22,634	68,527	3.03	2.37E-05
APIP	S	87	0.962	4.65E-03	81				
APOL1	S; S	352; 355	1; 1	2.53E-03	59	6305	4500	0.71	5.33E-03
ARHGEF11	S; T	663; 668	1; 1	1.93E-10	106	12,686	29,402	2.32	4.24E-04
	S	1295	1	6.04E-03	52	7700	11,195	1.45	1.11E-03
	S	1155	1	3.31E-47	146	1696	3062	1.81	1.02E-02
	S; S	1478; 1480	0.48; 0.48	2.20E-03	38				
ARHGEF12	S	309	1	1.82E-10	109	8015	23,551	2.94	9.07E-04
ARHGEF6	S	684	1	1.39E-10	126				
ASAP1	S	717	1	1.20E-107	116	4217	8616	2.04	1.35E-04
ASAP2	S	701	1	2.71E-52	185	11,289	17,685	1.57	2.02E-03
ATP8A1	S; T; S	25; 28; 29	0.966; 0.502; 0.502	5.82E-03	57	5114	8707	1.70	3.09E-05
	S; T	25; 28	0.764; 0.563	2.73E-03	62	5114	8707	1.70	3.09E-05
	S	29	0.767	2.73E-03	63	5114	8707	1.70	3.09E-05
AVP	S	83	0.996	1.57E-03	69	6536	4234	0.65	8.03E-03
BAIAP3	S	113	0.528	4.57E-03	58	10,732	21,332	1.99	6.38E-04
	S	115	0.981	1.52E-16	133	1866	3885	2.08	3.13E-03
BASP1	S	164	0.996	8.79E-03	42	7903	10,069	1.27	1.46E-02
	T	36	1	4.87E-24	90				
	S; S; T	194; 195; 196	0.333; 0.333; 0.333	1.91E-03	61				
	T	196	0.683	3.52E-06	63				
BCLAF1	S	177	1	8.49E-31	158	84,318	208,327	2.47	2.02E-07
	S	385	1	5.55E-93	218	31,132	135,860	4.36	4.16E-07
	S	512	1	8.04E-16	107	9441	20,570	2.18	3.11E-06
	S	496	1	1.35E-19	173	70,549	155,420	2.20	2.09E-05
	S	397; 402	1; 1	3.19E-129	256	44,945	69,960	1.56	2.82E-05
	T	494	0.567	2.69E-02	43	4370	8650	1.98	1.10E-04
	S	648	1	9.96E-03	65	797	2439	3.06	2.65E-04

Table 4 (continued)

DEG name	Phosphorylated amino acid residue	Phosphorylated position	Phosphorylated probabilities	PEP	Score	Phosphorylated level (N)	Phosphorylated level (T)	Ratio (T/N)	*P* value (*t* test)
	S	285	0.907	2.15E-31	167	23,981	39,296	1.64	3.62E-04
	S; S	287; 290	0.908; 0.999	2.15E-31	167	20,077	36,892	1.84	4.90E-04
	S	658	0.995	2.86E-13	162	36,901	49,609	1.34	8.48E-04
	S	222	0.998	9.35E-121	119	16,902	13,214	0.78	7.70E-03
	S	198	0.98	2.82E-35	94				
	S	217	0.528	3.48E-29	76				
CALD1	S	207	1	1.37E-06	119	98,098	323,267	3.30	2.31E-06
CASC4	S	366	1	1.16E-03	73				
CASK	S; S	570; 571	0.78; 0.739	5.24E-05	88	3606	7644	2.12	3.28E-04
	S	569	0.379	8.01E-16	79				
CBX8	S	190	0.513	2.77E-04	83				
CCDC48	S	480	0.841	1.19E-21	150	3504	2952	0.84	1.04E-01
	T	476	0.504	2.94E-11	136				
CCDC86	S	91	1	8.60E-16	91	11,730	18,273	1.56	5.06E-03
	S	18	0.998	1.72E-03	61	9461	12,076	1.28	1.46E-02
	S	47	0.988	8.54E-17	121				
CDC42EP4	S	292	0.789	6.03E-10	41				
CDK14	S	95	1	1.18E-02	75	2416	3471	1.44	5.63E-03
CENPA	S; S	17; 19	0.998; 0.984	7.74E-04	68	2107	18,118	8.60	3.01E-06
CHD3	S; S	712; 713	0.481; 0.481	1.47E-02	50				
CHGA	S; S	322; 333	1; 1	1.06E-26	183	296,230	566,530	1.91	4.87E-05
	S; S	322; 333	1; 1	1.06E-26	147	207,873	320,807	1.54	2.39E-04
	S; S	112; 113	1; 1	0.00E+00	287	320,767	437,363	1.36	8.38E-04
	S	207	1	3.51E-32	154	7755	9573	1.23	1.97E-03
	S	300	1	1.45E-131	233	280,203	169,087	0.60	2.61E-03
	S	142	1	2.90E-55	180	437,597	568,253	1.30	3.19E-03
	S	125	0.567	2.10E-05	93	18,890	23,102	1.22	7.15E-03
	S	126	0.873	1.02E-07	120	20,108	27,926	1.39	1.99E-02
	S	136	1	7.15E-06	108	126,907	149,643	1.18	3.08E-02
	S	203	1	3.97E-102	225	63,186	74,743	1.18	4.94E-02
	S; S; S	397; 398; 402	0.543; 0.543; 0.914	8.64E-27	145	38,199	34,450	0.90	6.23E-02
	S	370	0.989	3.96E-61	200	119,240	151,717	1.27	6.51E-02
	S	402	1	1.44E-38	185	123,567	116,303	0.94	7.89E-02

Table 4 (continued)

DEG name	Phosphorylated amino acid residue	Phosphorylated position	Phosphorylated probabilities	PEP	Score	Phosphorylated level (N)	Phosphorylated level (T)	Ratio (T/N)	*P* value (*t* test)
	S	218	1	2.58E-25	180	37,874	34,815	0.92	1.12E-01
	S; S	105; 112	0.8261	3.88E-90	99	2083	2441	1.17	1.58E-01
	S	438	0.98	3.04E-120	119	11,305	10,366	0.92	2.55E-01
	S; S	396; 402	0.731; 0.99	8.64E-27	145	67,782	66,289	0.98	4.30E-01
	S	98; 112	0.686; 0.843	3.26E-34	67				
	S	436	0.997	1.77E-167	127				
CHGB	S	225	1	4.87E-30	175	194,330	26,293	0.14	6.87E-07
	S	367	1	1.70E-07	146	85,298	10,118	0.12	7.46E-07
	S	335	1	5.81E-71	223	553,550	73,696	0.13	2.05E-06
	S; S; S	236; 239; 245	0.531; 1; 0.965	4.20E-73	205	248,397	14,007	0.06	3.67E-06
	S; S	146; 149	0.999; 0.999	1.30E-150	236	321,833	101,210	0.31	5.28E-06
	T	243	0.978	1.47E-45	161	143,047	2755	0.02	5.36E-06
	S; S	182; 183	1; 1	1.80E-03	100	80,795	13,041	0.16	7.03E-06
	S; Y	335; 341	1; 1	2.35E-06	98	220,190	39,598	0.18	8.29E-06
	S; S	239; 245	0.992; 1	4.20E-73	205	407,313	23,721	0.06	1.01E-05
	S	160	1	1.77E-17	140	50,520	12,595	0.25	1.17E-05
	S	626	1	1.85E-99	214	339,777	89,045	0.26	1.18E-05
	S	259; 263; 272	1; 1; 0.857	1.51E-53	157	260,217	35,935	0.14	1.23E-05
	S	298	0.981	3.28E-14	142	88,621	25,139	0.28	1.31E-05
	S	98	0.966	1.32E-30	169	16,941	1615	0.10	1.41E-05
	S	391	1	1.30E-04	112	209,063	29,849	0.14	1.44E-05
	S; S	144; 146	0.941; 0.751	3.58E-98	136	19,345	10,016	0.52	1.53E-05
	S; S; T	237; 239; 243	0.819; 0.935; 0.598	1.47E-45	161	227,790	11,221	0.05	1.53E-05
	S	301	0.999	5.51E-20	128	85,508	21,593	0.25	1.88E-05
	S	617	1	8.30E-152	246	312,090	68,957	0.22	2.13E-05
	Y	624	0.995	8.86E-43	152	68,357	15,724	0.23	2.23E-05
	T	271	0.973	1.38E-88	219	322,700	69,163	0.21	2.23E-05
	Y; S	401; 405	1; 1	2.41E-02	51	7666	1759	0.23	2.34E-05
	S	149	1	2.83E-147	264	584,753	166,957	0.29	2.80E-05
	S; S	377; 380	1; 1	4.73E-42	181	945,707	144,227	0.15	3.27E-05
	S; S	626; 631	0.996; 0.863	3.45E-35	140	84,147	25,399	0.30	3.33E-05
	S	294	0.807	3.74E-09	133	23,609	5551	0.24	3.77E-05
	S	293	0.992	1.97E-30	180	104,456	26,549	0.25	4.48E-05

Table 4 (continued)

DEG name	Phosphorylated amino acid residue	Phosphorylated position	Phosphorylated probabilities	PEP	Score	Phosphorylated level (N)	Phosphorylated level (T)	Ratio (T/N)	*P* value (*t* test)
	S	311	1	6.58E-209	232	930,043	206,513	0.22	5.91E-05
	S; T	631; 632	0.591; 0.586	3.45E-35	124	22,832	7174	0.31	5.94E-05
	S; S; S; T; S	235; 236; 239; 243; 245	0.643; 0.589; 0.589; 0.589; 0.589	1.47E-45	161	146,517	7750	0.05	7.50E-05
	T	492	1	6.83E-05	85	92,934	34,420	0.37	9.99E-05
	S	317	0.988	1.45E-59	184	150,487	43,938	0.29	1.70E-04
	Y; S	142; 149	0.981; 0.96	6.42E-108	134	22,916	11,918	0.52	1.87E-04
	S; S; S	314; 320; 323	0.739; 1; 1	1.83E-50	161	57,813	21,261	0.37	4.40E-04
	S	130	1	4.86E-03	80	1039	214	0.21	5.96E-04
	S; S; S	314; 317; 320	0.959; 0.959; 0.959	8.63E-27	145	41,766	12,932	0.31	6.63E-04
	S	46	1	3.06E-04	94	994	401	0.40	1.63E-02
	S; T; Y	329; 330; 341	0.355; 0.355; 0.98	1.56E-02	43				
	S; S	99; 100	0.651; 0.651	8.57E-07	62				
	S	93	0.989	5.88E-05	88				
	S	217	0.757	1.02E-02	78				
CHMP2B	S	199	1	3.83E-06	121	11,233	17,076	1.52	6.05E-03
CIC	S; S	2303; 2315	0.697; 0.741	2.08E-04	75				
	S	2304; 2315	0.563; 0.831	2.08E-04	75				
	S; S	2152; 2153	0.5; 0.5	1.43E-02	49				
	S	2153	0.795	1.43E-02	49				
CLASP2	T	594	0.618	2.50E-06	99	7092	16,081	2.27	2.64E-04
	S	596	0.848	7.26E-05	57				
CTAGE5	S	536	0.954	4.01E-03	54	5494	8403	1.53	1.09E-03
	S; S	594; 596	0.962; 0.997	2.71E-03	51	2316	3679	1.59	2.24E-03
	S; S	137; 139	0.5; 0.5	8.61E-34	89	2602	3220	1.24	3.50E-02
	S	139	0.861	8.61E-34	89	2602	3220	1.24	3.50E-02
	S	647	1	1.79E-02	59				
CYBRD1	Y	252	0.662	1.47E-02	49				
DCLK1	S	337	0.911	9.87E-04	71				
	S	364	0.807	1.08E-03	48				
DENR	S	73	1	4.03E-03	61				
DMXL2	S	2640	1	3.59E-05	79				
	S	2399	0.839	2.63E-04	58				
DOCK11	T; S; S	294; 295; 296	0.333; 0.333; 0.333	1.02E-02	45				

Table 4 (continued)

DEG name	Phosphorylated amino acid residue	Phosphorylated position	Phosphorylated probabilities	PEP	Score	Phosphorylated level (N)	Phosphorylated level (T)	Ratio (T/N)	*P* value (*t* test)
DOCK7	S; T	900; 909	0.9; 0.402	2.45E-06	47	1576	2651	1.68	9.54E-03
ELAVL4	S	33	0.999	4.54E-04	80	6680	11,145	1.67	9.07E-04
EPB41L2	S	715	0.607	1.49E-02	56	4934	9864	2.00	7.50E-05
	S	87	1	5.02E-03	99	9974	25,384	2.54	1.55E-04
	S	718	0.971	9.87E-03	81	4771	9142	1.92	4.81E-03
	S; S	38; 39	0.5; 0.5	1.38E-02	50				
	S	39	0.88	3.99E-81	111				
EPB49	S	333	1	4.66E-15	152	21,088	48,603	2.30	2.12E-05
	S	226	1	2.45E-73	205	66,329	117,453	1.77	1.15E-04
	S; S	92; 96	0.734; 0.978	2.86E-03	56	4181	9523	2.28	3.97E-04
	S	92	0.994	4.97E-08	103	27,533	42,218	1.53	5.58E-04
	S	156	1	6.79E-03	92	2009	4972	2.47	1.18E-03
	S	289	0.998	3.78E-05	134	8120	15,700	1.93	1.35E-03
	S	26	0.927	5.87E-04	69				
EPS15L1	S	229	1	1.50E-12	79	1597	2107	1.32	8.98E-02
	S	255	0.759	1.29E-04	79				
FKBP5	S	13	0.91	9.79E-06	43				
FLVCR1	S	536	0.965	5.83E-04	83	5787	10,532	1.82	2.55E-04
FOXK1	S	445	1	1.27E-06	87	3949	9911	2.51	1.37E-03
GAL	S	116	0.991	1.09E-82	227	161,450	28,762	0.18	1.20E-06
	S; S; S	116; 117; 123	0.658; 0.658; 0.684	3.21E-10	98	11,171	6908	0.62	4.26E-03
	S	116; 123	0.878; 0.716	2.09E-04	74	11,171	6908	0.62	4.26E-03
GATAD2A	S	100; 107; 113; 114	1; 0.87; 0.581; 0.548	3.91E-07	52				
GH1	S	176	1	3.20E-216	194	580,220	43,527	0.08	1.93E-06
	T	174	0.578	1.80E-03	70				
	S; S	132; 134	0.428; 0.428	1.85E-10	51				
GH2	S	176	1	6.34E-05	131				
	T; S	76; 77	0.481; 0.481	1.63E-02	37				
GNAS	S	995	1	1.21E-04	115	11,879	32,931	2.77	2.32E-05
GPATCH8	S	1081	1	1.74E-02	60	2087	4025	1.93	5.01E-03
H1FX	S	31	0.996	1.62E-02	80	5113	13,633	2.67	4.62E-05
HIST1H1D	S	105	0.969	7.22E-03	74	5296	22,242	4.20	8.93E-06
	S	37	1	3.45E-10	128	57,689	15,516	0.27	2.58E-04

Table 4 (continued)

DEG name	Phosphorylated amino acid residue	Phosphorylated position	Phosphorylated probabilities	PEP	Score	Phosphorylated level (N)	Phosphorylated level (T)	Ratio (T/N)	*P* value (*t* test)
HNRNPA1	S	6	1	1.83E-13	144	59,421	186,063	3.13	7.49E-06
HTATSF1	S	702	1	2.14E-175	268	288,110	160,883	0.56	1.95E-04
	S	624	1	1.72E-69	202	204,193	125,980	0.62	2.23E-04
	S	529	1	1.68E-56	192	88,307	60,457	0.68	2.99E-04
	S; S	713; 714	1; 1	1.56E-26	142	44,719	23,576	0.53	4.06E-04
	S	721	1	2.71E-03	131	34,573	22,836	0.66	1.16E-03
	S; S; S	597; 600; 607	1; 1; 1	1.27E-106	208	20,769	11,906	0.57	2.31E-03
	S	642	1	1.66E-199	294	239,173	191,277	0.80	5.55E-03
	S	579	1	3.61E-80	210	202,810	176,810	0.87	3.93E-02
	S	676	1	7.74E-152	254	366,127	394,907	1.08	1.47E-01
	S	453	0.989	1.37E-31	165	93,516	101,601	1.09	2.04E-01
	S; S	445; 452	0.704; 0.857	8.12E-04	56	15,981	14,532	0.91	3.02E-01
	S	616	1	1.23E-04	117	11,426	11,535	1.01	9.22E-01
	S	548	0.997	4.34E-04	69				
IGFBP5	T	123	0.346	2.19E-04	56				
IPCEF1	S	411	1	6.48E-10	113	2761	8305	3.01	4.03E-05
ITGA2B	S	880	0.996	2.38E-03	60				
ITPR1	S; T; S; S; Y; Y	1177; 1178; 1180; 1181; 1183	0.843; 0.855; 0.896; 0.55; 0.55	2.27E-02	37				
ITPR2	S	1687	0.966	8.73E-03	44	125,980	84,783	0.67	2.20E-03
KBTBD11	S; S	310; 314	0.989; 0.838	1.26E-03	57	2029	5855	2.89	1.34E-04
KIF13B	S	1381	0.98	5.62E-03	78	6201	20,094	3.24	4.31E-05
	S	1382	0.654	7.49E-03	74				
KIF16B	S; T; T; T	31; 33; 34; 36	0.25; 0.25; 0.25; 0.25	2.62E-02	47				
KIF1A	S	1370	0.98	1.89E-33	131	20,803	21,162	1.02	9.30E-01
LIMA1	T	487	0.577	5.99E-04	75	2533	3843	1.52	2.94E-02
	S	698	1	9.90E-03	79	4890	18,709	3.83	1.00E-05
	S	490	0.983	1.43E-10	119	6800	11,621	1.71	3.83E-05
	S	686	1	0.00E+00	141	3725	5941	1.59	1.17E-02
	S	726	1	2.48E-04	57				
MAP4	T	521	1	3.18E-40	153	66,008	110,437	1.67	1.71E-04
	S	1073	1	6.49E-06	91	11,125	28,354	2.55	2.17E-04
	S	280	0.981	5.00E-05	82	30,879	33,386	1.08	1.59E-01
	T	282	0.605	7.94E-06	109				

Table 4 (continued)

DEG name	Phosphorylated amino acid residue	Phosphorylated position	Phosphorylated probabilities	PEP	Score	Phosphorylated level (N)	Phosphorylated level (T)	Ratio (T/N)	*P* value (*t* test)
	S	507	0.999	8.64E-07	115				
	S	636	1	8.51E-06	77				
	S	928	0.975	1.89E-03	105				
MARCKS	S	27	0.96	1.32E-26	143	9538	82,612	8.66	3.86E-06
	S	26	0.878	8.86E-22	126	10,104	57,201	5.66	8.79E-06
	T	150	0.998	2.15E-16	140	7219	27,996	3.88	1.52E-05
	S	145	0.959	1.58E-04	79	2120	3439	1.62	8.15E-03
	S	147	0.936	5.11E-04	73				
	S; T	118; 120	0.499; 0.499	2.84E-58	66				
	S; T; S	128; 130; 138	0.323; 0.323; 0.323	3.44E-05	53				
	S; T	118; 120	0.499; 0.499	2.84E-58	66				
	S	101	1	7.07E-58	115				
MPP2	T; S	141; 145	0.833; 0.998	1.77E-68	80	4500	5589	1.24	1.22E-03
	T; S	138; 145	0.537; 0.988	6.46E-35	63				
MYH14	S	1969	1	5.84E-67	84	249	413	1.66	2.86E-01
NBEAL1	S	24	0.805	1.12E-02	35				
NCOA7	S	295	0.99	3.21E-03	45				
	S; T; S	208; 210; 211	0.87; 0.475; 0.475	6.29E-06	61				
	S; S	209; 211	0.77; 0.849	1.45E-04	79				
NDRG1	S; S	333; 336	0.728; 0.85	1.03E-02	50	3618	7439	2.06	3.36E-04
NGEF	S; S	485; 487	0.914; 0.914	1.29E-02	44	12,102	18,559	1.53	1.83E-03
NPDC1	S	307	1	9.47E-04	96	4714	20,392	4.33	4.33E-05
	S	314	1	1.93E-02	86	4139	5242	1.27	4.50E-02
NUP155	S	992	0.997	5.58E-06	120	6885	16,363	2.38	7.92E-05
	S	994	0.602	5.58E-06	120	6885	16,363	2.38	7.92E-05
OGFR	S	378	1	7.10E-04	61				
OTUB1	S	18	0.48	7.04E-03	34				
OXR1	S	204	0.889	2.36E-07	100				
PDLIM4	S	112	0.923	3.16E-04	75	9266	15,989	1.73	2.03E-03
PEA15	S	116	1	8.87E-06	138	18,264	123,410	6.76	1.32E-05
PGM5	S	122	0.54	2.66E-64	85				
PKM2	S	37	0.912	1.63E-02	47				
PLEC	S	720	0.995	1.49E-02	82	6049	13,023	2.15	3.16E-04

Table 4 (continued)

DEG name	Phosphorylated amino acid residue	Phosphorylated position	Phosphorylated probabilities	PEP	Score	Phosphorylated level (N)	Phosphorylated level (T)	Ratio (T/N)	*P* value (*t* test)
	S	1721	1	1.18E-02	55	3016	5604	1.86	9.12E-04
	S	4406	0.909	1.61E-15	97				
PLXNC1	S	978	1	3.76E-03	47	2450	4156	1.70	3.71E-03
POMC	S	55	0.997	1.64E-56	167	499,933	41,941	0.08	7.79E-07
	S	108	1	7.15E-166	277	379,447	90,008	0.24	3.01E-06
	T	58	0.759	1.26E-45	159	75,285	1928	0.03	8.83E-06
	S	168	1	3.56E-34	127	17,243	8453	0.49	8.78E-04
	S	208	1	1.38E-05	58				
	S	125	1	1.04E-02	54				
PRKAR2B	S	114	1	4.14E-31	139	37,944	26,707	0.70	6.75E-04
PRKCD	Y	514	0.511	4.36E-02	33				
PRKG1	T	515	0.543	4.49E-15	123				
PXN	S; S	302; 303	0.5; 0.5	1.30E-03	55	1185	1696	1.43	2.16E-02
	S	322	0.702	5.72E-19	89	4056	7646	1.88	4.60E-02
	T; S	318; 320	0.259; 0.259	4.20E-06	54				
	T	318	0.291	4.31E-19	96				
QSOX2	S	578	0.821	1.21E-12	81				
	S	579	0.556	5.21E-33	72				
RCAN1	S; S	163; 167	1; 1	1.21E-25	100	5957	12,269	2.06	1.21E-03
RRBP1	S	615	0.996	3.41E-04	55				
SCG3	S	37	1	2.80E-38	149	54,239	25,082	0.46	1.50E-04
	S	359	0.468	1.85E-02	36				
SET	S	63	1	1.18E-16	87				
SLC2A4	T; S	486; 488	0.5; 0.5	1.85E-10	91				
SLC46A1	S	458	1	1.60E-05	107	19,669	26,410	1.34	4.09E-02
SLC7A14	S	465; 468	0.998; 0.939	1.03E-05	67				
SLC8A2	S	622	1	7.55E-34	97	1039	1666	1.60	1.40E-01
SMARCA2	S	1568; 1572	1; 1	3.09E-10	108	8702	21,740	2.50	1.06E-05
SNAP23	S	110	1	3.54E-04	83	5323	11,357	2.13	6.07E-04
SNX17	S	336	0.658	4.46E-05	89	5947	11,510	1.94	1.05E-03
	S; S; T; S; S	331; 333; 334; 335; 336	0.2; 0.2; 0.2; 0.2; 0.2	1.79E-03	67				
SORBS2	S; T; T; S	370; 371; 374; 376	0.238; 0.238; 0.238; 0.238	1.88E-02	34				
SORT1	S	825	0.999	1.99E-04	99	4842	5538	1.14	1.42E-01

Table 4 (continued)

DEG name	Phosphorylated amino acid residue	Phosphorylated position	Phosphorylated probabilities	PEP	Score	Phosphorylated level (N)	Phosphorylated level (T)	Ratio (T/N)	*P* value (*t* test)
SPAG9	S; S	730; 732	0.834; 0.554	2.29E-17	145	21,879	108,870	4.98	2.23E-07
	S	730; 732; 733	0.577; 0.507; 0.91	5.14E-44	145	11,070	44,110	3.98	4.65E-06
SPARCL1	S	80		9.37E-38	176	44,342	10,604	0.24	1.86E-05
	S	92	0.999	1.61E-28	188	100,790	28,141	0.28	1.91E-05
	S; S	80; 84	0.999; 1	9.37E-38	176	57,751	20,002	0.35	5.38E-05
	S	231	1	5.61E-70	176	20,394	7396	0.36	5.25E-04
	S	295	1	2.83E-21	152	24,777	14,058	0.57	1.15E-03
	S	198	0.997	1.10E-05	53	2334	2083	0.89	1.92E-01
	S; T; S	231; 238; 240	0.331; 0.331; 0.331	1.44E-02	38				
	S; S	76; 80	0.999; 0.995	7.77E-05	77				
SPTB	S	2123; 2124; 2125	0.653; 0.693; 0.653	1.43E-23	154	9038	16,844	1.86	4.11E-04
	S	36	0.964	1.15E-18	148	6818	10,720	1.57	7.93E-04
	S	2124; 2125	0.582; 0.983	4.77E-17	137	18,958	25,412	1.34	5.27E-03
	S; S	2125; 2128	0.86; 1	8.08E-10	116	12,384	10,854	0.88	7.41E-02
	S	1226	1	4.33E-03	63				
SRRM2	S	2398	0.899	1.67E-02	70	2052	6736	3.28	7.74E-07
	S	455; 456	0.657; 0.864	4.72E-04	99	8692	22,507	2.59	1.78E-06
	S	2702; 2706	1; 1	1.13E-03	78	6822	21,190	3.11	4.31E-06
	S	1132	0.767	5.10E-03	79	6423	23,060	3.59	4.83E-06
	S; S	903; 908	0.756; 0.93	1.17E-02	89	7024	17,287	2.46	1.19E-05
	S; S; T	901; 902; 903	0.4476; 0.447; 0.849	1.17E-02	89	7916	19,551	2.47	1.62E-05
	S	1691	0.505	1.44E-02	60	3402	9542	2.81	1.81E-05
	S; S	2044; 2046	1; 1	1.07E-02	63	11,261	26,216	2.33	2.12E-05
	S	1329	1	3.46E-05	113	12,581	33,168	2.64	2.86E-05
	S	454	0.946	1.16E-03	94	9678	23,505	2.43	2.97E-05
	S; S; S	1690; 1691; 1693	0.501; 0.501; 0.664	1.44E-02	60	1233	3849	3.12	3.92E-05
	T	2397	0.949	9.09E-03	125	1856	5793	3.12	4.14E-05
	S; S	484; 486	1; 1	8.82E-03	66	2800	13,671	4.88	5.19E-05
	S; S	875; 876	1; 1	2.22E-05	118	15,580	35,770	2.30	5.73E-05
	S; S	2692; 2694;	0.997; 0.999	2.02E-04	103	9902	30,084	3.04	7.07E-05
	S	2581	0.964	1.55E-02	61	3557	11,007	3.09	7.34E-05
	S	1124	0.999	1.38E-03	104	14,424	35,744	2.48	9.98E-05
	S; S	1443; 1444	0.933; 0.899	5.07E-03	82	4248	12,065	2.84	1.49E-04

Table 4 (continued)

DEG name	Phosphorylated amino acid residue	Phosphorylated position	Phosphorylated probabilities	PEP	Score	Phosphorylated level (N)	Phosphorylated level (T)	Ratio (T/N)	*P* value (*t* test)
	S; T	857; 866	0.761; 0.779	5.23E-03	63	1771	5578	3.15	1.74E-04
	S	1014	0.984	5.61E-04	65	2459	11,814	4.81	2.24E-04
	S; S	351; 353	0.982; 0.994	5.54E-03	85	9186	27,782	3.02	2.36E-04
	S; T	1925; 1927	1; 1	1.78E-02	72	3013	9448	3.14	3.54E-04
	S; S	2727; 2729	1; 0.999	1.24E-02	57	2764	11,511	4.16	4.64E-04
	S; S	295; 297	1; 0.999	3.32E-04	77	8935	20,961	2.35	7.87E-04
	S	1112	0.834	4.10E-05	83	3678	7472	2.03	1.16E-03
	S; S	952; 954	1; 0.978	1.24E-02	84	6685	12,365	1.85	1.24E-03
	S; S	778; 780	1; 0.999	1.17E-04	112	31,177	58,376	1.87	1.42E-03
	T; S	1003; 1012	1; 0.693	1.98E-15	123	1958	4374	2.23	3.06E-03
	S	1102	0.567	4.10E-05	87	10,436	15,924	1.53	5.33E-03
	S; S	1497; 1499	0.93; 0.93	5.98E-03	66	11,049	15,474	1.40	1.06E-02
	S	322; 323	0.646; 0.847	2.10E-17	101	1813	2549	1.41	1.28E-02
	S	1103	0.993	3.29E-15	154	8557	9123	1.07	3.32E-01
	S; S; S	1477; 1482; 1483	1; 1; 1	1.00E-07	128	10,775	11,809	1.10	3.56E-01
	S	1010	0.996	3.50E-03	55				
	T	458	0.551	1.25E-02	75				
	S; S	1517; 1519	0.993; 0.995	5.19E-03	65				
	T; S	1063; 1064	0.496; 0.496	2.73E-02	79				
	S	377; 398; 400	0.991; 0.415; 0.415	3.40E-04	37				
	S	395	0.953	3.40E-04	37				
	T	1177	0.855	1.04E-02	55				
	S	1083	0.994	3.88E-03	96				
	T; T; S; T; S; S	315; 316; 317; 318; 322; 323	0.325; 0.325; 0.325; 0.325; 0.325; 0.325	3.79E-03	50				
	T; S; T	316; 317; 318	0.399; 0.399; 0.399	1.72E-04	57				
	S	1069	0.307	6.58E-03	66				
	S; S; S; S; S	1539; 1541; 1542; 1550; 1552	0.334; 0.334; 0.334; 0.499; 0.499	2.63E-03	54				
	S; S	1101; 1103	0.96; 0.955	4.10E-05	83				
SSBP3	S	347	1	4.55E-14	121	5331	8383	1.57	4.80E-03
STIM1	S	257	1	1.74E-02	78				
STK39	S	385	1	1.13E-219	188	27,341	40,397	1.48	7.42E-04
STX1A	S	14	1	4.88E-57	182	72,880	183,350	2.52	9.68E-06
STXBP5L	S; S; S	819; 820; 823	0.346; 0.346; 0.831	1.68E-02	44				

Table 4 (continued)

DEG name	Phosphorylated amino acid residue	Phosphorylated position	Phosphorylated probabilities	PEP	Score	Phosphorylated level (N)	Phosphorylated level (T)	Ratio (T/N)	*P* value (*t* test)
SYN1	S; S	551; 553	1; 1	1.08E-22	130	8100	33,111	4.09	3.59E-04
TCEA1	S	100	1	1.20E-47	197	66,104	140,043	2.12	8.61E-05
TCF12	T; S; T	581; 582; 584	0.256; 0.256; 0.256	3.44E-02	44				
TLN2	T	1843	1	1.10E-02	93	7613	8825	1.16	1.17E-02
TNKS1BP1	S	672	1	1.03E-03	70	6115	19,567	3.20	2.19E-05
	S; S	1620; 1621	1; 1	1.38E-16	138	7581	16,197	2.14	4.57E-05
	S	221	1	1.47E-02	62	6177	15,957	2.58	6.76E-05
	S	494	0.984	1.15E-12	88				
	S	494; 498	0.492; 0.492	1.22E-05	38				
TPI1	S	58	1	5.49E-61	200	57,287	111,203	1.94	2.76E-05
	S	249	0.992	7.14E-37	110				
TPMT	S	14	0.806	4.23E-05	86				
TRIM3	S	7	1	8.45E-07	73				
TSC2	S; S; S	1385; 1386; 1387	0.313; 0.313; 0.313	1.56E-11	74				
USP24	S	2047	1	7.77E-03	92	24,339	33,164	1.36	4.29E-03
WBP4	S	262	0.996	5.26E-03	90	4151	7080	1.71	4.96E-04

DEG, differentially expressed gene; *LogFC*, $\log_2$(fold change); *LogFC > = 1*, upregulated DEG; *LogFC <= − 1*, downregulated DEGs; *T*, NFPA; *N*, control pituitaries; *Ratio (T/N)*, ratio of phosphorylation level of NFPAs to controls

Table 5 Functional characteristics of 130 overlapped molecules between phosphoproteins and invasive DEGs in NFPAs, clustered with GO and KEGG pathway enrichments. Count means the number of genes enriched in each item

Category	Functional characteristics	Count	%	Fold enrichment	*P* value	Gene name of overlapped molecule
Annotation cluster 1						
GOTERM_CC_DIRECT	GO:0005913~cell–cell adherens junction	11	8.73	5.05	6.35E-05	ALDOA, TNKS1BP1, LIMA1, PGM5, CALD1, ASAP1, EPS15L1, H1FX, NDRG1, PLEC, CHMP2B
GOTERM_BP_DIRECT	GO:0098609~cell–cell adhesion	10	7.94	5.16	1.34E-04	ALDOA, TNKS1BP1, LIMA1, CALD1, ASAP1, EPS15L1, H1FX, NDRG1, PLEC, CHMP2B
GOTERM_MF_DIRECT	GO:0098641~cadherin binding involved in cell–cell adhesion	10	7.94	4.73	2.58E-04	ALDOA, TNKS1BP1, LIMA1, CALD1, ASAP1, EPS15L1, H1FX, NDRG1, PLEC, CHMP2B
Annotation cluster 2						
KEGG_PATHWAY	hsa04611:Platelet activation	10	7.94	10.58	2.53E-07	AKT1, TLN2, STIM1, GNAS, SNAP23, PRKG1, ARHGEF12, ITPR1, ITPR2, ITGA2B
Annotation cluster 3						
GOTERM_MF_DIRECT	GO:0005085~guanyl-nucleotide exchange factor activity	6	4.76	6.98	1.66E-03	NGEF, ARHGEF6, DOCK7, ARHGEF12, DOCK11, ARHGEF11
GOTERM_BP_DIRECT	GO:0043547~positive regulation of GTPase activity	12	9.52	2.97	2.25E-03	NGEF, ARHGEF6, TSC2, ASAP2, ASAP1, GNAS, ARHGEF12, CDC42EP4, DOCK11, ARHGEF11, STXBP5L, SPTB
GOTERM_MF_DIRECT	GO:0005089~Rho guanyl-nucleotide exchange factor activity	5	3.97	8.91	2.34E-03	NGEF, ARHGEF6, ARHGEF12, DOCK11, ARHGEF11
GOTERM_MF_DIRECT	GO:0005096~GTPase activator activity	8	6.35	3.94	4.17E-03	ARHGEF6, TSC2, ASAP2, ASAP1, ARHGEF12, CDC42EP4, ARHGEF11, STXBP5L
GOTERM_BP_DIRECT	GO:0051056~regulation of small GTPase mediated signal transduction	5	3.97	5.22	1.52E-02	NGEF, ARHGEF6, TSC2, ARHGEF12, ARHGEF11
GOTERM_BP_DIRECT	GO:0035023~regulation of Rho protein signal transduction	4	3.17	6.91	1.98E-02	NGEF, ARHGEF6, ARHGEF12, ARHGEF11
GOTERM_BP_DIRECT	GO:0043065~positive regulation of apoptotic process	7	5.56	3.27	2.00E-02	AKT1, NGEF, BCLAF1, ARHGEF6, ARHGEF12, GAL, ARHGEF11
Annotation cluster 4						
GOTERM_MF_DIRECT	GO:0008017~microtubule binding	6	4.76	3.96	1.76E-02	KIF1A, MAP4, NDRG1, CLASP2, KIF16B, KIF13B
GOTERM_CC_DIRECT	GO:0005874~microtubule	7	5.56	3.33	1.83E-02	KIF1A, STIM1, MAP4, NDRG1, CLASP2, KIF16B, KIF13B
GOTERM_CC_DIRECT	GO:0005871~kinesin complex	3	2.38	8.39	4.91E-02	KIF1A, KIF16B, KIF13B

Table 5 (continued)

Category	Functional characteristics	Count	%	Fold enrichment	*P* value	Gene name of overlapped molecule
Annotation cluster 5						
GOTERM_BP_DIRECT	GO:0018107~peptidyl-threonine phosphorylation	3	2.38	11.05	2.97E-02	AKT1, STK39, PRKCD
GOTERM_MF_DIRECT	GO:0004672~protein kinase activity	7	5.56	2.68	4.61E-02	AKT1, AVP, CASK, STK39, PRKCD, CDK14, DCLK1
Annotation cluster 6						
GOTERM_BP_DIRECT	GO:1903779~regulation of cardiac conduction	4	3.17	10.00	7.32E-03	SLC8A2, STIM1, ITPR1, ITPR2
KEGG_PATHWAY	hsa04020:Calcium signaling pathway	5	3.97	3.84	3.79E-02	SLC8A2, STIM1, GNAS, ITPR1, ITPR2
Annotation cluster 7						
KEGG_PATHWAY	hsa04611:Platelet activation	10	7.94	10.58	2.53E-07	AKT1, TLN2, STIM1, GNAS, SNAP23, PRKG1, ARHGEF12, ITPR1, ITPR2, ITGA2B
KEGG_PATHWAY	hsa04270:Vascular smooth muscle contraction	8	6.35	9.41	1.64E-05	CALD1, GNAS, PRKG1, ARHGEF12, PRKCD, ITPR1, ARHGEF11, ITPR2
KEGG_PATHWAY	hsa04915:Estrogen signaling pathway	6	4.76	8.34	6.44E-04	AKT1, FKBP5, GNAS, PRKCD, ITPR1, ITPR2
GOTERM_BP_DIRECT	GO:0050796~regulation of insulin secretion	5	3.97	10.44	1.30E-03	STX1A, MARCKS, GNAS, ITPR1, ITPR2
KEGG_PATHWAY	hsa04922:Glucagon signaling pathway	5	3.97	6.95	5.21E-03	AKT1, ACACA, GNAS, ITPR1, ITPR2
KEGG_PATHWAY	hsa04730:Long-term depression	4	3.17	9.17	8.74E-03	GNAS, PRKG1, ITPR1, ITPR2
KEGG_PATHWAY	hsa05205:Proteoglycans in cancer	6	4.76	4.13	1.34E-02	AKT1, ANK1, ARHGEF12, ITPR1, PXN, ITPR2
KEGG_PATHWAY	hsa04970:Salivary secretion	4	3.17	6.40	2.30E-02	GNAS, PRKG1, ITPR1, ITPR2
KEGG_PATHWAY	hsa04540:Gap junction	4	3.17	6.25	2.44E-02	GNAS, PRKG1, ITPR1, ITPR2
KEGG_PATHWAY	hsa04022:cGMP–PKG signaling pathway	5	3.97	4.35	2.55E-02	AKT1, SLC8A2, PRKG1, ITPR1, ITPR2
KEGG_PATHWAY	hsa04912:GnRH signaling pathway	4	3.17	6.05	2.66E-02	GNAS, PRKCD, ITPR1, ITPR2
KEGG_PATHWAY	hsa04750:Inflammatory mediator regulation of TRP channels	4	3.17	5.62	3.22E-02	GNAS, PRKCD, ITPR1, ITPR2
KEGG_PATHWAY	hsa04020:Calcium signaling pathway	5	3.97	3.84	3.79E-02	SLC8A2, STIM1, GNAS, ITPR1, ITPR2
GOTERM_BP_DIRECT	GO:0030168~platelet activation	4	3.17	4.87	4.84E-02	AKT1, PRKCD, ITPR1, ITPR2

(ratio of T/N = 2.32, P = 4.24E-04); Ser1295 (ratio of T/N = 1.45, P = 1.11E-03); Ser115 (ratio of T/N = 1.81, P = 1.02E-02); Ser1478 and Ser1480 in ARHGEF11; and Ser1687 (ratio of T/N = 0.67, P = 2.20E-03) in ITPR2 (Table 6; Supplemental Fig. 1.2); (iii) estrogen signaling pathway involved in phosphorylation at residues Ser122 and Ser124 in AKT1; Ser13 in FKBP5; Ser995 (ratio of T/N = 2.77, P = 2.32E-05) in GNAS; Tyr514 in PRKCD; Ser1177, Thr1178, Ser1180, and Tyr1181 in ITPR1; and Ser1687 (ratio of T/N = 0.67, P = 2.20E-03) in ITPR2 (Table 6; Supplemental Fig. 1.3); (iv) Fc gamma R-mediated phagocytosis involved in phosphorylation at residues Ser122 and Ser124 in AKT1; Ser701 (ratio of T/N = 1.57, P = 2.02E-03) in ASAP2; Ser717 (ratio of T/N = 2.04, P = 1.35E-04) in ASAP1; Ser27 (ratio of T/N = 8.66, P = 3.86E-06); Ser26 (ratio of T/N = 5.66, P = 8.79E-06), Thr150 (ratio of T/N = 3.88, P = 1.52E-05), Ser145 (ratio of T/N = 1.62, P = 8.15E-03), Ser147, Ser118, Thr120, Ser128, Thr130, Ser138, and Ser101 in MARCKS; and Tyr514 in PRKCD (Table 6; Supplemental Fig. 1.4); (v) glucagon signaling pathway involved in phosphorylation at residues Ser122 and Ser124 in AKT1; Ser29 (ratio of T/N = 2.98, P = 6.08E-05) in ACACA; Ser995 (Ratio of T/N = 2.77, P = 2.32E-05) in GNAS; Ser1177, Thr1178, Ser1180, and Tyr1181 in ITPR1; and Ser1687 (ratio of T/N = 0.67, P = 2.20E-03) in ITPR2 (Table 6; Supplemental Fig. 1.5); (vi) proteoglycans in cancer involved in phosphorylation at residues Ser122 and Ser124 in AKT1; Ser781 (ratio of T/N = 3.58, P = 4.13E-06), Ser1428 (ratio of T/N = 1.72, P = 1.74E-05), Thr961 (ratio of T/N = 1.61, P = 4.31E-04), Ser960 (ratio of T/N = 1.70, P = 5.29E-04), Thr961 (ratio of T/N = 1.70, P = 5.29E-04), Ser1607 (ratio of T/N = 0.76, P = 3.19E-03), Thr1684, Ser1686, Ser1686, and Thr1688 in ANK1; Ser309 (ratio of T/N = 2.94, P = 9.07E-04) in ARHGEF12; Ser1177, Thr1178, Ser1180, and Tyr1181 in ITPR1; Ser302 (ratio of T/N = 1.43, P = 2.16E-02), Ser303 (ratio of T/N = 1.43, P = 2.16E-02), Ser322 (ratio of T/N = 1.88, P = 4.60E-02), Thr318, and Ser320 in PXN; and Ser1687 (ratio of T/N = 0.67, P = 2.20E-03) in ITPR2 (Table 6; Supplemental Fig. 1.7); (vii) insulin signaling pathway involved in phosphorylation in residues Ser122 and Ser124 in AKT1; Ser114 (ratio of T/N = 0.7, P = 6.75E-04) in PRKAR2B; Thr486 and Ser488 in SLC2A4; Ser1385, Ser1386, and Ser1387 in TSC2; and Ser29 (ratio of T/N = 2.98, P = 6.08E-05) in ACACA (Table 6; Supplemental Fig. 1.8); (viii) gap junction involved in phosphorylation at residues Ser995 (ratio of T/N = 2.77, P = 2.32E-05) in GNAS; Thr515 in PRKG1; Ser1177, Thr1178, Ser1180, and Tyr1181 in ITPR1; and Ser1687 (ratio of T/N = 0.67, P = 2.20E-03) in ITPR2 (Table 6; Supplemental Fig. 1.10); (ix) cGMP–PKG signaling pathway involved in phosphorylation at residues Ser122 and Ser124 in AKT1; Ser622 (ratio of T/N = 1.60, P = 1.40E-01) in SLC8A2; Thr515 in PRKG1; Ser1177, Thr1178, Ser1180, and Tyr1181 in ITPR1; and Ser1687 (ratio of T/N = 0.67, P = 2.20E-03) in ITPR2 (Table 6; Supplemental Fig. 1.11); (x) GnRH signaling pathway involved in phosphorylation at residues Ser995 (ratio of T/N = 2.77, P = 2.32E-05) in GNAS; Tyr514 in PRKCD; Ser1177, Thr1178, Ser1180, and Tyr1181 in ITPR1; and Ser1687 (ratio of T/N = 0.67, P = 2.20E-03) in ITPR2 (Table 6; Supplemental Fig. 1.12); (xi) inflammatory mediator regulation of TRP channels involved in phosphorylation at residues Ser995 (ratio of T/N = 2.77, P = 2.32E-05) in GNAS; Tyr514 in PRKCD; Ser1177, Thr1178, Ser1180, and Tyr1181 in ITPR1; and Ser1687 (ratio of T/N = 0.67, P = 2.20E-03) in ITPR2 (Table 6; Supplemental Fig. 1.13); and (xii) calcium signaling pathway involved in phosphorylation at residues Ser622 (ratio of T/N = 1.60, P = 1.40E-01) in SLC8A2; Ser257 in STIM1; Ser995 (ratio of T/N = 2.77, P = 2.32E-05) in GNAS; Ser1177, Thr1178, Ser1180, and Tyr1181 in ITPR1; and Ser1687 (ratio of T/N = 0.67, P = 2.20E-03) in ITPR2 (Table 6; Supplemental Fig. 1.14). These findings clearly demonstrate that phosphorylation participates in invasiveness-related signaling pathways in invasive NFPAs.

Hub molecules identified with protein–protein interaction analysis of 130 overlapped molecules (phosphoproteins; invasive DEGs)

The PPI network was constructed using molecules with combined scores greater than 0.4, based on 130 overlapped molecules (phosphoproteins; invasive DEGs) (Fig. 3a; Supplemental Table 9). Some overlapped molecules (phosphoproteins; invasive DEGs) in PPI networks trend to be co-expressed or co-localized with high combined score, the difference might be related to functional differences between the overlapped molecules, and various co-expression and co-localization might be reflected in the molecular characteristics or structures of two molecules [31], which help to understand the function and biological mechanisms of NFPA invasiveness. Among 130 overlapped molecules (phosphoproteins; invasive DEGs), some between molecules had very high combined score; for example, SNAP23 and STX1A, AKT1 and TSC2, CHD3 and GATAD2A, SPTB and ANK1, ALDOA and TPI1, POMC and AVP, STIM1 and ITPR1, SCG3 and CHGA, DMTN and ADD2, CHGB and SCG3, ALDOA and PKM, STIM1 and ITPR2, PKM and TPI1, POMC and GAL, SYN1 and STX1A, DMTN and ADD3, and HNRNPA1 and SRRM2 had the combined score over 0.95 (Supplemental Table 9).

The hub molecules based on the PPI network play important roles in a molecular network system, which also reflects its crucial roles in a biological system such as NFPA invasive behavior system. The entire PPI network was analyzed using MCODE, and one module was obtained with module score = 5.778 (Fig. 3b). Thus, a total of 10 hub molecules were

Table 6 Statistically significant KEGG signaling pathways identified from 130 overlapped molecules between phosphoproteins and invasive DEGs in NFPAs. Count means the number of genes enriched in each pathway

Category	Pathway name	Count	%	Fold enrichment	*P* value	Benjamini	Gene name of overlapped molecule
KEGG_PATHWAY	hsa04611:Platelet activation	10	7.94	10.58	2.53E-07	3.61E-05	AKT1, TLN2, STIM1, GNAS, SNAP23, PRKG1, ARHGEF12, ITPR1, ITPR2, ITGA2B
KEGG_PATHWAY	hsa04270:Vascular smooth muscle contraction	8	6.35	9.41	1.64E-05	1.17E-03	CALD1, GNAS, PRKG1, ARHGEF12, PRKCD, ITPR1, ARHGEF11, ITPR2
KEGG_PATHWAY	hsa04915:Estrogen signaling pathway	6	4.76	8.34	6.44E-04	3.02E-02	AKT1, FKBP5, GNAS, PRKCD, ITPR1, ITPR2
KEGG_PATHWAY	hsa04666:Fc gamma R-mediated phagocytosis	5	3.97	8.19	2.89E-03	9.82E-02	AKT1, ASAP2, ASAP1, MARCKS, PRKCD
KEGG_PATHWAY	hsa04922:Glucagon signaling pathway	5	3.97	6.95	5.21E-03	1.39E-01	AKT1, ACACA, GNAS, ITPR1, ITPR2
KEGG_PATHWAY	hsa04730:Long-term depression	4	3.17	9.17	8.74E-03	1.89E-01	GNAS, PRKG1, ITPR1, ITPR2
KEGG_PATHWAY	hsa05205:Proteoglycans in cancer	6	4.76	4.13	1.34E-02	2.40E-01	AKT1, ANK1, ARHGEF12, ITPR1, PXN, ITPR2
KEGG_PATHWAY	hsa04910:Insulin signaling pathway	5	3.97	4.98	1.64E-02	2.55E-01	AKT1, PRKAR2B, SLC2A4, TSC2, ACACA
KEGG_PATHWAY	hsa04970:Salivary secretion	4	3.17	6.40	2.30E-02	3.09E-01	GNAS, PRKG1, ITPR1, ITPR2
KEGG_PATHWAY	hsa04540:Gap junction	4	3.17	6.25	2.44E-02	2.98E-01	GNAS, PRKG1, ITPR1, ITPR2
KEGG_PATHWAY	hsa04022:cGMP-PKG signaling pathway	5	3.97	4.35	2.55E-02	2.85E-01	AKT1, SLC8A2, PRKG1, ITPR1, ITPR2
KEGG_PATHWAY	hsa04912:GnRH signaling pathway	4	3.17	6.05	2.66E-02	2.75E-01	GNAS, PRKCD, ITPR1, ITPR2
KEGG_PATHWAY	hsa04750:Inflammatory mediator regulation of TRP channels	4	3.17	5.62	3.22E-02	3.02E-01	GNAS, PRKCD, ITPR1, ITPR2
KEGG_PATHWAY	hsa04020:Calcium signaling pathway	5	3.97	3.84	3.79E-02	3.26E-01	SLC8A2, STIM1, GNAS, ITPR1, ITPR2

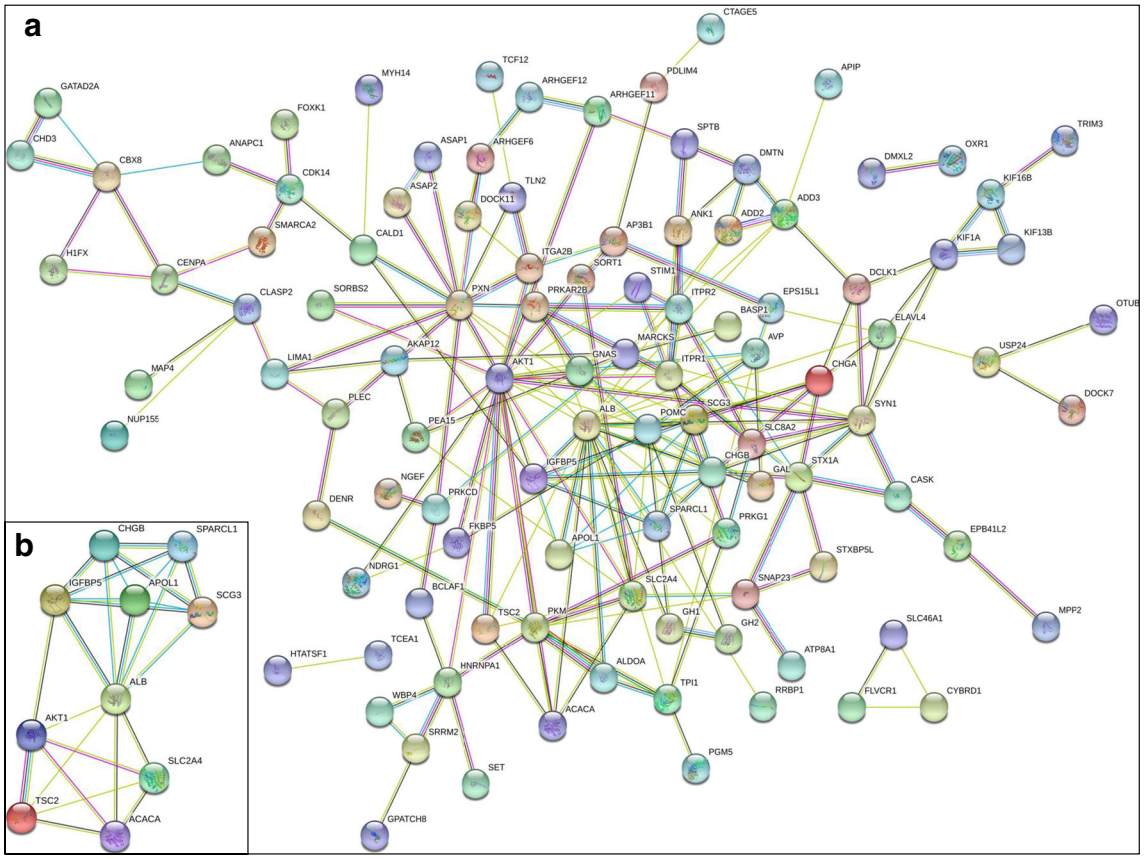

Fig. 3 The hub molecules were identified with protein–protein interaction (PPI)-based molecular complex detection (MCODE) using 130 overlapped molecules (phosphoproteins; invasive DEPs) in NFPAs. **a** The protein–protein interactions (PPIs) with combined scores greater than 0.4 were selected to construct PPI network. **b** The entire PPI network was analyzed using molecular complex detection (MCODE), and one module was obtained with module score = 5.778. The different colored nodes represent different query proteins and first shell of interactors. The white nodes represent second shell of interactors. The empty nodes represent the proteins with unknown 3D structure. The filled nodes represent the proteins with known or predicted 3D structure

identified in invasive NFPAs (Table 7), including SCG3 (secretogranin-3), TSC2 (tuberin), ALB (serum albumin), AKT1 (RAC-alpha serine/threonine-protein kinase), APOL1 (apolipoprotein L1), ACACA (acetyl-CoA carboxylase 1), SPARCL1 (SPARC-like protein 1), SLC2A4 (solute carrier family 2 facilitated glucose transporter member 4), CHGB (secretogranin-1), and IGFBP5 (insulin-like growth factor-binding protein 5). These hub molecules not only had the differential expression at the mRNA level but also had the changed level of phosphorylation. These hub molecules assisted in improving the understanding of the key molecular mechanisms underlying NFPA invasiveness, and the results may help the further study of the biological mechanism of NFPA invasive behavior. It also clearly demonstrated that phosphorylation of these hub molecules played important roles in NFPA invasive behavior; for example, phosphorylation occurred at residues Ser37 (ratio T/N = 0.46, P = 1.5E-04) in SCG3; Ser1385, Ser1386, and Ser1387 in TSC2; Ser82 (ratio T/N = 0.74, P = 3.24E-04) in ALB; Ser122 and Ser124 in AKT1; Ser352 (ratio T/N = 0.71, P = 5.33E-03) and Ser355 (ratio T/N = 0.71, P = 5.33E-03) in APOL1; Ser29 (ratio of T/N = 2.98, P = 6.08E-05) in ACACA; Ser76, Ser80 (ratio T/N = 0.24, P = 1.86E-05), Ser84 (ratio T/N = 0.35, P = 5.38E-05), Ser92 (ratio T/N = 0.28, P = 1.91E-05), Ser198 (ratio T/N = 0.89, P = 1.92E-01), Ser231, Thr238, Ser240, and Ser295 (ratio T/N = 0.57, P = 1.15E-053) in SPARCL1; Thr486 and Ser488 in SLC2A4; and Thr123 in IGFBP5; and CHGB was phosphorylated at 50 residues (41 Ser, 5 Thr, and 4 Tyr residues) (Table 7). The hub molecules (phosphoproteins; invasive DEGs) SLC2A4 and TSC2 were involved in insulin signaling pathway, ACACA was involved in insulin signaling pathway and glucagon signaling pathway, and AKT1 was involved in insulin signaling pathway, glucagon signaling pathway, cGMP–PKG signaling pathway, proteoglycans in cancer, Fc gamma R-mediated phagocytosis, estrogen signaling pathway, and platelet activation pathway (Table 6). It clearly demonstrated that one signaling pathway included multiple hub molecules, and one hub molecule was involved in multiple signaling pathways, to display a real signaling pathway network system in NFPA invasive behavior. Those hub molecules played the crucial roles in the signaling pathway network system in the invasive behavior of NFPAs,

Table 7 A total of 10 hub molecules in invasive NFPAs identified with PPI analysis of 130 overlapped molecules (invasive DEG; phosphoproteins)

Protein accession ID	DEG name	DEG level				Protein name	Phosphorylation level							
		logFC	AveExpr	*t*	*P* value		Phosphopeptide	Phosphorylated site	Phosphorylated position	Phosphorylated probabilities	PEP	Score	Ratio (T/N)	*P* value (*t* test)
Q8WXD2	SCG3	1.2843	10.4326	4.3052	1.72E-03	Secretogranin-3	ELS*AERPLNEQIAEAEEDKIK	S	37	1	2.80E-38	149	0.46	1.50E-04
							LFPAPS*EKSHEETDSTK	S	359	0.468	1.85E-02	36		
P49815	TSC2	2.1795	10.7866	6.3857	9.73E-05	Tuberin	S*SSSPELQTLQDILGDPGDK	S; S; S	1385; 1386; 1387	0.313; 0.313; 0.313	1.56E-11	74		
P02768-1	ALB	1.9536	6.1289	4.5055	1.27E-03	Serum albumin	TCVADES*AENCDK	S	82	1	1.24E-47	197	0.74	3.24E-04
P31749	AKT1	1.1801	6.8509	5.4900	3.11E-04	RAC-alpha serine/threonine-protein kinase	S*GSPSDNSGAEEMEVSLAKPK	S; S	122; 124	0.457; 0.457	1.16E-07	92		
A5PL32	APOL1	− 1.1936	9.8189	− 3.2480	9.26E-03	Apolipoprotein L1	VTEPIS*AES*GEQVER	S; S	352; 355	1; 1	2.53E-03	59	0.71	5.33E-03
Q13085	ACACA	1.1822	6.8754	3.3664	7.62E-03	Acetyl-CoA carboxylase 1	FIIGSVSEDNS*EDEISNLVK	S	29	1	3.35E-32	154	2.98	6.08E-05
Q14515	SPARCL1	− 3.1871	13.6134	− 4.7627	8.66E-04	SPARC-like protein 1	EES*HEQS*AEQGK	S	80		9.37E-38	176	0.24	1.86E-05
							SSS*QELGLK	S	92	0.999	1.61E-28	188	0.28	1.91E-05
							SKEES*HEQS*AEQGK	S; S	80; 84	0.999; 1	9.37E-38	176	0.35	5.38E-05
							EHANS*KQEEDNTQSDDILEE SDQPTQVSK	S	231	1	5.61E-70	176	0.36	5.25E-04
							HIQETEWQS*QEGK	S	295	1	2.83E-21	152	0.57	1.15E-03
							DQGNQEQDPNIS*NGEEEEEKE PGEVGTHNDNQER	S	198	0.997	1.10E-05	53	0.89	1.92E-01
							EHANS*KQEEDNT*QS* DDILEESDQPTQVSK	S; T; S	231; 238; 240	0.331; 0.331; 0.331	1.44E-02	38		
							S*KEES*HEQSAEQGK	S; S	76; 80	0.999; 0.995	7.77E-05	77		
P14672	SLC2A4	− 1.3065	5.1362	− 4.4148	1.45E-03	Solute carrier family 2, facilitated glucose transporter member 4	T*PSLLEQEVKPSTELEYLGPDEND	T; S	486; 488	0.5; 0.5	1.85E-10	91		
P05060	CHGB	− 1.3288	14.5253	− 3.2997	8.51E-03	Secretogranin-1	SETHAAGHS*QEK	S	225	1	4.87E-30	175	0.14	6.87E-07
							GRGS*EEYR	S	367	1	1.70E-07	146	0.12	7.46E-07
							AS*EEEPEYGEEIK	S	335	1	5.81E-71	223	0.13	2.05E-06
							EKSS*QES*GEETGS*QENHPQESK	S; S; S	236; 239; 245	0.531; 1; 0.965	4.20E-73	205	0.06	3.67E-06
							ADEPQWSLYPSDS*QVS*EEVK	S; S	146; 149	0.999; 0.999	1.30E-150	236	0.31	5.28E-06
							SSQESGEET*GSQENHPQESK	T	243	0.978	1.47E-45	161	0.02	5.36E-06
							GERGEDS*S*EEK	S; S	182; 183	1; 1	1.80E-03	100	0.16	7.03E-06
							AS*EEEPEY*GEEIK	S; Y	335; 341	1; 1	2.35E-06	98	0.18	8.29E-06
							SSQES*GEETGS*QENHPQESK	S; S	239; 245	0.992; 1	4.20E-73	205	0.06	1.01E-05
							S*QREDEEEEEGENYQK	S	160	1	1.77E-17	140	0.25	1.17E-05
							SAEFPDFYDS*EEPVSTHQEAENEKDR	S	626	1	1.85E-99	214	0.26	1.18E-05
							S*QEES*EEGEEDATS*EVDK	S	259; 263; 272	1; 1; 0.857	1.51E-53	157	0.14	1.23E-05
							SSQGGS*LPSEEK	S	298	0.981	3.28E-14	142	0.28	1.31E-05
							DPADASEAHES*SSR	S	98	0.966	1.32E-30	169	0.10	1.41E-05
							NYPS*LELDK	S	391	1	1.30E-04	112	0.14	1.44E-05
							ADEPQWSLYPS*DS*QVSEEVK	S; S	144; 146	0.941; 0.751	3.58E-98	136	0.52	1.53E-05
							EKSS*QES*GEET*GSQENHPQESK	S; S; T	237; 239; 243	0.819; 0.935; 0.598	1.47E-45	161	0.05	1.53E-05
							SSQGGSLPS*EEK	S	301	0.999	5.51E-20	128	0.25	1.88E-05
							S*AEFPDFYDSEEPVSTHQEAENEKDR	S	617	1	8.30E-152	246	0.22	2.13E-05
							S*AEFPDFY*DSEEPVSTHQEAENEKDR	Y	624	0.995	8.86E-43	152	0.23	2.23E-05
							SQEESEEGEEDAT*SEVDK	T	271	0.973	1.38E-88	219	0.21	2.23E-05
							M#AHGY*GEES*EEER	Y; S	401; 405	1; 1	2.41E-02	51	0.23	2.34E-05
							ERADEPQWSLYPSDSQVS*EEVK	S	149	1	2.83E-147	264	0.29	2.80E-05
							PQS*EES*WDEEDKR	S; S	377; 380	1; 1	4.73E-42	181	0.15	3.27E-05
							SAEFPDFYDS*EEPVS*THQEAENEK	S; S	626; 631	0.996; 0.863	3.45E-35	140	0.30	3.33E-05
							SS*QGGSLPSEEK	S	294	0.807	3.74E-09	133	0.24	3.77E-05
							S*SQGGSLPSEEK	S	293	0.992	1.97E-30	180	0.25	4.48E-05
							GHPQEES*EESNVSMASLGEK	S	311	1	6.58E-209	232	0.22	5.91E-05

Table 7 (continued)

Protein accession ID	DEG name	DEG level				Protein name	Phosphorylation level							
		logFC	AveExpr	*t*	*P* value		Phosphopeptide	Phosphorylated site	Phosphorylated position	Phosphorylated probabilities	PEP	Score	Ratio (T/N)	*P* value (*t* test)
							SAEFPDFYDSEEPVS*T*HQEAENEK	S; T	631; 632	0.591; 0.586	3.45E-35	124	0.31	5.94E-05
							EKS*S*QES*GEET*GS*QENHPQESK	S; S; S; T; S	235; 236; 239; 243; 245	0.643; 0.589; 0.589; 0.589; 0.589	1.47E-45	161	0.05	7.50E-05
							WQQQGDLQDT*KENR	T	492	1	6.83E-05	85	0.37	9.99E-05
							GHPQEES*EESNVS*M#ASLGEK	S	317	0.988	1.45E-59	184	0.29	1.70E-04
							ADEPQWSLY*PSDSQVS*EEVK	Y; S	142; 149	0.981; 0.96	6.42E-108	134	0.52	1.87E-04
							GHPQEES*EESNVS*MAS*LGEK	S; S; S	314; 320; 323	0.739; 1; 1	1.83E-50	161	0.37	4.40E-04
							WAEGGGHS*R	S	130	1	4.86E-03	80	0.21	5.96E-04
							GHPQEES*EES*NVS*MASLGEK	S; S; S	314; 317; 320	0.959; 0.959; 0.959	8.63E-27	145	0.31	6.63E-04
							CIIEVLSNALS*K	S	46	1	3.06E-04	94	0.40	1.63E-02
							DHHS*THYRASEEPEY*GEEIK	S; T; Y	329; 330; 341	0.355; 0.355; 0.98	1.56E-02	43		
							DPADASEAHESS*S*RGEAGAP GEEDIQGPTK	S; S	99; 100	0.651; 0.651	8.57E-07	62		
							LLRDPADAS*EAHESSSR	S	93	0.989	5.88E-05	88		
							S*ETHAAGHS*QEK	S	217	0.757	1.02E-02	78		
P24593	IGFBP5	− 2.6828	10.6639	− 4.1430	2.20E-03	Insulin-like growth factor-binding protein 5	EHEEPT*TSEMAEETYSPK	T	123	0.346	2.19E-04	56		

DEG, differentially expressed gene; *LogFC*, $\log_2$(fold change). *LogFC* > = *1*, upregulated DEG; *LogFC* <= − *1*, downregulated DEGs; *Ratio (T/N)*, the ratio of phosphorylation level of NFPAs to controls

which might be the effective panel biomarker and multitherapeutic targets for NFPA invasiveness.

Discussion

Phosphorylation is one of the important protein PTMs (ranging from 400 to 600 PTMs in humans [16]) that cause the diversity of proteins, namely proteoforms or protein species [17]. Proteoform or protein species is defined as a primary amino acid sequence + PTMs + spatial conformation + binding partners + cofactors + localization + a defined function [17]. The number of proteoforms (at least 1,000,000 proteoforms in humans) is much more than the number of transcripts (at least 100,000 transcripts in humans) and genes (about 20,300 genes in humans) [32, 33]. Proteoform is the basic unit in a proteome and is the final performer of gene functions. In-depth investigation of proteoforms in human proteome will directly benefit the discovery of reliable biomarkers for accurate molecular mechanisms, therapeutic targets, personalized medicine, or precision medicine in human pituitary adenomas [32]. Therefore, proteoforms have important scientific merit in the entire medical science and life science [34, 35]. The studies on PTMs directly benefit the characterization of proteoforms. This study focused on phosphoproteomic profiling in human NFPA tissues, which belongs to our long-term research program in proteomics, PTMs, and proteoforms in human pituitary adenomas. TMT labeling–TiO_2 enrichment–LC-MS/MS was an effective quantitative proteomics approach [36] and identified a total of 2982 phosphorylation sites within 1035 phosphoproteins, with quantitative information for 1660 (1660/2982 = 55.67%) phosphorylation sites and qualitative information for 1322 (1322/2982 = 44.33%) phosphorylation sites, in NFPA tissues relative to controls. It is the first large-scale phosphoproteomic profiling of NFPAs with quantitative information, and those identified phosphoproteins participated in multiple biological process and signaling pathways, including cell–cell adherens junction, cadherin binding involved in cell–cell adhesion, cell–cell adhesion, SNARE interactions in vesicular transport, SNAP receptor activity, SNARE complex, histone H2B ubiquitination, histone monoubiquitination, endodermal cell fate commitment, Cdc73/Paf1 complex, myosin II complex and filament, oxygen transporter activity, oxygen transport, haptoglobin binding, haptoglobin–hemoglobin complex, hemoglobin complex, cAMP-dependent protein kinase complex, protein kinase A catalytic subunit binding, cAMP-dependent protein kinase regulator activity, ESCRT III complex disassembly, positive regulation of viral release from host cell, and eukaryotic 43S preinitiation complex. Also, 31 statistically significant signaling pathways were mined with KEGG pathway analysis from 1035 phosphoproteins in NFPAs, including platelet activation, mRNA surveillance pathway, RNA transport, spliceosome, endocytosis, proteoglycans in cancer, mTOR signaling pathway, insulin signaling pathway, MAPK signaling pathway, SNARE interactions in vesicular transport, gap junction, focal adhesion, glucagon signaling pathway, estrogen signaling endoplasmic reticulum, and GnRH signaling pathway. Those data provided the largest phosphorylation profiling and phosphorylation-mediated signaling pathway systems, which are the precious resource to deeply investigate biological functions of protein phosphorylations in NFPAs, and identify the reliable and effective new biomarkers for patient stratification, prognostic/predictive assessment, and personalized treatment of NFPAs.

Tumor invasiveness is a very challenging clinical problem in NFPAs, which causes the different therapeutic strategies after neurosurgery [37–39]. Investigation of tumor invasiveness in NFPAs is always very interesting and meaningful. Some researchers have focused on several invasiveness-related molecules including pituitary tumor-transforming gene (PTTG), vascular endothelial growth factor (VEGF), hypoxia inducible factor-1a (HIF-1a), fibroblast growth factor-2 (FGF-2), and matrix metalloproteinases (MMPs) such as MMP-2 and MMP-9, and their interacted complex molecular network in human pituitary adenoma [4, 38, 40]. However, the world of molecules of invasive NFPAs is very complex; these molecules [4, 38, 40] are only the partial molecules, which cannot represent the entire molecular world of NFPA invasive behavior. Multiomics-based molecular pathway networks [4, 15, 30] are an effective strategy and approach to study NFPA invasiveness, and annotate the interactome in invasive NFPA, and also are the real way to resolve its clinical invasiveness challenge, for in-depth clarification of its molecular mechanism of NFPA invasiveness and discovery of reliable invasiveness-related biomarkers for diagnosis, prognostic/predictive assessment, and therapeutic targets for personalized therapy [6, 7, 16, 41, 42]. This study used transcriptomics data between invasive NFPAs and control pituitaries, from the public GEO database, which was integrated with the identified phosphoprotein data. An overlapped analysis between 1035 phosphoproteins and 2751 DEGs in invasive NFPAs relative to controls revealed 130 overlapped molecules (phosphoproteins; invasive DEGs). Those 130 overlapped molecules were involved in multiple biological processes, including cell–cell adherens and regulation, platelet activation, GTPase signaling and regulation, microtubule and its regulation, protein kinase activity and peptidyl-threonine phosphorylation, and calcium signaling pathway and regulation. Thereby, those phosphoproteins participated in the corresponding biological functions in NFPA invasive behaviors. We have clearly demonstrated the important roles of phosphorylation in invasive NFPA pathogenesis.

Furthermore, based on 130 overlapped molecules (phosphoproteins; invasive DEGs), 12 statistically significant signaling pathways (Table 6; Supplemental Fig. 1) were identified to associate with tumor invasiveness, and the identified

phosphoproteins were involved in these signaling pathways. For example, the platelet activation pathway included phosphoproteins (invasive DEGs) AKT1, TLN2, STIM1, GNAS, SNAP23, PRKG1, ARHGEF12, ITPR1, ITPR2, and ITGA2B; the vascular smooth muscle contraction pathway included phosphoproteins (invasive DEGs) CALD1, GNAS, PRKG1, ARHGEF12, PRKCD, ITPR1, ARHGEF11, and ITPR2; the estrogen signaling pathway included phosphoproteins (invasive DEGs) AKT1, FKBP5, GNAS, PRKCD, ITPR1, and ITPR2; Fc gamma R-mediated phagocytosis included phosphoproteins (invasive DEGs) AKT1, ASAP2, ASAP1, MARCKS, and PRKCD; the glucagon signaling pathway included phosphoproteins (invasive DEGs) AKT1, ACACA, GNAS, ITPR1, and ITPR2; proteoglycans in cancer included phosphoproteins (invasive DEGs) AKT1, ANK1, ARHGEF12, ITPR1, PXN, and ITPR2; the insulin signaling pathway included phosphoproteins (invasive DEGs) AKT1, PRKAR2B, SLC2A4, TSC2, and ACACA; the gap junction pathway included phosphoproteins (invasive DEGs) GNAS, PRKG1, ITPR1, and ITPR2; the cGMP–PKG signaling pathway included phosphoproteins (invasive DEGs) AKT1, SLC8A2, PRKG1, ITPR1, and ITPR2; the GnRH signaling pathway included phosphoproteins (invasive DEGs) GNAS, PRKCD, ITPR1, and ITPR2; inflammatory mediator regulation of TRP channels included phosphoproteins (invasive DEGs) GNAS, PRKCD, ITPR1, and ITPR2; and the calcium signaling pathway included phosphoproteins (invasive DEGs) SLC8A2, STIM1, GNAS, ITPR1, and ITPR2. These KEGG signaling pathways formed the signaling pathway profiling of NFPA invasive behavior and mutually interacted through hub molecules. Interestingly, PPI network-based MCODE analysis identified 10 hub molecules (phosphoproteins; DEGs) in invasive NFPAs (Table 7; Fig. 3b), namely SLC2A4, TSC2, AKT1, SCG3, ALB, APOL1, ACACA, SPARCL1, CHGB, and IGFBP5. Comparative analysis of these hub molecules with the nodes of signaling pathways (Table 6; Supplemental Fig. 1) found that one signaling pathway might include multiple hub molecules, and one hub molecule might be involved in multiple signaling pathways [43]; for example, the insulin signaling pathway included hub molecules SLC2A4, TSC2, and AKT1; and AKT1 was involved in insulin signaling pathway, cGMP–PKG signaling pathway, glucagon signaling pathway, estrogen signaling pathway, platelet activation pathway, Fc gamma R-mediated phagocytosis, and proteoglycans in cancer. These signaling pathways and hub molecules formed the real signaling pathway network system for NFPA invasive behavior, which is offering great promise to clarify the molecular mechanisms of NFPA invasive behavior; determine the effective panel of biomarkers [11] for patient stratification, prognostic/predictive assessment, and personalized treatment of invasive NFPAs; and discover multitherapeutic targets for personalized therapy for patients suffering of invasive NFPAs [44–46].

Currently, the diagnosis of NFPA invasive behaviors mainly relies on tumor morphological changes observed by neurosurgery and nuclear magnetic resonance (NMR) image changes at its middle or late stages, and it is very difficult to determine its invasiveness at its early stage [9, 10]. Even at its middle or late stages, NMR image and morphological change-based diagnosis of invasive behavior of NFPAs are also not fully accurate. In this study, the identified invasiveness-related, phosphorylation-mediated signaling pathways and pathway network-based hub molecules (phosphoproteins; invasive DEGs) have the potential for establishing panel of biomarkers allowing early prediction of invasive behavior and focusing on therapeutic targets to prevent its progression and accurate prognostic/predictive assessment of invasive behavior after neurosurgery, in order to personalize the treatment of invasive NFPA patients. Here, 10 pathway–network-based hub molecules (phosphoproteins; invasive DEGs) were taken for further discussion in the context of PPPM in invasive NFPAs. AKT1 is a crucial component in the PI3K–Akt signaling pathway that is required for VEGF-A mRNA expression in GH3 cells induced by 17alpha-estradiol [47], and the anticancer drug precursor methylseleninic acid (MSeA) can decrease AKT phosphorylation to inhibit the growth and survival of human umbilical vein endothelial cells [48], and AKT1-mutant estrogen receptor (ER)-positive metastatic breast cancer has a longer survival duration on mTOR inhibitor therapy [49]. Thus, AKT is an important therapeutic target potentially capable of improving the treatment results of solid tumors [50]. ACACA is acetyl-CoA carboxylase 1 that catalyzes the ATP-dependent carboxylation of acetyl-CoA, a rate-limiting step in fatty acid biosynthesis [51]. A study found that ACACA is a potent therapeutic target for anticancer therapy [52]. Also, phospho-ACACA protein is an independent prognostic/predictive factor for human gastric cancer without lymph node metastasis [53]. TSC2, tuberin, is a well-known suppressor of the mTOR pathway [54]. SPARCL1 can suppress cancer metastasis and recruit macrophases by activation of canonical WNT/β-catenin signaling [55], or it can suppress cancer cell proliferation and migration via the MEK/ERK signaling [56]. SLC2A4, namely solute carrier family 2 facilitated glucose transporter member 4, encodes glucose transporter 4 protein (GLUT4), which has been identified as a promising therapeutic target for cancer, because the putative antimicrobial peptides (AMPs) can serve as a therapeutic drug in treating cancer by inhibiting SLC2A4 that is responsible for the production of energy for cancer cells during angiogenesis [57]. IGFBP5 is the insulin-like growth factor binding protein 5, which acts as a tumor suppressor, and is often dysregulated in human cancers to associate with tumorigenicity and metastasis; thus, IGFBP5 might be a novel therapeutic target for human melanoma [58, 59]. Furthermore, clinical findings demonstrate the potential of IGFBP5 as an effective biomarker predicting the response to therapy and clinical outcome of

cancer patients [60]. SCG3 is secretogranin-3 [61, 62], CHGB is secretogranin-1 [63, 64], ALB is serum albumin [65, 66], and APOL1 is apolipoprotein L1 [67–69]; these molecules were found to be phosphorylated in this study, and they can be secreted into body fluid thus having the potential for the early prediction and prognostic assessment of invasive behavior of NFPAs from the molecular view of point.

Thereby, PTMs are the main factor to result in proteoforms—the final functional forms of a gene/protein. In the context of proteoforms, we focused on an important PTM—phosphorylation that is involved in many biological processes and cell signaling transductions, in NFPA pathogenesis. Further, we integrated the phosphoproteomics and transcriptomics data in invasive NFPAs to obtain phosphorylation-mediated molecular events in invasive NFPAs, which is the precious resource to (i) benefit the understanding of molecular mechanisms of NFPA invasive behavior, (ii) discover effective therapeutic targets to prevent the occurrence and progression of invasive NFPAs, and (iii) develop effective phosphorylation-related biomarkers for prognostic/predictive assessment to stratify NFPA patients into invasive and noninvasive groups who will undergo personalized therapeutic approaches after neurosurgery. This study may serve as an example of effective contribution to the paradigm shift from experimental medicine to PPPM in pituitary adenomas.

Strength and limitation

This study provided the first large-scale phosphoproteomic profiling with 2982 phosphorylation sites within 1035 phosphoproteins in NFPAs and the corresponding phosphorylation-mediated functional characteristics and signaling pathway networks. Moreover, 1035 phosphoproteins were integrated with transcriptomics data (2751 DEGs) in invasive NFPAs relative to controls, which obtained 130 overlapped molecules (phosphoproteins; invasive DEGs), followed by pathway network analysis to obtain 12 statistically significant signaling pathways and 10 hub molecules associated with NFPA invasive behaviors. These findings offer an increasing promise for insights into the molecular mechanisms, determination of effective therapeutic targets, and discovery of effective pathway network-based panel of biomarkers for patient stratification, prognostic/predictive assessment, and personalized treatment of NFPA patients. However, one must realize that those phosphoproteomic data (4 NFPAs vs. 4 controls) and transcriptomics (4 invasive NFPAs vs. 3 controls from GEO database) were derived from a limited sample size. In order to transit those findings into routine practice, a significantly expanded sample size will be needed to further validate and study in detail the molecular mechanisms, functional roles, and potentially therapeutic targets of these identified phosphorylation-involved signaling pathways and hub molecules in NFPA patients. One should also try their best to address the signaling pathway alterations at the proteoform level for real evidence-based PPPM in invasive NFPAs.

Moreover, one should note the potential bias resource of phosphoproteomics analysis due to the different ethnic origin of the samples. Because the post-mortem control pituitary tissue samples were very difficult to be obtained, this phosphoproteomics study used control pituitary tissues from three subjects from the USA of Caucasian ethnic origin and one subject of African-American ethnic origin, and NFPA tissues from 4 Chinese patients (Table 1). It is also important to emphasize yet another limitation as a source of potential differences in phosphorylation—it is the fact that all control samples were taken post-mortem, while NFPA tissues were taken as biopsies from the living patients. For future thorough investigation of phosphorylation level of each phosphoprotein in NFPAs and control pituitary tissues, we would recommend to investigate the variations of phosphorylation levels among different ethnic origin of the samples (American Caucasian, African-American, and Chinese tissue samples). However, for transcriptomics data (DEG data) between 4 invasive NFPAs and 3 control pituitary tissues in the GEO database, these NFPAs and control pituitary tissue samples were from the same ethnic origin. After the overlapped analysis of phosphoproteins and DEG data, the bias of phosphoproteomics derived from ethnic origin of samples would be adjusted. Also, our previous study investigated the heterogeneity of human control pituitary proteome and identified differentially expressed proteins (DEPs) in the group of different genders (male vs. female), in the group of different ages (30-, 40-, and 50-year-old groups), and in the group of different ethnic origin (white vs. black), of control pituitary tissues [70]. The heterogeneity of human control pituitary proteomes did not significantly affect the differences (DEPs) between NFPAs and control pituitary tissues [71, 72]. It clearly indicated that the pituitary adenoma disease-induced differences might be much larger than, or different from, the gender-, age-, and ethnic origin-induced differences, or the potential differences arising from the type of the tissue origin (post-mortem vs. biopsies), in pituitary tissue proteome, which might help to assure our phosphoproteomics results.

Conclusions and expert recommendation

Protein phosphorylation is an important molecular event in the pathological process of NFPA. This study is the first report to provide the large-scale phosphorylation site profiling with quantitative information and the potential biological functions of protein phosphorylation in human NFPA tissues relative to controls, with TMT-labeled TiO_2 enrichment–LC-MS/MS method, bioinformatics, and pathway network analysis.

A total of 2982 phosphorylation sites within 1035 phosphoproteins and their involved functional characteristics and signaling pathways were identified in NFPAs. Further, the identified phosphoproteins in NFPAs were integrated with DEG data in invasive NFPAs relative to controls, which revealed a set of overlapped molecules (phosphoproteins; invasive DEGs), followed by analysis of functional characteristics and signaling pathway alterations of those overlapped molecules to reveal the important protein phosphorylation in the pathological process of invasive NFPAs. A total of 130 overlapped molecules (phosphoproteins; invasive DEGs) and their functional characteristics were revealed, and 12 statistically significant signaling pathways were identified to associate the invasive characteristics of invasive NFPAs. Ten hub molecules (phosphoproteins; DEGs) were identified with PPI network-based MCODE analysis in invasive NFPAs, including SLC2A4, TSC2, AKT1, SCG3, ALB, APOL1, ACACA, SPARCL1, CHGB, and IGFBP5. Those findings are the precious resource for new phosphoprotein biomarkers to take deep insight into the molecular mechanisms of NFPAs, prognostic/predictive assessment, patient stratification, and personalized treatment of invasive NFPAs, which might contribute to the development of PPPM in pituitary adenomas [45, 46, 73, 74].

We recommend to strengthen the studies of the large-scale phosphoproteins and their involved signaling pathways in NFPA pathogenesis, and to integrate phosphoproteomics data and transcriptomics data [15, 74] for invasive NFPAs to discover reliable and effective phosphoprotein biomarkers for molecular mechanism clarification of NFPA invasive behavior. These invasiveness-related phosphoprotein biomarkers might be used to discriminate invasive NFPAs from noninvasive NFPAs for patient stratification. The stratified patients (invasive vs. noninvasive NFPAs) will accept the corresponding prognostic assessment and personalized treatment, which will directly contribute to the predictive medicine and personalized medicine in NFPAs. Further, the invasiveness-related biomarkers might benefit the early-stage diagnostics of invasive NFPAs to let invasive NFPA patients undergo an early-stage medical treatment and prevent its progression, or the invasiveness-specific biomarkers might be developed into therapeutic targets for personalized drug treatment to prevent the occurrence and progression of NFPA invasive behavior. These will directly contribute to the predictive, preventive, and personalized medicine applied in NFPA patients.

Acknowledgments The authors also acknowledge Professor Xuejun Li from Xiangya Hospital and Professor Dominic M. Desiderio from University of Tennessee Health Science Center to assist in obtaining human tissues.

Author contributions D.L. analyzed data, prepared figures and tables, and wrote the manuscript draft. J.J., N.L., M.L., and S.W. participated in partial data analysis and bioinformatics. X.Z. conceived the concept, designed and instructed the experiments, analyzed the data, obtained the phosphoproteomic data, supervised the results, coordinated, wrote and critically revised the manuscript, and was responsible for its financial supports and the corresponding works. All authors approved the final manuscript.

Funding information This work was supported by the Shandong First Medical University Talent Introduction Funds (to X.Z.), the Hunan Provincial Hundred Talent Plan (to X.Z.), the SCIBP supported project (No. SCIBP2019090006), and China "863" Plan Project (Grant No. 2014AA020610-1 to XZ).

Compliance with ethical standards

Competing interests The authors declare that they have no conflict of interest.

Ethical approval Four pituitary adenoma tissue samples, obtained from the Department of Neurosurgery of Xiangya Hospital, Central South University, were approved by the Xiangya Hospital Medical Ethics Committee of Central South University. Post-mortem control pituitary tissue samples, obtained from the Memphis Regional Medical Center (n = 5), were approved by the University of Tennessee Health Science Center Internal Review Board.

Abbreviations ACACA, acetyl-CoA carboxylase 1; ACN, acetonitrile; AGC, automatic gain control; AKT, protein kinase B; AKT1, RAC-alpha serine/threonine-protein kinase; ALB, serum albumin; AMPK, AMP-activated protein kinase; APOL1, apolipoprotein L1; ATF2, activating transcription factor 2; BP, biological process; CC, cellular component; cGMP, cyclic nucleotide cGMP; CHGB, secretogranin-1; DEG, differentially expressed gene; DEP, differentially expressed protein; DTT, dithiothreitol; r-ERG channel, rat *ether-à-go-go*-related (ERG) channel; ERK, extracellular signal–regulated kinase; ESCRT, endosomal sorting complex required for transport; ESI-TRAP, electrospray ionization-ion trap; FC, fold change; FDR, false discovery rate; FGF-2, fibroblast growth factor-2; FPA, functional pituitary adenoma; GEO, Gene Expression Omnibus; GH, growth hormone; GH3, pituitary growth hormone 3; GnRH, gonadotropin-releasing hormone; GO, Gene Ontology; HCD, high-energy collision dissociation; HIF-1a, hypoxia-inducible factor-1a; HPLC, high-performance liquid chromatography; IGF-1, insulin growth factor-1; IGFBP5, insulin-like growth factor-binding protein 5; KEGG, Kyoto Encyclopedia of Genes and Genomes; LC, liquid chromatography; MAPK, mitogen-activated protein kinase; MCODE, molecular complex detection; MF, molecular function; MMPs, matrix metalloproteinases; MS/MS, tandem mass spectrometry; mTOR, mammalian target of rapamycin; NCBI, National Center for Biotechnology Information; NFκB, nuclear factor kappa-B; NFPA, nonfunctional pituitary adenoma; NMR, nuclear magnetic resonance; PACAP, pituitary adenylyl cyclase activating polypeptide; PI3K, phosphatidylinositol 3 kinase; PKG, protein kinase G; PPI, protein–protein interaction; PTM, post-translational modification; PTTG, pituitary tumor-transforming gene; RSK, ribosomal S6 kinase; SCG3, secretogranin-3; Ser or S, serine; SLC2A4, solute carrier family 2 facilitated glucose transporter member 4; S/N, signal-to-noise; SNAP, soluble N-ethylmaleimide-sensitive fusion attachment protein; SNARE, soluble N-ethylmaleimide-sensitive factor attachment protein receptor; SPARCL1, SPARC-like protein 1; TFA, trifluoroacetic acid; Thr or T, threonine; TMT, tandem mass tag; TSC2, Tuberin; TRH, thyrotropin-releasing hormone; Tyr or Y, tyrosine; VEGF, vascular endothelial growth factor

References

1. Melmed S. Mechanisms for pituitary tumorigenesis: the plastic pituitary. J Clin Invest. 2003;112:1603–18. https://doi.org/10.1172/JCI20401.
2. Melmed S. Pathogenesis of pituitary tumors. Nat Rev Endocrinol. 2011;7:257–66. https://doi.org/10.1038/nrendo.2011.40.
3. Melmed S. Pituitary tumors. Endocrinol Metab Clin N Am. 2015;44:1–9. https://doi.org/10.1016/j.ecl.2014.11.004.
4. Zhan X, Desiderio DM. Editorial: Molecular network study of pituitary adenomas. Front Endocrinol. 2020;11:26. https://doi.org/10.3389/fendo.2020.00026.
5. Cheng T, Wang Y, Lu M, Zhan X, Zhou T, Li B, et al. Quantitative analysis of proteome in non-functional pituitary adenomas: clinical relevance and potential benefits for the patient. Front Endocrinol. 2019;10:854. https://doi.org/10.3389/fendo.2019.00854.
6. Wang Y, Cheng T, Lu M, Mu Y, Li B, Li X, et al. TMT-based quantitative proteomics revealed follicle-stimulating hormone (FSH)-related molecular characterizations for potentially prognostic assessment and personalized treatment of FSH-positive non-functional pituitary adenomas. EPMA J. 2019;10:395–414. https://doi.org/10.1007/s13167-019-00187-w.
7. Zhan X, Desiderio DM, Wang X, Zhan X, Guo T, Li M, et al. Identification of the proteomic variations of invasive relative to noninvasive nonfunctional pituitary adenomas. Electrophoresis. 2014;35(15):2184–94.
8. Losa M, Mortini P, Barzaghi R, Ribotto P, Terreni MR, Marzoli SB, et al. Early results of surgery in patients with nonfunctioning pituitary adenoma and analysis of the risk of tumor recurrence. J Neurosurg. 2008;108(3):525–32. https://doi.org/10.3171/JNS/2008/108/3/0525.
9. Meij BP, Lopes MB, Ellegala DB, Alden TD, Laws ER Jr. The long-term significance of microscopic dural invasion in 354 patients with pituitary adenomas treated with transsphenoidal surgery. J Neurosurg. 2002;96(2):195–208. https://doi.org/10.3171/jns.2002.96.2.0195.
10. Selman WR, Laws ER Jr, Scheithauer BW, Carpenter SM. The occurrence of dural invasion in pituitary adenomas. J Neurosurg. 1986;64(3):402–7. https://doi.org/10.3171/jns.1986.64.3.0402.
11. Cheng T, Zhan X. Pattern recognition for predictive, preventive, and personalized medicine in cancer. EPMA J. 2017;8:51–60. https://doi.org/10.1007/s13167-017-0083-9.
12. Grech G, Zhan X, Yoo BC, Bubnov R, Hagan S, Danesi R, et al. EPMA position paper in cancer: current overview and future perspectives. EPMA J. 2015;6:9. https://doi.org/10.1186/s13167-015-0030-6.
13. Zhan X, Desiderio DM. The use of variations in proteomes to predict, prevent, personalize treatment for clinically non-functional pituitary adenomas. EPMA J. 2010;1:439–59. https://doi.org/10.1007/s13167-010-0028-z.
14. Hu R, Wang X, Zhan X. Multi-parameter systematic strategy for predictive, preventive, and personalized medicine in cancer. EPMA J. 2013;4:2. https://doi.org/10.1186/1878-5085-4-2.
15. Lu M, Zhan X. The crucial role of multiomic approach in cancer research and clinically relevant outcomes. EPMA J. 2018;9(1):77–102. https://doi.org/10.1007/s13167-018-0128-8.
16. Zhan X, Long Y, Lu M. Exploration of variations in proteome and metabolome for predictive diagnostics and personalised treatment algorithms: innovative approach and examples for potential clinical application. J Proteome. 2018;188:30–40. https://doi.org/10.1016/j.jprot.2017.08.020.
17. Zhan X, Li B, Zhan X, Schlüter H, Jungblut PR, Coorssen JR. Innovating the concept and practice of two-dimensional gel electrophoresis in the analysis of proteomes at the proteoform level. Proteomes. 2019;7(4):36. https://doi.org/10.3390/proteomes704003.
18. Guo T, Wang X, Li M, Yang H, Li L, Peng F, et al. Identification of glioblastoma phosphotyrosine-containing proteins with two-dimensional Western blotting and tandem mass spectrometry. Biomed Res Int. 2015;2015:134050.
19. Singh V, Ram M, Kumar R, Prasad R, Roy BK, Singh KK. Phosphorylation: implications in cancer. Protein J. 2017;36:1–6. https://doi.org/10.1007/s10930-017-9696-z.
20. Golden RJ, Chen B, Li T, Braun J, Manjunath H, Chen X, et al. An argonaute phosphorylation cycle promotes microRNA-mediated silencing. Nature. 2017;542:197–202. https://doi.org/10.1038/nature21025.
21. Tsai CF, Wang YT, Yen HY, Tsou CC, Ku WC, Lin PY, et al. Large-scale determination of absolute phosphorylation stoichiometries in human cells by motif-targeting quantitative proteomics. Nat Commun. 2015;6:6622. https://doi.org/10.1038/ncomms7622.
22. Sergina NV, Rausch M, Wang D, Blair J, Hann B, Shokat KM, et al. Escape from HER-family tyrosine kinase inhibitor therapy by the kinase-inactive HER3. Nature. 2007;445(7126):437–41.
23. Shah KN, Bhatt R, Rotow J, Rohrberg J, Olivas V, Wang VE, et al. Aurora kinase A drives the evolution of resistance to third-generation EGFR inhibitors in lung cancer. Nat Med. 2019;25(1):111–8. https://doi.org/10.1038/s41591-018-0264-7.
24. Kreuzer J, Edwards A, Haas W. Multiplexed quantitative phosphoproteomics of cell line and tissue samples. Methods Enzymol. 2019;626:41–65. https://doi.org/10.1016/bs.mie.2019.07.027.
25. Li Z, Li M, Li X, Xin J, Wang Y, Shen QW, et al. Quantitative phosphoproteomic analysis among muscles of different color stability using tandem mass tag labeling. Food Chem. 2018;249:8–15. https://doi.org/10.1016/j.foodchem.2017.12.047.
26. Carretero L, Llavona P, López-Hernández A, Casado P, Cutillas PR, de la Peña P, et al. ERK and RSK are necessary for TRH-induced inhibition of r-ERG potassium currents in rat pituitary GH3 cells. Cell Signal. 2015;27(9):1720–30. https://doi.org/10.1016/j.cellsig.2015.05.014.
27. Zhao S, Feng J, Li C, Gao H, Lv P, Li J, et al. Phosphoproteome profiling revealed abnormally phosphorylated AMPK and ATF2 involved in glucose metabolism and tumorigenesis of GH-PAs. J Endocrinol Investig. 2019;42(2):137–48. https://doi.org/10.1007/s40618-018-0890-4.
28. Delcourt N, Thouvenot E, Chanrion B, Galéotti N, Jouin P, Bockaert J, et al. PACAP type I receptor transactivation is essential for IGF-1 receptor signalling and antiapoptotic activity in neurons. EMBO J. 2007;26(6):1542–51.
29. Beranova-Giorgianni S, Zhao Y, Desiderio DM, Giorgianni F. Phosphoproteomic analysis of the human pituitary. Pituitary. 2006;9(2):109–20.
30. Long Y, Lu M, Cheng T, Zhan X, Zhan X. Multiomics-based signaling pathway network alterations in human non-functional pituitary adenomas. Front Endocrinol. 2019;10:835. https://doi.org/10.3389/fendo.2019.00835.
31. Ota M, Gonja H, Koike R, Fukuchi S. Multiple-localization and hub proteins. PLoS One. 2016;11:e0156455. https://doi.org/10.1371/journal.pone.0156455.
32. Zhan X, Li N, Zhan X, Qian S. Revival of 2DE-LC/MS in proteomics and its potential for large-scale study of human proteoforms. Med One. 2018;3:e180008. https://doi.org/10.20900/mo.20180008.
33. Zhan X, Yang H, Peng F, Li J, Mu Y, Long Y, et al. How many proteins can be identified in a 2-DE gel spot within an analysis of a complex human cancer tissue proteome? Electrophoresis. 2018;39:965–80. https://doi.org/10.1002/elps.201700330.

34. Aebersold R, Agar JN, Amster IJ, Baker MS, Bertozzi CR, Boja ES, et al. How many human proteoforms are there? Nat Chem Biol. 2018;14(3):206–14. https://doi.org/10.1038/nchembio.2576.
35. Smith LM, Kelleher NL. Proteoforms as the next proteomics currency. Science. 2018;359(6380):1106–7. https://doi.org/10.1126/science.aat1884.
36. Broncel M, Treeck M. Label-based mass spectrometry approaches for robust quantification of the phosphoproteome and total proteome in Toxoplasma gondii. Methods Mol Biol. 2020;2071:453–68. https://doi.org/10.1007/978-1-4939-9857-9_23.
37. Serioli S, Doglietto F, Fiorindi A, Biroli A, Mattavelli D, Buffoli B, et al. Pituitary adenomas and invasiveness from anatomo-surgical, radiological, and histological perspectives: a systematic literature review. Cancers (Basel). 2019;11(12). https://doi.org/10.3390/cancers11121936.
38. Zheng X, Li S, Zhang W, Zang Z, Hu J, Yang H. Current biomarkers of invasive sporadic pituitary adenomas. Ann Endocrinol (Paris). 2016;77(6):658–67. https://doi.org/10.1016/j.ando.2016.02.004.
39. Øystese KA, Evang JA, Bollerslev J. Non-functioning pituitary adenomas: growth and aggressiveness. Endocrine. 2016;53(1):28–34. https://doi.org/10.1007/s12020-016-0940-7.
40. Yang Q, Li X. Molecular network basis of invasive pituitary adenoma: a review. Front Endocrinol. 2019;10:7. https://doi.org/10.3389/fendo.2019.00007.
41. Zhan X, Desiderio DM. Editorial: Systems biological aspects of pituitary tumors. Front Endocrinol. 2016;7:86. https://doi.org/10.3389/fendo.2016.00086.
42. Zhan X, Long Y. Exploration of molecular network variations in different subtypes of human nonfunctional pituitary adenomas. Front Endocrinol. 2016;7:13. https://doi.org/10.3389/fendo.2016.00013.
43. Zhan X, Long Y, Zhan X, Mu Y. Consideration of statistical vs. biological significances for omics data-based pathway network analysis. Med One. 2017;1:e170002. https://doi.org/10.20900/mo.20170002.
44. Seifirad S, Haghpanah V. Inappropriate modeling of chronic and complex disorders: how to reconsider the approach in the context of predictive, preventive and personalized medicine, and translational medicine. EPMA J. 2019;10(3):195–209. https://doi.org/10.1007/s13167-019-00176-z.
45. Janssens JP, Schuster K, Voss A. Preventive, predictive, and personalized medicine for effective and affordable cancer care. EPMA J. 2018;9(2):113–23. https://doi.org/10.1007/s13167-018-0130-1.
46. Zhan X, Desiderio DM, editors. Molecular network study of pituitary adenomas. Lausanne: Frontiers Media SA; 2020. ISBN: 978-2-88963-602-0. https://doi.org/10.3389/978-2-88963-602-0.
47. Banerjee S, Saxena N, Sengupta K, Banerjee SK. 17alpha-Estradiol-induced VEGF-A expression in rat pituitary tumor cells is mediated through ER independent but PI3K-Akt dependent signaling pathway. Biochem Biophys Res Commun. 2003;300(1):209–15. https://doi.org/10.1016/s0006-291x(02)02830-9.
48. Wang Z, Jiang C, Ganther H, Lü J. Antimitogenic and proapoptotic activities of methylseleninic acid in vascular endothelial cells and associated effects on PI3K-AKT, ERK, JNK and p38 MAPK signaling. Cancer Res. 2001;61(19):7171–8.
49. Smyth LM, Zhou Q, Nguyen B, Yu C, Lepisto EM, Arnedos M, et al. Characteristics and outcome of AKT1 E17K-mutant breast cancer defined through AACR Project GENIE, a clinicogenomic registry. Cancer Discov. 2020;10(4):526–35. https://doi.org/10.1158/2159-8290.CD-19-1209.
50. Iida M, Harari PM, Wheeler DL, Toulany M. Targeting AKT/PKB to improve treatment outcomes for solid tumors. Mutat Res. 2020;819-820:111690. https://doi.org/10.1016/j.mrfmmm.2020.111690.
51. Hunkeler M, Hagmann A, Stuttfeld E, Chami M, Guri Y, Stahlberg H, et al. Structural basis for regulation of human acetyl-CoA carboxylase. Nature. 2018;558(7710):470–4. https://doi.org/10.1038/s41586-018-0201-4.
52. Stoiber K, Nagło O, Pernpeintner C, Zhang S, Koeberle A, Ulrich M, et al. Targeting de novo lipogenesis as a novel approach in anticancer therapy. Br J Cancer. 2018;118(1):43–51. https://doi.org/10.1038/bjc.2017.374.
53. Fang W, Cui H, Yu D, Chen Y, Wang J, Yu G. Increased expression of phospho-acetyl-CoA carboxylase protein is an independent prognostic factor for human gastric cancer without lymph node metastasis. Med Oncol. 2014;31(7):15. https://doi.org/10.1007/s12032-014-0015-7.
54. Alkharusi A, Lesma E, Ancona S, Chiaramonte E, Nyström T, Gorio A, et al. Role of prolactin receptors in lymphangioleiomyomatosis. PLoS One. 2016;11(1):e0146653. https://doi.org/10.1371/journal.pone.0146653.
55. Zhao SJ, Jiang YQ, Xu NW, Li Q, Zhang Q, Wang SY, et al. SPARCL1 suppresses osteosarcoma metastasis and recruits macrophages by activation of canonical WNT/β-catenin signaling through stabilization of the WNT-receptor complex. Oncogene. 2018;37(8):1049–61. https://doi.org/10.1038/onc.2017.403.
56. Ma Y, Xu Y, Li L. SPARCL1 suppresses the proliferation and migration of human ovarian cancer cells via the MEK/ERK signaling. Exp Ther Med. 2018;16(4):3195–201. https://doi.org/10.3892/etm.2018.6575.
57. Aruleba RT, Adekiya TA, Oyinloye BE, Kappo AP. Structural studies of predicted ligand binding sites and molecular docking analysis of Slc2a4 as a therapeutic target for the treatment of cancer. Int J Mol Sci. 2018;19(2):386. https://doi.org/10.3390/ijms19020386.
58. Wang J, Ding N, Li Y, Cheng H, Wang D, Yang Q, et al. Insulin-like growth factor binding protein 5 (IGFBP5) functions as a tumor suppressor in human melanoma cells. Oncotarget. 2015;6(24):20636–49. https://doi.org/10.18632/oncotarget.4114.
59. Duan C, Allard JB. Insulin-like growth factor binding protein-5 in physiology and disease. Front Endocrinol. 2020;11:100. https://doi.org/10.3389/fendo.2020.00100.
60. Güllü G, Karabulut S, Akkiprik M. Functional roles and clinical values of insulin-like growth factor-binding protein-5 in different types of cancers. Chin J Cancer. 2012;31(6):266–80. https://doi.org/10.5732/cjc.011.10405.
61. Lloyd RV, Jin L. Analysis of chromogranin/secretogranin messenger RNAs in human pituitary adenomas. Diagn Mol Pathol. 1994;3(1):38–45. https://doi.org/10.1097/00019606-199403010-00007.
62. Lloyd RV, Jin L, Kulig E, Fields K. Molecular approaches for the analysis of chromogranins and secretogranins. Diagn Mol Pathol. 1992;1(1):2–15. https://doi.org/10.1097/00019606-199203000-00002.
63. Jin L, Chandler WF, Smart JB, England BG, Lloyd RV. Differentiation of human pituitary adenomas determines the pattern of chromogranin/secretogranin messenger ribonucleic acid expression. J Clin Endocrinol Metab. 1993;76(3):728–35. https://doi.org/10.1210/jcem.76.3.7680355.
64. d'Herbomez M, Do Cao C, Vezzosi D, Borzon-Chasot F, Baudin E, groupe des tumeurs endocrines (GTE France). Chromogranin A assay in clinical practice. Ann Endocrinol (Paris). 2010;71(4):274–80. https://doi.org/10.1016/j.ando.2010.04.004 Epub 2010 Jun 9.
65. Cruz-Topete D, Christensen B, Sackmann-Sala L, Okada S, Jorgensen JO, Kopchick JJ. Serum proteome changes in acromegalic patients following transsphenoidal surgery: novel biomarkers of disease activity. Eur J Endocrinol. 2011;164(2):157–67. https://doi.org/10.1530/EJE-10-0754.

66. Tang KT, Yang HJ, Choo KB, Lin HD, Fang SL, Braverman LE. A point mutation in the albumin gene in a Chinese patient with familial dysalbuminemic hyperthyroxinemia. Eur J Endocrinol. 1999;141(4):374–8. https://doi.org/10.1530/eje.0.1410374.
67. Liu X, Zheng W, Wang W, Shen H, Liu L, Lou W, et al. A new panel of pancreatic cancer biomarkers discovered using a mass spectrometry-based pipeline. Br J Cancer. 2017;117(12):1846–54. https://doi.org/10.1038/bjc.2017.365.
68. Lin X, Hong S, Huang J, Chen Y, Chen Y, Wu Z. Plasma apolipoprotein A1 levels at diagnosis are independent prognostic factors in invasive ductal breast cancer. Discov Med. 2017;23(127):247–58.
69. Hu CA, Klopfer EI, Ray PE. Human apolipoprotein L1 (ApoL1) in cancer and chronic kidney disease. FEBS Lett. 2012;586(7):947–55. https://doi.org/10.1016/j.febslet.2012.03.002.
70. Zhan X, Desiderio DM. Heterogeneity analysis of the human pituitary proteome. Clin Chem. 2003;49(10):1740–51. https://doi.org/10.1373/49.10.1740.
71. Moreno CS, Evans CO, Zhan X, Okor M, Desiderio DM, Oyesiku NM. Novel molecular signaling and classification of human clinically nonfunctional pituitary adenomas identified by gene expression profiling and proteomic analyses. Cancer Res. 2005;65(22):10214–22. https://doi.org/10.1158/0008-5472.CAN-05-0884.
72. Zhan X, Wang X, Long Y, Desiderio DM. Heterogeneity analysis of the proteomes in clinically nonfunctional pituitary adenomas. BMC Med Genet. 2014;7:69. https://doi.org/10.1186/s12920-014-0069-6.
73. Golubnitschaja O, Costigliola V, EPMA. General report & recommendations in predictive, preventive and personalised medicine 2012: white paper of the European Association for Predictive, Preventive and Personalised Medicine. EPMA J. 2012;3(1):14. https://doi.org/10.1186/1878-5085-3-14.
74. Hu R, Wang X, Zhan X. Multi-parameter systematic strategies for predictive, preventive and personalised medicine in cancer. EPMA J. 2013;4(1):2. https://doi.org/10.1186/1878-5085-4-2.

Abbreviations for all particular genes and proteins can be found in the Supplemental Table 1 and the UniProtKB database at the following link: https://www.expasy.org/.